PHYSIOLOGICAL CHANGES AND DNA DAMAGE REPAIR IN ARCTIC AND ANTARCTIC *Pseudogymnoascus* spp. IN RESPONSE TO ULTRAVIOLET-B RADIATION

WONG HAO JIE

INSTITUTE FOR ADVANCED STUDIES
UNIVERSITY OF MALAYA
KUALA LUMPUR

2019

PHYSIOLOGICAL CHANGES AND DNA DAMAGE REPAIR IN ARCTIC AND ANTARCTIC *Pseudogymnoascus* spp. IN RESPONSE TO ULTRAVIOLET-B RADIATION

WONG HAO JIE

THESIS SUBMITTED IN FULFILMENT OF THE REQUIREMENTS FOR THE DEGREE OF MASTER OF PHILOSOPHY

INSTITUTE FOR ADVANCED STUDIES
UNIVERSITY OF MALAYA
KUALA LUMPUR

2019

UNIVERSITY OF MALAYA

ORIGINAL LITERARY WORK DECLARATION

Name of Candidate: **WONG HAO JIE**

Matric No: **HGT150012**

Name of Degree: **MASTER OF PHILOSOPHY**

Title of Thesis:

"**PHYSIOLOGICAL CHANGES AND DNA DAMAGE REPAIR IN ARCTIC AND ANTARCTIC *Pseudogymnoascus* spp. IN RESPONSE TO ULTRAVIOLET-B RADIATION**"

Field of Study: **MARINE BIOTECHNOLOGY**

I do solemnly and sincerely declare that:

(1) I am the sole author/writer of this Work;
(2) This Work is original;
(3) Any use of any work in which copyright exists was done by way of fair dealing and for permitted purposes and any excerpt or extract from, or reference to or reproduction of any copyright work has been disclosed expressly and sufficiently and the title of the Work and its authorship have been acknowledged in this Work;
(4) I do not have any actual knowledge nor do I ought reasonably to know that the making of this work constitutes an infringement of any copyright work;
(5) I hereby assign all and every rights in the copyright to this Work to the University of Malaya ("UM"), who henceforth shall be owner of the copyright in this Work and that any reproduction or use in any form or by any means whatsoever is prohibited without the written consent of UM having been first had and obtained;
(6) I am fully aware that if in the course of making this Work I have infringed any copyright whether intentionally or otherwise, I may be subject to legal action or any other action as may be determined by UM.

Candidate's Signature Date:

Subscribed and solemnly declared before,

Witness's Signature Date:

Name: Assoc.
Designation:

ABSTRACT

Solar radiation drives almost all biological activities on Earth and regulates the morphology of many organisms as well as their biochemical and developmental processes. Soil microorganisms such as fungi within the polar regions can be continuously exposed to considerable solar UV radiation in the summer. Prolonged exposure to UV radiation can cause DNA damage and negatively affect cellular and physiological processes such as transcription, growth and reproduction. Physiological and cellular responses of four polar fungal strains of *Pseudogymnoascus* spp. (HND16 R2-1 sp.2 and HND16 R4-1 sp.1 isolated from Hornsund, Svalbard in the Arctic; AK07KGI1202 R1-1 sp.3 and AK07KGI1202 R1-1 sp.4 isolated from King George Island in maritime Antarctica) toward UVB radiation were examined. All strains were identified through BLAST and phylogenetic analysis using three DNA markers comprising ITS, LSU and *MCM7*. Phylogenetic analysis indicates that all the strains are closely related and formed a cluster that is a mixture of clades A, B and C of genus *Pseudogymnoascus*, despite being isolated from the opposite poles. The first part of this study was to determine the physiological responses of the fungi, including growth, pigmentation, and conidia production, toward UVB exposure over a period of 10 days. UVB radiation was supplied with a daily dosage of 6.1 kJ m^{-2} d^{-1} in a 12/12 h day/night cycle of PAR at 15°C. All strains showed significant growth rate reduction between 22 and 35% when compared to controls. Pigment production was not induced throughout the 10-day exposure to UV-B radiation. Based on scanning electron microscope imaging, UVB radiation exposure inhibited conidia production in all the *Pseudogymnoascus* strains except for HND16 R4-1 sp.1. The aim of the second part of this study was to compare the repair pathway of UV-induced DNA damage under two repair conditions: (i) light condition that induces photoreactivation (Phr) and (ii) and dark condition that induces nucleotide excision repair (NER) pathways. Two types of

DNA damage, namely cyclobutane pyrimidine dimers (CPDs) and pyrimidine 6-4 pyrimidone photoproducts (6-4PPs) were quantified using ELISA during repair incubation at 0, 2, 6, and 10 hours. Results showed that Antarctic strains were more resistant to UVB-induced CPD compared to Arctic strains, with CPD concentration being three-fold lower in the former strains. CPDs were repaired significantly faster in light than in dark conditions. For 6-4PPs, their repair rates were not significantly different between the two conditions. The expression of two DNA repair genes, *RAD2* and *PHR1* (each encoding a protein in NER and Phr, respectively) during the repair duration of 0 and 2 hours in the two different repair conditions were then measured using qPCR to determine the principal DNA repair pathway. The expression of *PHR1* was downregulated and *RAD2* was upregulated after UVB exposure in both light and dark repair conditions. However, the expression of *PHR1* was induced by light without UVB radiation, suggesting the expression of *PHR1* can be promoted in the presence of light. These observations suggest that the Phr pathway may not be involved in the repairing of UVB-induced DNA damage in *Pseudogymnoascus*, and that *PHR1* may carry out a different function in these fungi. The difference in *RAD2* expression between the two repair conditions was insignificant, suggesting an alternative repair mechanism may be involved in the repairing of CPDs in the presence of light. Findings from this study clearly demonstrate the effects of UVB irradiation on the growth and the reproduction of *Pseudogymnoascus* sp., suggesting the potential impact of increased UV radiation on the ecosystem functions of polar soil fungi, such as in the Arctic and Antarctic. In addition, this study provides some insights on the DNA repair mechanisms employed by these polar fungi to mitigate UV-induced DNA damage, on which studies were lacking previously in polar fungi.

Keywords: stress responses • nucleotide excision repair • photoreactivation • cyclobutane pyrimidine dimers • pyrimidine 6-4 pyrimidone photoproducts

ABSTRAK

Sinaran suria memacu hampir semua aktiviti biologi di bumi dan mengawal proses morfologi kebanyakan organisma serta pelbagai proses biokimia dan perkembangan mereka. Mikroorganisma tanah seperti kulat di kawasan kutub mungkin terdedah secara berterusan kepada sinaran UV matahari pada musim panas. Pendedahan yang berpanjangan kepada sinaran UV boleh menyebabkan kerosakan DNA dan memberi kesan negatif kepada proses selular dan fisiologi seperti transkripsi, pertumbuhan dan pembiakan. Gerak balas fisiologi dan selular daripada empat strain kulat *Pseudogymnoascus* spp. (HND16 R2-1 sp.2 dan HND16 R4-1 sp.1 dipencilkan dari *Hornsund, Svalbard* di *Arctic*; AK07KGI1202 R1-1 sp.3 dan AK07KGI1202 R1-1 sp.4 dipencilkan dari *King George Island*, *Antarctica*) terhadap sinaran UVB telah dikaji. Kesemua strain dikenal pasti melalui analisi *BLAST* dan filogenetik dengan menggunakan tiga penanda DNA yang terdiri daripada ITS, LSU dan *MCM7*. Analisi filogenetik menunjukkan bahawa kesemua strain adalah berkait rapat dan membentuk satu kelompok campuran klad A, B dan C dalam genus *Pseudogymnoascus*, walaupun dipencilkan dari kutub yang bertentangan. Bahagian pertama kajian ini adalah untuk menentukan gerak balas fisiologi kulat termasuk pertumbuhan, pigmentasi, dan penghasilan konidium terhadap keadaan simulasi UVB selama 10 hari. Dos harian sinaran UVB sebanyak 6.1 kJ m^{-2} d^{-1} dibekalkan dalam kitaran siang/malam bagi PAR 12/12 jam pada 15°C. Kesemua strain menunjukkan pengurangan kadar pertumbuhan di antara 22 dan 35% berbanding dengan kawalan. Penghasilan pigmen tidak dikesan sepanjang tempoh 10 hari pendedahan kepada sinaran UVB. Berdasarkan kepada pengimejan mikroskop elektron, penghasilan konidium bagi kesemua strain *Pseudogymnoascus* telah direncatkan akibat pendedahan sinaran UVB, kecuali HND16 R4-1 sp.1. Tujuan bahagian kedua kajian ini adalah untuk membandingkan tapak jalan pembaikpulihan DNA di bawah dua keadaan: (i) keadaan bercahaya yang mengaruhkan pemfotoreaktifan (Phr) dan (ii) keadaan gelap yang mengaruhkan pembaikpulihan eksisi nukleotida (NER). Dua jenis kerosakan DNA iaitu dimer pirimidin siklobutana (CPD) dan fotoproduk pirimidi 6-4 piramidon (6-4PP) telah

diukur dengan menggunakan ELISA semasa pengeraman pembaikpulihan pada 0, 2, 6, dan 10 jam. Hasil kajian menunjukkan bahawa strain Antartika adalah lebih rintang terhadap CPD yang dijanakan oleh UVB berbanding strain Artik, dengan kepekatan CPD yang tiga kali ganda lebih rendah. CPD dibaikpulih dengan lebih cepat dalam keadaan bercahaya, berbanding dengan keadaan gelap. Bagi 6-4PP, kadar pembaikpulih adalah tidak berbeza dengan berertinya di antara kedua-dua keadaan. Pengekspresan kedua-dua gen pembaikpulih DNA, *RAD2* dan *PHR1* (masing-masing mengekodkan protein dalam NER and Phr) telah diukur disepanjang tempoh pembaikpulihan untuk 0 dan 2 jam bagi dua keadaan pembaikpulihan yang berbeza dengan menggunakan PCR kuantitatif untuk mengenal pasti tapak jalan utama pembaikpulihan DNA. Pengekspresan *PHR1* menurun manakala pengekspresan *RAD2* meningkat selepas sinaran UVB dalam kedua-dua keadaan pembaikpulih yang bercahaya dan gelap. Bagaimanapun, pengekspresan *PHR1* telah diaruhkan oleh sinaran cahaya tanpa UVB, justeru mencadangkan bahawa pengekspresan *PHR1* boleh dicetuskan dalam keadaan bercahaya. Pemerhatian ini mencadangkan bahawa tapak jalan Phr mungkin tidak terlibat dalam pembaikpulihan kerosakan DNA yang dijanakan oleh UVB dalam *Pseudogymnoascus*, dan berkemungkinan menjalankan fungsi yang lain dalam kulat tersebut. Perbezaan pengekspresan *RAD2* di antara kedua-dua keadaan pembaikpulih adalah tidak bererti, justeru mencadangkan terlibatnya suatu mekanisme alternatif pembaikpulih DNA semasa pembaikpulih CPD dalam keadaan sinaran cahaya. Penemuan kajian ini ternyata menunjukkan kesan penyinaran UVB terhadap pertumbuhan dan pembiakan *Pseudogymnoascus* sp., mencadangkan kesan peningkatan sinaran UV yang berpotensi terhadap fungsi ekosistem kulat tanah, terutamanya di tanah yang terdedah di Artik dan Antartika. Di samping itu, kajian ini memberi gambaran mengenai mekanisme pembaikpulih DNA dalam kulat kutub untuk mengurangkan kerosakan DNA yang dijanakan oleh UV, yang mana kajian dalam kulat kutub sebelum ini adalah kurang.

Kata kunci: tindak balas ketegangan • baikpulih eksisi nukleotida • pemfotoreaktifan • dimer pirimidin siklobutana • fotoproduk pirimidi 6-4 piramidon

ACKNOWLEDGEMENTS

I would like to express my sincere gratitude to all the key persons and entities, who made possible for the development of this cruel fungal torturing experiment and for me to undertaking my Master degree of Philosophy in the oldest and most prestigious university in the land of Malaya. I believe I can't thank all the following persons enough for their kindness and supports in building me as a mad scientist during the three years of lab wars.

Dr. Siti Aisah Alias ❧ The Queen of our lab, thanks to her guidance on academia and provided us enough resources to fight the war against the *Pseudogymnoascus*, the national and international critics and to mark the lands we colonized with our papers.

Dr. Nuradilla Mohamad-Fauzi ❧ The General of our lab that helped in developing the fungal torturing procedures to extract the finest essence from the *Pseudogymnoascus* with all the crushing, vortexing, flicking and pipetting in order to winning the wars.

Dr. Mohammed Rizman-Idid ❧ The Cryptanalyst of our lab that helped breaching the fungal security systems and gained excess to the contents of encrypted message between *Pseudogymnoascus* and its alliances.

Prof. Peter Convey ❧ The Consultant in our lab that helped in developing papers and correcting my very bad grammar to make it readable for all the other scientists.

Thanks to all my fellow lab mates, **Natasha Tajuddin**, **Lee Li Chuen**, **Dr Abiramy Krishnan**, **Nurlizah Abu Bakar**, **Yasoga Supramaniam** and **Dr. Vejeysri Vello** for all the peer supports, discussions and critics that helped developed better strategies against all the difficulties and problems that I faced during the lab wars.

My parents ❧ Thanks to their financial and mental support throughout these 3 years, without their support I wouldn't make it to the end of this journey.

Ministry of Higher Education ❧ for awarding me the MyMaster Scholarship for 2 of 6 semesters that I was enrolled and provide funding through Higher Centre of Excellence (HiCoE) for the IOES (IOES-2014G: "Microbial response and adaptation towards atmospheric changes – Comparisons of response and adaptation of Antarctic and tropical fungi induced by changes in sea-air temperature and ultraviolet radiation") that make possible to complete this project.

Lastly, the polar fungi ***Pseudogymnoascus*** from both poles that continuously sacrificed themselves to be zapped by UV for generations throughout their lineage

Cheers to the victory of the lab wars,

Wong Hao Jie (**Maccus**)
Master of Philosophy
February 1st, 2019

TABLE OF CONTENTS

LIST OF FIGURES

LIST OF TABLES

LIST OF SYMBOLS AND ABBREVIATIONS

+G	:	Plus gamma
+I	:	Plus invariable
6-4PP	:	Pyrimidine (6-4) pyrimidone photoproducts
A/T/C/G	:	Adenine/Thymine/Cytosine/Guanine
ACT1	:	Actin
AER	:	Alternative excision repair
AGE	:	Agarose gel electrophoresis
AIC	:	Akaike information criterion
ATP	:	Adenosine triphosphate
BAS	:	Biotrophy-associated secreted
BEAST	:	Bayesian evolutionary analysis sampling trees
BI	:	Bayesian inference
BLAST	:	Basic local alignment search tool
BLR	:	Blue light receptor
BP	:	Base pair
BS	:	Bootstrap
C	:	Carbon
CDA	:	Czapex-Dox agar
COI	:	Cytochrome oxidase
CPD	:	Cyclobutane pyrimidine dimers
CRY	:	Cryptochrome
CS	:	Conserved site
C_T	:	Cycle threshold
DEL	:	DP-E2F-like

DEPC	:	Diethylpyrocarbonate
DHI	:	Dihydrolopoamide drhydrogenase
DLD	:	Dihydrolopoamide drhydrogenase
DNA	:	Deoxyribonucleic acid
dNTP	:	Deoxynuclotide triphosphates
DP	:	Cell-death protein
E2F	:	E2 transcription factor
EDTA	:	Ethylenediaminetetraacetic acid
EES	:	Effective sample size
EHE	:	Extracellular hydrolytic enzymes
ELISA	:	Enzyme-linked immunosorbent assay
EPF	:	Entomopathogenic fungi
EPS	:	Extracellular polymetric substances
ESR	:	Environmental stress response
FSB	:	Fostat Sørencen buffer
G1/G2	:	Growth phase 1/2
GAPDH	:	Glyceraldehyde 3-phosphate dehydrogenase
gDNA	:	Genomic DNA
GIS	:	Glg1-2-suppressor
gIUV	:	Global UV-B surfaces
GTP	:	General time reversible model
HMG	:	High-mobility group
IGS	:	Intergenic spacer
ITS	:	Internal transcribed spacer
K2P	:	Kimura 2-parameter
KEGG	:	Kyoto encyclopedia of genes and genomic

LSU	:	Large subunit
M-value	:	Gene-stability value
MAA	:	Mycosporine-like amino acid
MANOVA	:	Multivariate analysis of variance
MAP	:	Mitogen-activated protein
MCM7	:	Minichromosomal maintenance unit
MEGA	:	Molecular evolutionary genetic analysis
ML	:	Maximum likelihood
MMS	:	Methyl methane sulfonate
MP	:	Maximum parsimony
MUS	:	Mutagen sensitive
MUSCLE	:	Multiple sequence comparison by log-expectation
MYB	:	Myeloblatosis
MYC	:	Mycosporine
NADH	:	Nicotinamide adenine dinucleotide
NCBI	:	National Centre for Biotechnology Information
NER	:	Nucleotide excision repair
NJ	:	Neighbour joining
ODS	:	Ozone depleting substances
OHP	:	Overhead projector
O_SO_4	:	Osmium tetroxide
p	:	Significant level
PAR	:	Photosynthetically active radiation
PAUP	:	Phylogenetic analysis using parsimony
PDB	:	Phosphate-buffered saline
PCR	:	Polymerase chain reaction

PGK1	:	Phosphoglycerate kinase
PHL	:	Photolyase-like
Phr	:	Photoreactivation
PIS	:	Parsimony informative sites
PP	:	Posterior probability
qPCR	:	Quantitative polymerase chain reaction
R^2	:	Correlation coefficient
RAD	:	Radiation sensitive
RAxML	:	Randomized axelerated maximum likelihood
RNA	:	Ribonucleic acid
ROS	:	Reactive oxygen species
ROX	:	Rhodamine X
RPB2	:	RNA polymerase II subunit B
RPH	:	Resistance to phosphine
rRNA	:	Ribosomal RNA
SAR1	:	Secretion associated Ras related GTPase
SBF	:	SWI4/SWI6 protein complex
SD	:	Standard deviation
SEM	:	Standard error of mean
SEM	:	Scanning electron microscopy/micrograph
SS	:	Singleton
ssDNA	:	Single-stranded DNA
SSU	:	Small subunit
SWI	:	Switching
SYBR	:	Synergy brand
TAE	:	Tris-acetate-EDTA

TBS	:	Tree bisection-reconnection
TE	:	Tris-EDTA
TEF1α	:	Translational elongation factor 1-alpha
TET	:	Tetragnathidae
TIM	:	Transitional model
TOP1	:	Topoisomerase I
UV	:	Ultraviolet
UVDE	:	UV endonuclease
UVER	:	UVDE-dependent excision repair
UVR	:	Ultraviolet radiation
V	:	Volume/Version
VS	:	Variable site
WC	:	White complex
XP	:	Xenoderma pigmentosum
β-TUB	:	Beta tubulin
nm	:	Nanometer
%	:	Percent
h	:	Hour
kJ	:	Kilojoules
m	:	Meter
d	:	Day
s	:	Second
min	:	Minute(s)
kb	:	Kilobase
g	:	Gram(s)
L	:	Liter(s)

mg	:	Miligram(s)
ml	:	Mililiter(s)
mm	:	Milimeter(s)
µL	:	Microliter(s)
mM	:	Mili Molar
µ	:	Mean

LIST OF APPENDICES

CHAPTER 1: INTRODUCTION

1.1 Background

Solar radiation provides the energy that drives almost all biological activities on Earth, as well as underpins the environmental cues that regulate morphological and developmental processes in many organisms. The ultraviolet (UV) spectrum can be divided into three distinct wavelength bands of progressively increasing energy: UV-A (320-400 nm), UV-B (280-320 nm) and UV-C (100-280 nm) (Braga et al., 2015; Coblentz, 1932). The Earth's stratospheric ozone layer absorbs these bands differentially, completely absorbing wavelengths below 290 nm, thus only allowing UVA and UVB to penetrate the stratosphere and reach the planet's surface (Caldwell & Flint, 1997; Williamson et al., 2014).

The change in the intensity and duration of solar ultraviolet radiation (UVR) is most pronounced towards the Earth's poles, particularly in the Southern Hemisphere, being influenced by cloud transmittance, global atmospheric circulation and anthropogenic greenhouse gases (Bais et al., 2015; 2011; Stevenson, 2009). Exposure to high levels of UVR can be damaging, inducing many morphological, physiological and biochemical changes that can occur at many levels of the hierarchical organisation of biology, such as impacting individual cells, the organism itself, and even causing changes in community composition as well as ecosystem functioning and services (Mishra et al., 2017; Paul & Gwynn-Jones, 2003).

While today's public and scientific research communities are more concerned with climate change, particularly in the contexts of increasing atmospheric and oceanic temperatures, changing weather and precipitation patterns, and ocean acidification, it is important to recognize that solar radiation forms a key element of the physical environment for many organisms. Its biological impact in the polar regions has been a

focus of attention particularly in the southern regions, associated with the annual development of the Antarctic 'ozone hole', and studies have examined its impacts on organisms ranging from aquatic microbes to terrestrial plants (Day et al., 2001; Smith et al., 1992; Xiong & Day, 2001). It is often assumed that soil microbial communities are likely to be minimally affected by UVR, due to the physical characteristic of UVB wavelengths not able to penetrate deeper than 100 μm into the soil horizon (Johnson, 2003). However, a growing body of microbiological research on the effects of UVR gives clear evidence that its impacts are more complex and pervasive than widely expected.

Micro-fungi are amongst the simplest form of eukaryotic organisms and have been reported to thrive successfully in many stressful environments, and especially under exposure to UVR (Johnson, 2003; Rangel et al., 2011). Polar micro-fungi are most susceptible to environmental changes as well as the impacts caused by UV elevation due to their biome regime. One of the commonly polar isolated fungi is *Pseudogymnoascus* sp. (previously known as *Geomyces*) that has been widely investigated on difference stress resistance, including temperature (Tajuddin et al., 2018) and salinity (Kochkina et al., 2007) except toward UV radiation. Mechanisms that mitigate the effects of solar radiation in micro-fungi are relatively well established, but the impacts are often species-dependent and modulated by other environmental factors. Certain fungi produce pigment compounds act as sunscreens or antioxidants to minimize the damage generated from UV exposure, while most fungi have conserved deoxyribonucleic acid (DNA) repair mechanisms to mitigate the consequences of UV-induced lesions.

Nucleotide excision repair (NER) and photoreactivation (Phr) are particularly important in repairing UV-induced DNA lesions, cyclobutane pyrimidine dimers

(CPDs) and pyrimidine (6-4) pyrimidone photoproducts (6-4PPs) in fungi, thereby maintaining DNA integrity and assisting cell survival (Bluhm & Dunkle, 2008; Brancini et al., 2016; Chelico et al., 2006; Chelico et al., 2005; de Menezes et al., 2015). However, the physiological impacts of UV-induced DNA damage and the principal DNA repair pathway have not been characterised in polar micro-fungi. Therefore, this study aims to investigate the physiological responses of polar fungi toward UVB radiation in terms of growth, pigmentation and conidia production, as well as the principle DNA repair mechanism used to mitigate the UV-induced DNA damage.

1.2 Research Objectives

1.2.1 General Objective

To investigate the physiological, morphological, and biochemical effects of UVB exposure and DNA damage repair on *Pseudogymnoascus* spp. fungi isolated from polar soils.

1.2.2 Specific Objectives

a) To measure morphological variations occurring under UVB exposure, which includes pigmentation, conidia production and fungal growth based on colony extension rate.

b) To determine the levels of CPD and 6-4PP during DNA damage repair under light and dark conditions following UVB exposure.

c) To investigate the expression of genes involved in Phr and NER during repair under light and dark conditions after UVB exposure.

1.3 Research Questions

a) How does UVB radiation affect the growth rate, pigmentation and conidia production in *Pseudogymnoascus*?

b) Are UVB-induced DNA lesions being repaired faster in the light than in the dark conditions?

c) Which is the principal repair mechanism for UVB-induced DNA lesions in *Pseudogymnoascus* under these conditions?

1.4 Significance of Research

The findings of this study will contribute in the field of soil ecology as well as microbiology considering that UV radiation is an important source of energy and somewhat directly or indirectly influences microbial activities and nutrient cycles. Although the deleterious effects of UV radiation in micro-fungi are well documented (Braga et al., 2015; Paul & Gwynn-Jones, 2003), the protection mechanisms however, are not well elucidated. This study will provide insight into UV-induced DNA damages and the adaptive responses in polar fungi, especially the importance of conserving the Arctic and Antarctic environments, polar soils and its communities from the threats of ozone depletion and climate change. Such baseline information will also help in future studies when dealing with different aspects of environmental stressors and adaptation of microbial communities in soils from different latitudes. Thus, this will lead to better understanding of their ecosystem functions and roles in nutrient cycling and ways to improve the agriculture sector.

CHAPTER 2: LITERATURE REVIEW

2.1 Soil Ecosystem and Its Microorganisms

Major land masses on the Earth are made of soil – the naturally occurring organic material and minerals – that is an essential natural resource for most living organisms. Soil is the most complex habitat in all the substrates that control the soil biodiversity and regulate the activities of the organisms responsible for ecosystem functioning and evolution (Paul, 2014). A single gram of soil may contain billions of microorganisms of thousands of different species that shared interactive ecosystem functioning (Kozdroj & van Elsas, 2001; Paul, 2014). These microorganisms serve as producers and decomposers, regulating the major elements of biological building blocks in the ecosystem's biogeochemical cycles. Among the microorganisms in the soil, fungi play vital roles in the cycling of elements in the biosphere but are often neglected within microbiological and biogeochemical research fields.

2.1.1 Soil Fungi

The kingdom Fungi is the most diverse group of organisms on Earth, comprising more than 100,000 described species and the actual number of fungal species existing globally is expected to be as many as 3 to 5.1 million (Blackwell, 2011; Hawksworth, 2012). Soil is a habitat of high fungal diversity, which is especially highest in soils containing high organic matters. Based on the culture collection at Westerdijk Fungal Biodiversity Institute, the number of species of soil-inhabiting fungi is estimated to be approximately 3,300, including 150 species of nonculturable *Glomerales* (Gams, 2007). Generally, fungi are heterotrophs; unable to perform photosynthesis for chemical energy to be utilized for cellular and physiological processes. Instead, they produce various type of extracellular hydrolytic enzymes (EHEs) to catalyse the degradation of complex compounds into simple products, which are then absorbed for the use of cellular

functions. Thus, they play prominent roles in all ecosystems in nutrient cycling, functioning as decomposers, symbionts of animals and plants and as parasites, with the first two especially important for nutrient cycling (Smith & Read, 2010).

Ascomycetes and basidiomycetes are two major groups of fungi in natural ecosystems responsible for the regulation and redistribution of organic substances in terrestrial soils (Grinhut et al., 2007). Mycorrhizal fungi form intimate symbiotic connections to plants by acting as transporters for nutrient and water uptake, and in return the plant supplies carbohydrates (Bago et al., 2003; Finlay, 2008; Parniske, 2008). This group of fungi contributes significant global phosphate and carbon cycling and indirectly affects the primary productivity in terrestrial ecosystems (Fitter, 2005). Saprotrophic fungi actively decompose organic matter by secreting EHEs and thereby increase soil nutrient availability (Baldrian & Valášková, 2008). A large number of hydrolytic enzymes, including cellulase, hemicellulase protease, amylase, chitinase, pectinases, and gelatinase, have been reported to be secreted by various types of soil fungi (Baldrian & Valášková, 2008; Baldrian et al., 2011; Krishnan et al., 2016; Loperena et al., 2012). These enzymes are especially important for the functional ecosystem in polar soils that already limited by the low nutrient availability as well as the harsh abiotic factors.

2.1.2 Polar Soil Fungi

The Antarctic and Arctic are two regions located at the southernmost and northernmost part of the Earth. Polar soils are particularly interesting due to restricted nutrient and water availability, as well as the extreme cold conditions that push the limits of life, leading to polar soil organisms developing unique physiologies and functional capabilities to survive in the extreme environments.

The environmental similarity of the polar regions has led to observed similarities in community composition, as reported by several studies (Bridge & Newsham, 2009; Timling et al., 2014). Bipolar distribution of fungi was then reported by Cox et al. (2016), who compared fungal community structures in the Antarctic and higher North regions. As much as 50% of the observed bipolar fungi that do not occur in intermediate latitudes belong to the class *Leotiomycetes*, but other classes of fungi in *Ascomycota* and *Basidiomycota* also showed bipolar distributions (Cox et al., 2016). This observation was also supported by Tedersoo et al. (2014), who reported that biodiversity of *Leotiomycetes* increased toward the poles. Thus, these findings suggest that the fungal communities in the polar regions are primarily structured by environmental filtering and might have been well evolved and adapted to survive in these extreme environments.

Colder environments tend to select clades that possess protective cell walls that enable them to evolve and adapt to the particular environmental conditions. Several cold-adaptive responses have been well documented in psychrophilic or psychrotolerant fungi (Robinson, 2001). In the study of the evolution of soil fungi, Treseder et al. (2014) revealed that younger phyla associated with the loss of zoospores tend to reside in soils at higher latitudes and colder temperatures, indicating the importance of the cell wall in adapting to cold environments. Fungal cell walls are composed by β1,3/1,4/1,6 glucan-chitin cross-linked with cellular proteins and metabolites to generate a matrix that provides various functions in adapting to different environmental and biological factors (Latgé, 2007). Most fungal cell walls produce adhesive proteins or biofilms that enable them to adhere to the substratum, which has shown to be essential for infection and mating processes (Liu & Filler, 2011; Nobile et al., 2006; Sharifmoghadam & Valdivieso, 2008; Sheppard, 2011).

The modulation of cell wall components and structure also has been well documented in polar fungi in response to temperature and osmotic stress. For instance, the regulation of fatty acid components in the cell wall has been reported in various *Pseudogymnoascus* species in response to thermal and salinity stress (Konova et al., 2009; Pannkuk et al., 2014; Weinstein et al., 2000). Other cold-adaptive responses in polar fungi have been well discussed in detail by Robinson (2001) including the synthesis of trehalose and cryoprotectant sugars (Weinstein et al., 2000), the production of glycerol and mannitol (Weinstein et al., 1997), and the production of antifreeze proteins (Hoshino et al., 2003). However, the adaptive responses of polar fungi to UV are not well elucidated.

2.1.3 Systematics of *Pseudogymnoascus*

Among the fungal taxa under *Leotiomycetes*,the genus *Pseudogymnoascus* Raillo (1929) [previously known as *Geomyces* Traaen (1914)] is a common cultivable filamentous fungus that can be isolated from different substrates from temperate and polar regions. There are 10 species that have been described morphologically or genetically and that are recognized by the Westerdijk Fungal Biodiversity Institute, namely *P. roseus, P. vinaceus* (Raillo, 1929), *P. bhatti, P. caucasicus* (Samson, 1972), *P. alpinus* (Muller & von Arx, 1982), *P. appendiculatus, P. verrucosus* (Rice & Currah, 2006), *P. destructans*, *P. pannorum*, and *P. carnis* (Minnis & Lindner, 2013). This genus is described by its small, unicellular, oval- or pear-shaped arthroconidia produced from existing branched, tree-like cluster conidiophores. This group of fungi can be psychrotolerant or psychrophilic, as they have been reported to grow optimally from 10 to 20ºC depending on the species, culture substrate, and origin of isolates (Kuthubutheen & Pugh, 1979; Tajuddin et al., 2018).

Pseudogymnoascus fungi are capable of surviving in a harsh environment that is inhospitable to any human. According to the review by Ozerskaya et al. (2009) on permafrost fungi, *Pseudogymnoascus* has broad adaptive potential that might trigger certain protective mechanisms to overcome lower ambient temperature and continue to grow at a very slow rate. It is capable of switching cellular metabolism from glucose to lipid utilization in response temperature decreases and has been reported growing in negative temperature (Finotti et al., 1996; Hughes et al., 2003; Kochkina et al., 2007). *Pseudogymnoascus* has also been found in extreme high temperature and pressure environments around an active volcano on the *Vailulu'u* seamount near Samoa (Connell et al., 2009). *Pseudogymnoascus pannorum* was also reported to have high salt tolerance and capable of growing in three times the salinity of seawater (Kochkina et al., 2007; Poole & Price, 1971). In cold and low-nutrient polar environments, *Pseudogymnoascus* fungi produce different types of enzymes such as lipase, chitinase, urease, amylase, protease and cellulase to consume and metabolize diverse food sources (Fenice et al., 1997; Krishnan et al., 2016). One of the well-known pathogenic *Pseudogymnoascus* fungi is *P. destructans* that infects the nose of bats, causing white nose disease and the collapse of bat populations in temperate regions (Rhodes & Fisher, 2018).

2.2 Species Concepts and Identification of Fungal Species

Evolutionary species in the kingdom of *Fungi* are recognized using three distinct methods, morphology, biology and phylogenetic species identification (Cai et al., 2011; Taylor et al., 2000). Morphological species concept is the determination of species based on morphological structures and biological species concept is based on mating behaviour, whereas, phylogenetic species recognition emphasizes on nucleotide divergence between monophyletic lineages.

The most commonly used species concept for fungi is the morphological species concept. However, this method is often error-prone and frequently classifies genetically similar taxa as separate species. For example, *P. roseus* and *P. vinaceous* were previously classified as a separate species and then were later synonymized as a single species by Samson (1972) based on the pigments of the ascomata. Most recently, *P. pannorum* and *P. destructans* were being re-classified from *Geomyces* based on phylogenetic analysis using five markers of DNA sequence by Minnis and Lindner (2013).

The biological species concept is hardly applicable to fungi that lack of meiospores or those that reproduce asexually. Most species in *Pseudogymnoascsus* are known to reproduce homothallically with the formation of gymnothecia; however, their capacity for sexual reproduction is still unknown. Although the heterothallic system was reported in *P. destructans* isolates with the lack of a high-mobility group (HMG), a transcription factor, box domain (*MAT1-2-1*, unknown function), other *Pseudogymnoascus* species showed homothallic system with the presence of conserved HMG box proteins (*MAT1-2-1* and *MAT1-1-3*) (Palmer et al., 2014), even though no sexual reproduction activities were observed in laboratory conditions. Thus, it is impossible to define a species in *Pseudogymnoascus* based on the biological species concept alone for identification.

The identification of species under the phylogenetic species concept relies on the phylogenetic analysis of the DNA sequence of the marker genes or genomes. It is believed that the divergence of DNA sequences occurs throughout evolution before any observable changes in physiology and morphological characters. With the increase of recognised DNA markers and the ease of DNA sequencing, the phylogenetic species concept has been applied to reveal and identify numerous species complexes in

Neurospora crassa (Dettman et al., 2003), *Saccharomyces paradoxus* (Kuehne et al., 2007), and *Fusarium graminearum* (O'Donnell, 2000).

2.2.1 Identification and Marker Genes in Fungi

According to Hebert et al. (2003) "sole prospect for a sustainable identification capability lies in the construction of systems that employ DNA sequences as taxon 'barcodes' ". The most commonly used DNA barcoding marker for animals and some protists is mitochondrial cytochrome oxidase I (*COI*) (Aziz et al., 2016; Kosakyan et al., 2015). In fungi, *COI* functions equitable well with promising intraspecific and interspecific variability in *Penicillium* (Seifert et al., 2007) and *Cladonia* (Pino-Bodas et al., 2013); however, problems in amplifying the *COI* region in other fungi have been reported, including multiple copies and variable numbers of introns, which have proved *COI* inadequate for species-level identification in certain groups within *Ascomycota* (Geiser et al., 2007; Gilmore et al., 2009) and *Basidiomycota* (Vialle et al., 2009). Thus, an alternative marker in the nuclear ribosomal, internal transcribed spacer (ITS) region has been proposed to be used as DNA barcode in the fungi kingdom (Schoch et al., 2012).

Figure 2.1: Nuclear rDNA regions and its partitions in fungal genomic DNA.

Nuclear ribosomal deoxyribonucleic acid (rDNA) regions have been extensively used across many organisms for phylogenetic studies in the last two decades, but they are reported to be too conserved for most groups of fungi (Begerow et al., 2010). The eukaryotic rDNA consists of 18S (SSU), 5.8S and 28S (LSU) rDNA, and the larger

units are transcribed as a single unit by RNA polymerase I (Figure 2.1). The two spacers in between, as well as 5.8S, are referred to the ITS. The ITS region is the most frequently sequenced marker for fungal strain identification. It was recently suggested as the universal DNA barcode marker for fungi by Schoch et al. (2012) after six DNA markers including ITS, LSU, SSU, DNA-directed RNA polymerase II largest (*RPB1*) and second largest (*RPB2*) subunit, and minichromosome maintenance complex component 7 (*MCM7*) were evaluated. Intraspecific as well as intra-individual variability of ITS region have been reported in fungal sequences (Lindner & Banik, 2011; Smith et al., 2007). In comparisons of the performance between three nuclear ribosomal regions (ITS, LSU and SSU), ITS has clearly defined barcode gap and is generally superior to LSU and SSU in species discrimination (Schoch et al., 2012). Barcoding gap is the a threshold of difference between the average of inter- and intra-specific genetic distance within a group of organisms that enable the discovery of new species (Čandek & Kuntner, 2015) (Figure 2.2). However, additional markers are required for taxa with low ITS inter- or intra-specific variability such as in *Pseudogymnoascus* (Lorch et al., 2013), *Aspergillus* (Geiser et al., 2007), *Cladosporium* (Schubert et al., 2007), *Penicillium* (Skouboe et al., 1999), and *Fusarium* (O'Donnell & Cigelnik, 1997).

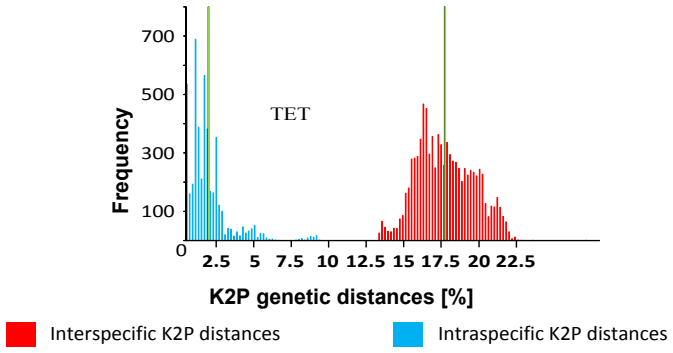

Figure 2.2: Example of barcoding gap graph derived from Čandek and Kuntner (2015). K2P and TET indicate Kimura 2-parameter model and the taxon Tetragnathidae, respectively.

Protein-coding genes are popular among the mycologists and have been widely used as *de facto* barcodes in phylogenetic analyses and species identification in several groups of fungi, including the utilization of *MCM7*. It has been reported to be more phylogenetically informative to resolve lower as well as higher level phylogenetic analyses across *Ascomycota*, especially in combination with the LSU sequences (Raja et al., 2011; Schmitt et al., 2009). In addition, *RPB2* is currently suggested as another viable alternative molecular marker for fungi due to its promising inter- and intraspecific variation, and high taxonomic sensitivity in fungal community studies (Schoch et al., 2012; Větrovský et al., 2016). *RPB2* remains not as commonly used as ITS, as it has low representation in GenBank and certain fungal species have been reported to contain intron(s) or cannot be amplified using universal primers (Schoch et al., 2012).

The utilization of multigene phylogeny in species identification can resolve the uncertainty of phylogenetic relationships obtained using in a single-gene approach. Tretter et al. (2013); (2014) and James et al. (2006) have reconstructed the evolution of fungi using multi-gene phylogenetic analyses. The multigene approach also has been used frequently to infer cryptic diversification (Bischoff et al., 2009; Rehner & Buckley, 2005) and to identify new species in fungi (Amalfi et al., 2010; Gilgado et al., 2005; Zhao et al., 2011). Thus, the application of multiple genes in phylogenetic analyses further strengthens the support of phylogenetic relationships in fungi.

2.2.2 The Phylogenetic Relationships of Species in *Pseudogymnoascus*

In recent decades, there has been development in the taxonomy of *Geomyces* and its allies following the re-evaluations and revisions of this taxa by Lorch et al. (2013) and Minnis and Lindner (2013). Lorch et al. (2013) reported that there were approximately

17 discrete species of *Geomyces* based on ITS and partial intergenic spacer (IGS) regions that could be accepted under a one name system of classification (Norvell, 2011). Lorch et al. (2013) also reported low genetic variation in the ITS region between species which would obscure the identification in *Geomyces*, a fact that is also supported by Gargas et al. (2009), Johnson et al. (2013) and Flieger et al. (2016). Minnis and Lindner (2013) then reclassified *P. destructans* and *P. pannorum* (previously classified under *Geomyces*) using five DNA markers, ITS, LSU, *MCM7*, *RBP2* and *TEF1*. The multi-gene phylogenetic tree constructed also proposed 13 clades of *Pseudogymnoacsus* (Clade A-M), in which nine were undefined species. Among the five gene sequences used by Minnis and Lindner (2013), *MCM7* showed the most parsimony-informative base pairs ratio, followed by *RBP2, TEF1*, ITS region and LSU, having the least. Similarly, Johnson et al. (2013) also suggested *MCM7* to be used as the genetic marker for *Pseudogymnoascus,* although the amplification process can be challenging in certain species. These sequences and DNA markers have been subsequently used for phylogenetic analyses in studies that involve *Pseudogymnoascus* and related species (Reynolds & Barton, 2014; Wilson et al., 2017).

Zhang et al. (2016) and Forsythe and Xu (2017) recently sequenced the complete mitochondrial genome of *P. destructans* and *P. pannorum* and and used 13 protein-coding genes for multi-gene phylogenetic analyses. The findings revealed that the variations in mitochondrial sequence provide sufficient information to infer *Pseudogymnoascus* among the *Leotiomycetes*, but the identification at species-level was unresolved. Phylogenomic analysis using 125 genes was recently performed by Reynolds et al. (2016), and the results demonstrated that *P. destructans* is closely related to *P. verrucosus* complex, confirming the placement from Minnis and Lindner (2013).

2.3 Variation in Climatic UV Radiation Across Latitudes

Solar UV radiation is conventionally divided into three internal wavelengths: UVA (315-400nm), UVB (280-315nm) and UVC (100-280nm) (Coblentz, 1932). The stratospheric ozone layer plays a major role in regulating the UV radiation reaching on the Earth by drastically reducing the penetration of radiation of wavelengths shorter than 320nm and completely excluding those below 290nm (Caldwell & Flint, 1997; Williamson et al., 2014). UVA radiation passes through the stratospheric ozone layer with slight debilitation contributing approximately 95% of the UV spectrum reaching the Earth's surface, while UVB is responsible for the remaining 5% (Christiaens et al., 2011).

Solar UV radiation varies considerably over the Earth's surface and the UVR intensity reduces toward the polar regions (McKenzie et al., 2007). A recent study conducted by Beckmann et al. (2014) using Global UVB Surfaces (glUV) showed a similar pattern applying the ozone monitoring instrument dataset from the year 2004 to 2013. (Figure 2.3). In contrast, the intra-annual UVB seasonality is relatively lowest near the equatorial zone and highest in mid-latitudes and polar region (Figure 2.4). This indicates that the organisms that inhabit the mid-latitudes and polar regions experience high variability of UVB radiation throughout the year following seasons.

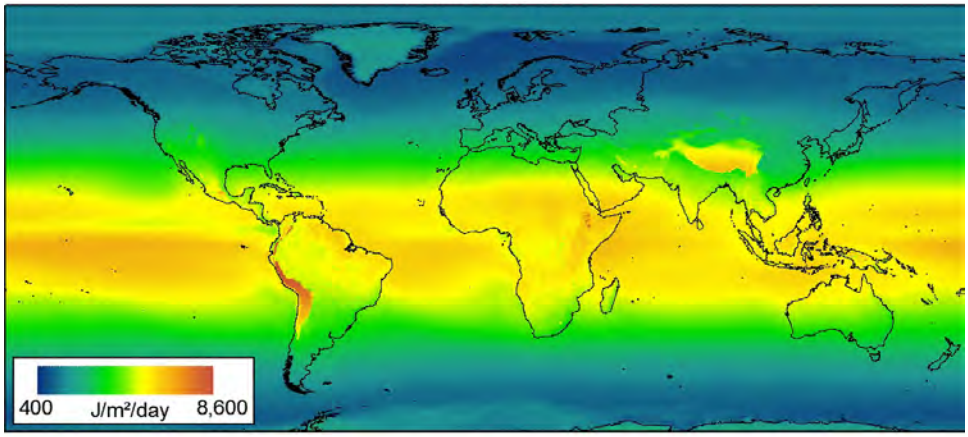

Figure 2.3: Annual mean UVB radiation illustrated using glUV dataset. Retrieved from Beckmann et al. (2014).

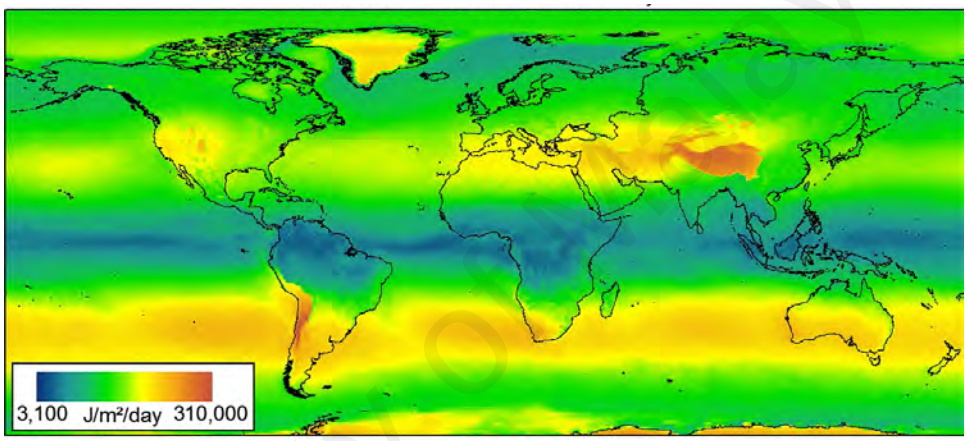

Figure 2.4: Annual UVB seasonality illustrated using glUV dataset. Retrieved from Beckmann et al. (2014).

During the summer, UVB radiation in the Northern and Southern polar circles (July and January, respectively) reaches the highest among the climate seasons according to the glUV illustration on two monthly mean UVB irradiances (Figure 2.5). In addition, the range of UVB values in the Southern Hemisphere is generally higher than the Northern Hemisphere according to the same illustration. According to the 2010 report on Scientific Assessment of Ozone Depletion, the high UVB intensity increment in the Southern Hemisphere is associated with the ozone hole, which also consistently reported by Langematz (2019). An updated time series of UVB radiation at the Earth's surface showed UVB irradiation increased by more than 20% for the past 20 years before the year 2000 (Figure 2.6) (Williamson et al., 2014). The increment of UVB

intensity in the Southern hemisphere suggests the inhabitants have encountered an increasing dosage of UVB for the past 20 years and might have adopted resistance toward UVB radiation.

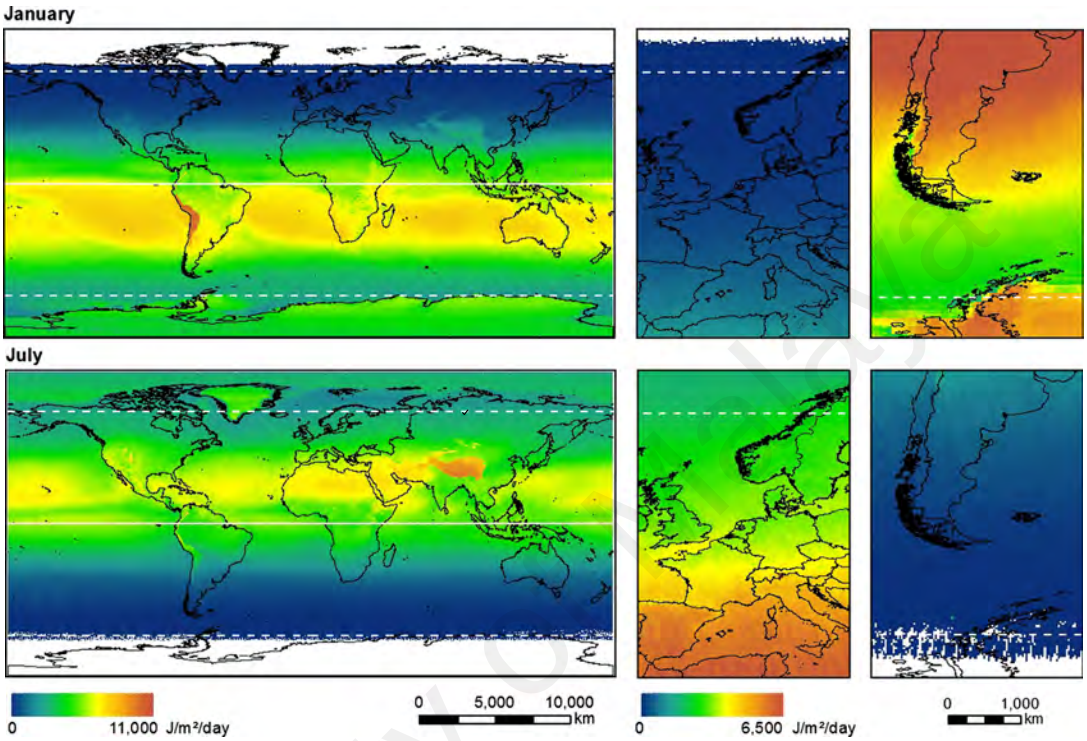

Figure 2.5: Two monthly mean UVB illustrated using glUV datasets. Retrieved from Beckmann et al. (2014).

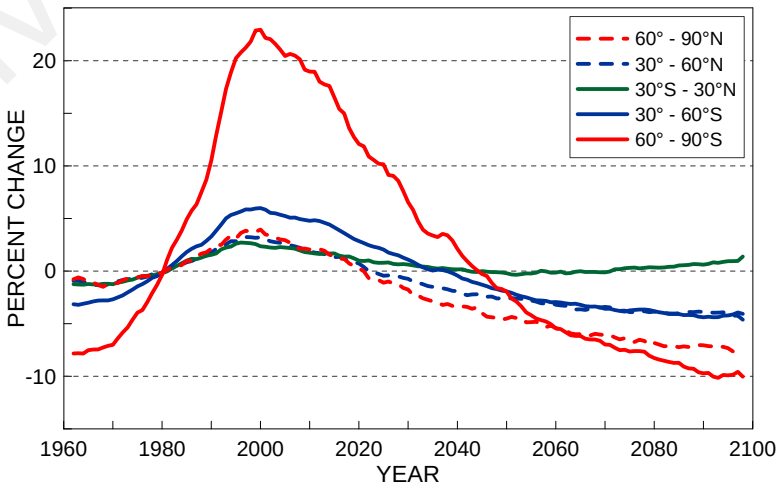

Figure 2.6: Observed and projected changes in annual mean erythemal clear-sky UVB radiation at Earth's surface across latitudes.

The loss of ozone in both the Arctic and the Antarctic resulted in an increase in UV radiation at the end of winter/early spring (Madronich et al., 1998; McKenzie et al., 2007). Even though the production chlorofluorocarbon and other ozone-depleting substances (ODS) has been drastically reduced by the implementation of the Montreal Protocol, the long-lived halogenated source gases in the atmosphere can substantially affect the ozone layer for several decades (WMO, 2011). The combination of ODS-derived chlorine and the change in circulation patterns in the ozone layer can delay the seasonal transport of ozone from the tropics and cause the major ozone depletion event in both the Arctic and the Antarctic (Manney et al., 2011). Such patterns are predicted to markedly influence the amount of UVB radiation received at the Earth's surface.

There are many factors that influence solar radiation reaching on the Earth surface including changes in total ozone, aerosols, clouds, locations, surface reflectivity (albedo), solar activity, gaseous pollutants in the troposphere and temperature in the stratosphere (Bais et al., 2015; WMO, 2011). The changes of ice and snow coverage in the polar regions are influenced by climate change effects. Ice and snow coverage area reflect UV radiation back to the atmosphere, and this reflection is largely enhanced by the redirection downward through the scattering of air molecules and cloud, a phenomenon known as albedo. A decrease of ice and snow coverage in the polar region resulting of the acceleration of surface warming are predicted to cause ice and snow to be disappeared for the next decades (Comiso et al., 2008; Overland et al., 2008). Thus, the organisms living below the ice will expose to higher UV radiation.

The stratospheric ozone layer allows the survival of organisms by debilitating the level of solar radiation reaching the Earth's surface, which completely eliminating solar UVC and greatly reduce UVB radiation. However, the stratospheric ozone layer itself is not sufficient to lower the UV radiation to non-lethal levels. All living organisms

protect themselves from solar UVA and UVB radiation through a combination of UV-absorbing pigments and employ variety DNA repair mechanisms designed to remove the damage induced by UV radiation (Britt, 2004).

2.4 Stress and Physiological Responses of Fungi towards UVR

Response and adaptive mechanisms that mitigate the effects of stress in micro-fungi are relatively widely investigated, but the impacts are often species-dependent and modulated by other environmental factors such as nutrient availability, moisture, and other environmental parameters (Gasch, 2003; Rangel, 2011). Many fungi show photomorphogenic responses to solar UVR exposure, particularly to UVA or near UV wavelengths (300-400 nm), with induction of sporulation, differentiation of the fruiting body, and the synthesis of photoprotective pigments and various secondary metabolites (Alves et al., 1984; Avalos & Estrada, 2010; Kurahashi et al., 2015; Mooney & Yager, 1990; Olmedo et al., 2013; Schumacher, 2017; Zhang et al., 2009). Deleterious effects of UVR are also apparent, including spore inactivation, delayed spore germination, reduced mycelial extension rate, and changing patterns of nitrogen and carbon uptake and deposition, as shown in various groups of fungi, including soil fungi (Duguay & Klironomos, 2000; Hughes et al., 2003), entomopathogenic fungi (Braga et al., 2002; Brancini et al., 2018; Brancini et al., 2016), plant pathogenic fungi (Cheng et al., 2014; de Menezes et al., 2015), and litter and phylloplane fungi (Gunasekera et al., 1997; Moody et al., 1999).

Temperature stress responses has been widely established in the fungi and many showed similar regulatory responses toward the stresses induced by UV radiation, including the regulation of heat shock proteins as well as the genes involved in carotenoid synthesis (Rodríguez-Romero & Corrochano, 2004; Rodríguez-Romero &

Corrochano, 2006). Thus, it is believed that these two stressor share similar regulatory pathways to mitigate the the stress induced in the natural environments.

2.4.1 Fungal Growth Under Light and UVR

Visible light is an important source of energy for fungal species. Many show photomorphogenic responses toward light and express photoresponsive proteins that are highly conserved across different species. Most fungi appear to be photoresponsive to light at the blue to near-UVA wavelength (~400-495 nm) according to Fuller et al. (2015), but the inhibitory effects of light also have been widely reported across many fungal species. Canessa et al. (2013) demonstrated growth retardation in *Botrytis cinerea* growing under white light (400-720 nm), and suggested the observation might be due to oxidative stress generated by light. Similarly, slight reduction in mycelial extension rate was also demonstrated in *Aspergillus fumigatus* (Fuller et al., 2013), *Cordyceps millitaris* (Yang & Dong, 2014), *F. graminearum* (Kim et al., 2014a), and *Colletotrichum acutatum* (Yu et al., 2013). However, Fuller et al. (2015) suggest that the influence of light on fungal growth can be a photoreceptor-mediated process, rather than a consequence of reactive oxygen species (ROS) generated by light.

In comparisons between different culture media, Leach (1971) reported that the growth of *Verticillium alboatrum* was stimulated by near-UV light during the log phase of growth in liquid culture, but the same light source showed inhibitory effects on fungal growth on plates. The opposite observation was reported in *Pellicularia filamentosa* under light illumination, whereby growth inhibition was observed in broth but enhanced in plate culture (Durbin, 1959). Thus, this suggests that fungal growth response toward UV and light depends on specie and the availability of moisture.

Although growth inhibition under light conditions has been well documented, there are fewer studies on the growth response in fungi toward UV radiation. UVB radiation for four hours completely inhibited the radial growth rate of *Penicillium chrysogenum* (formerly *Penicillium notatum*) and to a certain extent in *Aspergillus flavus* (Osman et al., 1989). Moody et al. (1999) investigated the responses of 12 litter and seven phylloplane fungal species to UVB radiation. Their findings revealed that *A. fumigatus* and four *Penicillium* spp. were sensitive to UVB radiation (1.7 kJ m^{-2} d^{-1}) with significant mean reduction of 20% on mycelial extension rate, while other fungi showed a small mean reduction rate of 1.3%. A similar observation was reported by Hughes et al. (2003) on Antarctic terrestrial fungi, which UVB radiation was reported to cause greater reductions on the extension rates of surface mycelial compared to submerged hyphae in all terrestrial strains tested, with *P. pannorum* demonstrating the highest UVB sensitivity. These observations suggest that fungi might experience significant impacts from UV radiation in the natural environment.

2.4.2 UV Induced Pigmentation in Fungi

A series of UV-protective mechanisms have evolved in fungi in response to the selective pressures imposed by solar radiation. Melanin, carotenoids and mycosporines are the three major pigments that are well documented in fungi and act as sunscreens or antioxidants to minimize the damage generated from UV exposure (Almeida-Paes et al., 2012b; Avalos & Limón, 2015; Belozerskaya et al., 2017; Volkmann et al., 2003).

Different melanins are able to absorb a wide range of radiation wavelengths including gamma ray, X-ray and UV radiation. This enables them to be excellent photoprotectants in many fungi (Dadachova & Casadevall, 2008; Huijser et al., 2011; Schweitzer et al., 2009). Certain melanotic fungi including *Cryptococcus neoformans*,

Exophiala (*Wangiella*) *dermatitidis*, *Alternaria alternata* and *Aspergilus versicolor* show advanced adaptation toward radiation by growing toward radiation sources, utilizing the energy for growth and metabolic changes (Braghini et al., 2009; Bryan et al., 2011; Dadachova et al., 2007; Dighton et al., 2008; Shuryak et al., 2014; Zhdanova et al., 2004). Under UV exposure, two eumelanin building blocks, 5,6-dihydroxyindole (DHI) and 5,6-dihydroxyindole-2-carboxylic acid (DHICA), have been reported to absorb and transduce photon energy into other forms of energy, reducing damage induced by UVR (Belozerskaya et al., 2017; Huijser et al., 2011; Meredith & Sarna, 2006; Riesz et al., 2006). Exposure to UVR in the melanotic fungus, *C. neoformans*, resulted in decreased adenine triphosphate (ATP) amount, which could be due to oxidation of nicotinamide adenine dinucleotide (NADH) by irradiated melanin or the utilization of available ATP for UV-induced DNA repair and in cellular metabolism and growth (Bryan et al., 2011; Dadachova et al., 2007).

Sporothrix complex (*S. schenckii, S. brasiliensis* and *S. globosa*) fungi are able to produce pyomelanin in the presence of L-tyrosine during the stationary phase, and this has been shown to increase the tolerance of *Sporothrix* cells toward UVR, but only during the first 30 seconds of exposure (Almeida-Paes et al., 2012a). Scanning electron microscopy (SEM) also showed that the pyomelanin covers the surface of *Sporothrix* cells and forms a protective layer against UVR, rather than polymerizing on the cell wall as observed in other groups of fungi (Almeida-Paes et al., 2012a). The deposition of melanin in the intra-colonial/extracellular polymeric substances (EPS) matrix was also reported in *Coniosporium* sp., developing an intra-colonial protective milieu against UV radiation, heat, desiccation and ROS (Gorbushina et al., 2003).

Most carotenoids mainly absorb in the visible spectrum of solar radiation and appear to protect the fungal cells primarily through quenching of ROS rather than against UV-induced DNA damage through UV absorption (Irazusta et al., 2013; Moliné et al., 2010b; Yan et al., 2011). Upon exposure to UVR, carotenoid compounds were accumulated in cells of various fungal taxa including *W. dermatitidis, Ustilago violacea, Sporidiobolus salmonicolor, Rhodotorula minuta, Rh. pinicola,* and *Cystofilobasidium capitatum* (Geis & Szaniszlo, 1984; Libkind et al., 2004; Moliné et al., 2010b; Will & Scovel, 1989). However, in other fungal species, such as *N. crassa* and *Sporobolomyces ruberrimus,* the accumulation of carotenoids was not induced by UVR (Blanc et al., 1976; Moliné et al., 2010b). Such differences could be due to the differing experimental irradiation spectra, as the types of ROS and resulting damage are dependent upon the wavelength experienced. A decrease in the carotenoid Raman signal under UVB radiation was also demonstrated in the Antarctic fungus, *Arthrobotr ferox,* interpreted as either the result of dissolution in the lipid matrix to maintain membrane fluidity, or photo-destruction of the pigments (Arcangeli & Cannistraro, 2000). Although differences in carotenoid accumulation are plainly observed across fungal species and treatments, the increased carotenoid content certainly improves the resistance and survival rate of cells exposed to UVR (Geis & Szaniszlo, 1984; Gutiérrez Pozo et al., 2012; Moliné et al., 2010b; Will & Scovel, 1989).

Many micro-fungi appear to produce mycosporine (MYC), with mycosporine-glutaminol-glucoside and mycosporine-glutamicol-glucoside being reported in most studied fungi (Table 2.1). The synthesis of mycosporine-like amino acids (MAA) was highly induced upon irradiation of photosynthetically active radiation (PAR) and UV radiation in various species of *Rhodoturola* and *Cryptococcus* (Libkind et al., 2004; Moliné et al., 2010a). A similar observation was also reported in *Xanthophyllomyces dendrorhous* under UVA radiation (Libkind et al., 2011), suggesting a photoprotective function. The absorption maxima of MYCs at a wavelength maximum close to 310 nm gives them potential as UV-protectant compounds, especially against damage induced by UVB radiation (Libkind et al., 2011; Moliné et al., 2010a). CPD accumulation is negatively correlated with MYC accumulation, and the high coefficient of determination between MYC concentration and survival suggests other protective mechanisms could be involved, presumably to guard against ROS (Moliné et al., 2010a). MYCs protect the cells primarily through the dissipation of photon energy from radiation without generating ROS (Conde et al., 2004). Also, MYCs have been demonstrated to possess antioxidant activity through the quenching of singlet oxygen, and their ability in quenching reactions is comparable to that of the MAA, mycosporine-glycine (Moliné et al., 2010a; Suh et al., 2003).

Table 2.1: List of fungal species with identified mycosporine compounds including; Mycosporine-Allanine (MYC_a), Mycosporine-glutaminol (MG_n), Mycosporine-glutaminol-glucoside (MGnG), Mycosporin-glutamicol (MG_c) and Mycosporine-glutamicol-glucoside (MG_cG). (+) and (-) indicate the presence and the absence of the compound, respectively.

Species	MYC_a	MG_n	MG_nG	MG_c	MG_cG	Reference
Ascochyta fabae	-	-	(+)	-	-	Pittet et al. (1983)
Ascochyta pisi	-	-	(+)	-	-	Bouillant et al. (1981)
Aureobasidium pullans	-	-	(+)	-	(+)	Kogej et al. (2006)
Aureobasidium sp.	-	-	(+)	-	(-)	Kogej et al. (2006)
Botryosphaeria-like fungi	(-)	(+)	(+)	(+)	(+)	Volkmann and Gorbushina (2006), Volkmann et al. (2003)
Cladophialophora-like fungi	(-)	(-,+)	(-)	(-)	(-)	Volkmann and Gorbushina (2006), Volkmann et al. (2003)
Cladosporium cladosporioides	-	-	(+)	-	(-)	Kogej et al. (2006)
Cladosporium herbarum	-	-	(+)	-	-	Bouillant et al. (1981)
Cladosporium sphaerospermum	-	-	(+)	-	(-)	Kogej et al. (2006)
Collectotrichum gramicola	(+)	-	-	-	-	Leite and Nicholson (1992)
Coniosporium apollinis	(-)	(-)	(+)	(-)	(-)	Gorbushina et al. (2003), Volkmann and Gorbushina (2006), Volkmann et al. (2003)
Coniosporium-like fungi	(-)	(-)	(+)	(+)	(+)	Volkmann and Gorbushina (2006), Volkmann et al. (2003)
Coniosporium perforans	(-)	(+)	(+)	(+)	(+)	Volkmann and Gorbushina (2006)
Coniosporium sp.	-	(-,+)	(+)	(-,+)	(+)	Gorbushina et al. (2003), Volkmann et al. (2003)
Coniosporium uncinatum	(-)	(+)	(+)	(+)	(+)	Gorbushina et al. (2003), Volkmann and Gorbushina (2006)
Cryptococcus steppossus	-	-	(+)	-	(-)	Moliné et al. (2010a)
Cryptococcus laurentii	-	-	(+)	-	-	Libkind et al. (2006) (2004)
Cryptococcus liquefaciens	-	-	(+)	-	(+)	Kogej et al. (2006)
Cryptococcus sp.	-	-	(+)	-	-	Libkind et al. (2005)
Dioszegia hungarica	-	-	(+)	-	-	Libkind et al. (2005)
Hortaea werneckii	(-)	(+)	(+)	(-)	(+)	Kogej et al. (2006; 2007), Volkmann and Gorbushina (2006)
Knufia cryptophialidica	(-)	(-)	(+)	(-)	(+)	Volkmann and Gorbushina (2006)
Phaeococcus chersonesus	-	(+)	(+)	(+)	(+)	Volkmann and Gorbushina (2006)
Phaeotheca fissurella	-	-	(+)	-	-	Gorbushina et al. (2003)
Phaeotheca triangularis	-	(-)	(+)	(-)	(-,+)	Kogej et al. (2006), Volkmann and Gorbushina (2006)
Pyronema omphalodes	-	-	(+)	-	-	Bernillon et al. (1984)
Rhodotorula laryngis	-	-	(+)	-	-	(Gorbushina et al., 2003), (Libkind et al., 2005)
Rhodotorula minuta	-	-	(+)	-	(-)	Libkind et al. (2006; 2004; 2005)
Rhodotorula pinicola	-	-	(+)	-	(-)	Libkind et al. (2006; 2004; 2005)
Rhodotorula slooffiae	-	-	(+)	-	-	Gorbushina et al. (2003), Libkind et al. (2005)
Rhodotorula sp.	-	-	(+)	-	(-)	Libkind et al. (2004)
Rhodotorula sp.	-	-	(+)	-	-	Libkind et al. (2005)
Sarcinomyces petricola	(-)	(+)	(+)	(-,+)	(-,+)	Volkmann and Gorbushina (2006), Volkmann et al. (2003)
Sarcinomyces sp.	(-)	(-)	(-,+)	(-)	(-)	Gorbushina et al. (2003),Volkmann and Gorbushina (2006)
Septoria nodorum	-	-	(+)	-	-	Bouillant et al. (1981)
Trichothecium roseum	-	(+)	-	-	-	Favre-Bonvin et al. (1987)
Trimmatostroma salinum	(-)	(+)	(+)	(-)	(+)	Kogej et al. (2006), Volkmann and Gorbushina (2006)
Xanthophyllomyces dendrorhous	-	-	(+)	-	-	Libkind et al. (2011)

2.4.3 Influence of Light and UV on Asexual Reproduction

Light regulates several aspects of biology in many organisms and it is especially important in the regulation of asexual reproduction activities in fungi. Sporulation is highly influenced by the wavelength of light the fungi are exposed to. As demonstrated by Vakalounakis and Christias (1981), sporulation in *Alternaria cichorii* is depending on the specific light wavelength, whereby near ultraviolet radiation (< 340 nm) induced sporulation and blue light inhibited. The results are in agreement with similar observations in *Bipolaris oryzae* (Honda & Yunoki, 1980), *Alternaria tomato* (Kumagai & Oda, 1969, 1973), *B. cinerea* (Tan, 1974, 1975; Tan & Epton, 1974), *Peronospora belbahrii* (Cohen et al., 2013) and *Peronospora effuse* (Choudhury & McRoberts, 2017). However, sporulation has been shown to be inhibited by both blue and white light in *Plasmopara viticola*, in which prolonged darkness is required to promote sporangium formation (Rumbolz et al., 2002). In another case, blue light (max 370 nm) increased sporulation in *Verticilium agaricinum* but inhibited growth at the same time (Osman & Valadon, 1979).

Reuveni et al. (1989) demonstrated the importance of the ratio of transmitted blue/UV light on the formation of spores in *B. cinerea*. The promotion of spore production can be achieved by lowering this ratio, thus suggesting the dependency on the light ratio for sporulation rather than solely the type of light. Besides blue/UV light ratio, the ratio of light/dark also has been reported to regulate spore production activities in fungi. *Phytophthora infestans* failed to produce conidia in continuous light conditions (Cohen et al., 1975). However, certain fungi are capable to reproduce asexually in a non-circadian dependent manner including *Peronospora tabacina* (Cohen, 1976) and *Magnaporthe oryzae* (Lee et al., 2006).

Other heat tolerance-related genes also have been frequently reported to be involved in the regulation of conidiation. Thompson et al. (2008) demonstrated that the disruption of *HSF1* and *HSF2* could affect the formation of asexual development in *N. crassa*. A similar observation also was demonstrated following *HSF1* gene disruption in *Coniothyrium minitans* (Hamid et al., 2013). A study on heat-shock protein 90 (HSP90) in *A. fumigatus* demonstrated that the disruption of *HSP90* led to downregulation of conidiation-specific transcription factors, including *BRLA, WETA* and *ABAA* (Lamoth et al., 2012). Thus, this suggests that there are similar signalling responses between heat stress and conidia production.

2.5 UV induced DNA damage and Its Repair Mechanisms

DNA damage is distinctly different from mutations; it is the modification of chemical structure of DNA generated by endogenous cellular processes or by exogenous factors derived from external environments. In contrast, mutation is the permanent alteration of DNA sequence as the results of unrepaired DNA damage or errors in replication. The two primary mutagenic UV-induced DNA lesions are cyclobutane pyrimidine dimers (CPDs) and pyrimidine 6-4 pyrimidone photoproducts (6-4 PP), and their Dewar isomers (Cadet et al., 2014; Douki & Cadet, 2014). Pyrimidine dimers are the most significant types of lesions compare to other UV-induced DNA lesions. About 75% of UV-induced damaged bases are made up of CPDs while 6-4 PP making up the rest with some degree of oxidatively damaged, DNA strand breaks and other photoproducts (Bowman et al., 1994; Britt, 2004; Pfeifer, 1997; Pfeifer et al., 2005). CPDs and 6-4 PP are majorly caused by direct UVB and UVC radiation absorption by DNA, however, UVC is completely attenuated in the ozone layer with small amount (1%) of UVB reaching the Earth's surfaces (Chelico & Khachatourians, 2008; Nascimento et al., 2010; Rastogi et al., 2010; Schuch et al., 2009).

Types of UVR based damage is determined by the nature and position of the nucleotides and the flexibility of the DNA strand. CPDs arise from a cycloaddition reaction between C5-C6 double bonds of two neighbouring bases in single-stranded DNA (ssDNA) (Becker & Wang, 1989; Cadet et al., 2012). 6-4PPs are formed by a noncyclic bond between the C5-C6 double bond of the 5'-end base and the C5 carbonyl group of a 3'end pyrimidine via spontaneous rearrangement of oxetane or azetidine (Cadet et al., 2012; Friedberg et al., 2005; Pattison & Davies, 2006). The 6-4PPs are promptly converted into their Dewar valence isomers upon exposing to UVB or UVB radiation that may further reverse to the formation of 6-4PPs when exposing to short wavelength UVR (Courdavault et al., 2005; Taylor et al., 1990). Figure 2.7 shows the summary of UVR-induced CPD and 6-4PP formation.

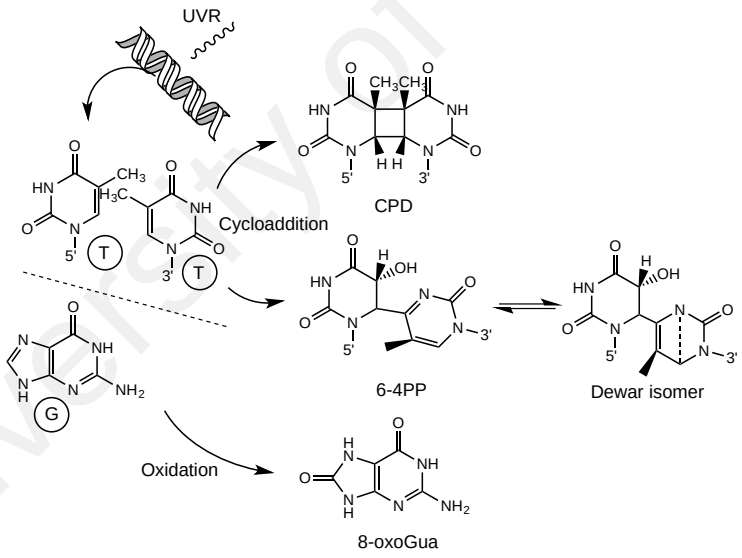

Figure 2.7: Pathways of UVR-induced CPD, 6-4PPs, and their Dewar isomers.

Of the two major photoproducts induced by UVR, CPDs are the most quantified photoproducts in fungi as they are formed in a relatively higher amount compared to 6-4PPs and there are many established standard protocols available to identify them. In between these two types of DNA damage, CPDs has been reported making up about

75% of the total UV-mediated DNA damage products, meanwhile the rest of the amount was 6-4PPs (Britt, 2004). UVB dose-related induction of CPD formation has been reported in the conidia of *A. fumigatus, A. nidulans* and *Metarhizium acridum* (Nascimento et al., 2010). The levels of UV-induced CPDs differed among species, with *A. fumigatus* having the most CPD formation followed by *A. nidulans* and *M. acridum*. In contrast, experimental exposure to UVC induced a saturated amount of CPD in *Beauveria bassiana* conidiospores over 1.5 h of radiation exposure (Chelico et al., 2005). This level of CPD formation was shown to impair the ability of *B. bassiana* to repair the damaged DNA *in vivo*. Thus, demonstrated the ability of many microbial cells to deploy photoprotective pigments to reduce the amount of UVR reaching cellular DNA.

Eukaryotes employ various DNA repair pathways to ensure the genome remains functionally intact. In general, fungi are similar to most eukaryotes in that they harbour two critically important pathways that repair CPD and 6-4PP, namely nucleotide excision repair (NER) and photoreactivation (Phr). NER is the most versatile and flexible repair mechanism that can repair CPD and is required to repair 6-4PPs in organisms that lack 6-4PP-specific repair systems. NER repairs by *de novo* synthesis involving multi-enzyme complexes that execute DNA repairing in an orderly manner of recognition, excision, synthesis and ligation (Dijk et al., 2014). Phr, in contrast, involves a direct reversal of the dimers using photolyases, which are light-dependent enzymes that utilize photon energy to split the covalent bond(s) between two bases (Faraji & Dreuw, 2017; Sancar, 1994). The repairing of 6-4PP has been reported to repair faster than CPDs, however, the majority amount of both types of DNA damage can be eliminated within hours, or in certain cases minutes upon promotion (Rastogi et al., 2010).

In most studies, the functional roles of NER and Phr in DNA repair in fungi were evaluated based on physiological assessment. Chelico et al. (2006) attempted to characterize the modes of repair in entomopathogenic fungi (EPF) by comparing post-UV spore germination under light and dark conditions, which are assumed to induce Phr and NER respectively. The findings of the study suggested that most EPF depend more on Phr than NER due to the greater survival rate of spores incubated in light conditions after irradiation by UVC. Alejandre-Durán et al. (2003) and Braga et al. (2002) also derived conclusions based on the same approach using *Fusarium oxysporum* f. sp. *lycopersici*, and *Verticillium lecanii* and *Aphanocladium album* respectively. Berrocal-Tito et al. (2007) investigated photoreactivation ability in *Trichoderma atroviride* by *in vivo PHR1* gene deletion and demonstrated that the Δ*PHR1* strain showed completely lost photoreactivation ability with a significant germination rate reduction after UVC exposure.

In-depth investigations using genetic manipulation techniques have shed more light on the UV-induced DNA repair in fungi. The disruption of genes in the cryptochrome/ photolyase gene family revealed that the expression of photolyase genes influences the expression of genes involved in NER as well in *Cercospora zeae-maydis* (Bluhm & Dunkle, 2008), *M. robertsii* (Fang & Leger, 2012) and *Trichoderma reesei* (Guzmán-Moreno et al., 2014). These observations suggest that NER activity could be enhanced by the expression of Phr genes during incubation in light conditions and improve the survival rate of the conidia, but the mechanism by which cryptochrome/ photolyase family proteins regulate NER remains poorly understood. Thus, experiments solely based on the physiological data is insufficient to derive conclusions for determining the mode of DNA repair in fungi.

In vitro insertion of a transposon containing the fungal photolyase gene *PHR1* in *Escherichia coli* bacteria have been used extensively to study photorepair ability in fungi. Berrocal-Tito et al. (2007) reported that *E. coli* harbouring *PHR1* from *T. atriviride* showed significant survival rates following UVC irradiation compared to controls when incubated in light conditions. Similar approaches using *PHR1* cDNA from *F. oxysporum* and *B. oryzae* also demonstrated improvement in post-UV survival rate (Alejandre-Durán et al., 2003; Kihara et al., 2004), suggesting *PHR1* indeed confers *in vivo* photorepair activities in fungi.

In contrast to photoreactivation, DNA damage response by NER is poorly characterized in filamentous fungi. This is due to the presence of a redundant NER pathway in filamentous fungi (Goldman et al., 2002). Early genetic and biochemical studies in the yeast, *S. cerevisiae* revealed that the genes involved in NER could be divided into two major classes (Prakash & Prakash, 2000). Mutations in class 1 genes have been reported to confer a relatively higher UV sensitivity and defect in performing incision on damaged DNA compared to mutations in class 2 genes in *S. ceverisiae* (Prakash & Prakash, 2000). Genes responsible for NER in *Schizosaccharomyces pombe*, *A. niger* (Goldman & Kafer, 2004) and *N. crassa* (Goldman et al., 2002) have also been identified and annotated, but their functional roles in NER still remained to be elucidated especially in filamentous fungi. Thus, it requires a more complex investigation to study the repair activities in filamentous fungi due to the involvement of redundant pathways. Table 2.2 lists reports on NER and Phr being functional in DNA repair in different fungal species.

Table 2.2: Functional DNA repair mechanisms, nucleotide excision repair (NER) or photoreactivation (Phr), available in different fungal species.

Species	NER	Phr	Citation
Aspergillus nidulans	(+)	(+)	Goldman and Kafer (2004)
Beauveria bassiana	(+)	(-)	Chelico and Khachatourians (2008); Lee et al. (2018)
Bipolaris oryzae	-	(+)	Kihara et al. (2004)
Candida albicans	(+)	(-)	Legrand et al. (2008)
Candida stellatoidea	-	(-)	Miller and Sarachek (1974)
Candida tropicalis	-	(-)	Miller and Sarachek (1974)
Cercospora zeae-maydis	(+)	(+)	Bluhm and Dunkle (2008)
Cordyceps militaris	-	(+)	Wang et al. (2018); (2017)
Fusarium oxysporium f.sp. *lycopersici*	-	(+)	Alejandre-Durán et al. (2003)
Metarhizium acridum		(+)	Brancini et al. (2018)
Metarhizium anisopliae	(+)	(-)	Pereira - Junior et al. (2018)
Neurospora crassa	(+)	(+)	Borkovich et al. (2004); Hatakeyama et al. (1998); Yajima et al. (1991)
Phycomyces blakesleeanus	-	(+)	Tagua et al. (2015)
Pseudogymnoascus destructans	(+)	(-)	Palmer et al. (2018)
Pseudogymnoascus sp.	(+)	(+)	Palmer et al. (2018)
Saccharomyces cerevisiae	(+)	(+)	Sancar (1985); Sebastian et al. (1990)
Schizosaccharomyces pombe	(+)	(-)	Fabre (1972); Lehmann (1996)
Sclerotinia sclerotiorum	-	(+)	Veluchamy and Rollins (2008)
Trichoderma harzianum	-	(+)	(1999); Berrocal-Tito et al. (2000)
Trichoderma atroviride	-	(+)	Berrocal-Tito et al. (2007)
Trichoderma reesei	-	(+)	Guzmán-Moreno et al. (2014)
Ustilago maydis	-	(+)	Brych et al. (2016)

(+) indicates the functional pathway in repairing UV-induced DNA damage
(-) indicates the pathway is deficient in repairing the damage

In an attempt to understand the relationship between photorepair and dark repair, Ishii et al. (1998) reported the existence of an alternative excision repair (AER) pathway in *N. crassa*. A similar finding was also reported in *S. pombe*, in which the pathway responsible for UV damage involved an endonuclease encoded by the gene *UVDE* (Yonemasu et al., 1997). Further genetic and biochemical analysis showed that *UVDE*-mediated excision repair removes UV damage more rapidly than NER and it also repairs both CPD and 6-4PP (Bowman et al., 1994; Yonemasu et al., 1997). These findings suggest an AER might exist in certain fungal species.

2.5.1.1 UV-induced DNA repair in *Pseudogymnoascus* spp.

Recently annotated genomes of *P. destructans*, as well as six closely related non-pathogenic *Pseudogymnoascus* species by Palmer et al. (2018) provide insight on the ability of this genus to perform NER and Phr. The study revealed that in the comparison between seven species of *Pseudogymnoascus*, *P. destructans* has lost a key enzyme, CPD phytolyase I, to perform Phr and another key enzyme, UVE1, which is essential to executing AER. In the same study, despite the other *Pseudogymnoascus* harbouring CPD photolyase I gene, only two strain tested, *P. verrucosus* and *P.* sp. 24MN13, displayed an increase in survival attributed to the activity of Phr. The study also reported that the *P. destructans* genome harbours genes for NER, thus confirming the possible roles of NER in UV-induced DNA repair. Extreme UV sensitivity recorded in *P. destructans* due to the loss of *UVE1* gene also suggests the importance of AER in the *Pseudogymnoascus* spp. in maintaining the DNA integrity against UV radiation.

CHAPTER 3: METHODOLOGY

3.1 Strains Selection and Culture Maintenance

Polar strains of *Pseudogymnoascus* spp. were obtained from the culture collection at the National Antarctic Research Centre, University of Malaya. Strains were selected based on 1) fungal colony morphology, 2) growth at different temperatures, 3) fungal colony pigmentation and 4) geographical of origins, which are listed in Table 3.1. 9 isolates were incubated at three different temperatures, 10, 15 and 20°C for strains selection after examining colony morphology to determine the optimal growth temperature for the study. The results are supplied in Appendix A.

Table 3.1: List of *Pseudogymnoascus* spp. selected for the study including the strain code, origin of isolate and person who isolated the strain

Taxon	Strain code	Locality	Isolated by
***Pseudogymnoascus* sp.**	AK07KGI1202 R1-1 sp.3 (**AKSP3**)	King George Island, Antarctic	Krishnan et al. (2016)
***Pseudogymnoascus* sp.**	AK07KGI1202 R1-1 sp.4 (**AKSP4**)	King George Island, Antarctic	Krishnan et al. (2016)
***Pseudogymnoascus* sp.**	HND16 R4-1 sp.1 (**HNDR4**)	Hornsund, Arctic	Ali (2016)
***Pseudogymnoascus* sp.**	HND16 R2-1 sp.2 (**HNDR2**)	Hornsund, Arctic	Ali (2016)

3.1.1 Culture Media Preparation

Czapex-Dox agar (CDA) was used throughout this study. CDA is a medium containing sodium nitrate and sucrose as the sole nitrogen and carbon sources, with other sources of essential ions such as potassium chloride, ferrous sulphate, magnesium glycerophosphate and potassium sulphate that are generally useful for the cultivation of fungi. CDA promoted more mycelial biomass compared to potato dextrose agar (Appendix B), which is required for section 3.5. CDA was prepared by suspending 45.4 g of CDA powder in 1 L of distilled water spiked with 0.1% of 34 mg ml^{-1} chloramphenicol stock solution (bioWorld, USA). Chloramphenicol was added to the media as a selective agent to reduce the possibility of bacterial contamination and

inhibit rapidly growing moulds including *Neurospora* and *Rhizopus* species (Downes, 1992). Prepared media was autoclaved at 121°C for 15 min and poured on 90 mm petri dishes (NEST, USA) after cooling down to around 50°C in the laminar flow to avoid condensation. The agar plates were then stored at 2-4°C in the dark as instructed by the manufacturer's protocol to prevent nutrient degradation until further use.

3.2 Verification of *Pseudogymnoacus* Isolates Based on Molecular DNA Sequences

3.2.1 Genomic DNA Extraction from Fungal Colonies

To confirm the identity and determine the phylogenetic relationship of the selected fungal strains, genomic DNA was extracted using the DNeasy® Plant Mini Kit (Qiagen, GER) following the manufacturer's instructions. Fungal colonies were cultured for 15 d prior to obtaining sufficient biomass for genomic DNA extraction. Fungal biomass was scraped off from the agar surface with a clean, sterile spatula and processed immediately. The fungal biomass was crushed with a sterile plastic pestle in 400 µL Buffer AP1 added with 4 µL RNase A in a 1.5 mL microcentrifuge tube, before proceeding with the rest of the kit's protocal. Extracted DNA was re-suspended in 200 µL AE elution buffer and stored at -20°C until further analysis. The amount of extracted gDNA was quantified by loading 1 µL of the sample on the NanoDrop™ spectrophotometers (Thermo Fisher Scientific Inc, USA) and the quality of successfully extracted gDNA was assessed using agarose gel electrophoresis (AGE).

3.2.2 Quality Assessment of Extracted gDNA

1% agarose gel was prepared by dissolving 0.15 g of molecular grade agarose powder (NextGene, MYS) in 15 mL 1× Tris-acetate-EDTA (TAE) buffer (1st Base, SGP) stained with 1: 10,000 (v/v) SYBR® Safe (Thermo Fisher Scientific Inc, USA). AGE was performed by loading 10 µL of gDNA mixed with 2 µL of 6× DNA loading dye (Thermo Fisher Scientific Inc, USA), and loading 5 µL of 1kb Plus DNA ladder (Thermo Fisher Scientific Inc, USA) as the size marker. AGE was conducted at 100 V for 25 min using electrophoresis power supply EV243 (Consort, BEL). Upon completion, the gel was visualized using the gel documentation system Platinum HD2 (UVItec, GBR) and UVItec software (UVItec, GBR). The fragment size and intensity of gDNA products were compared to 1kb Plus DNA ladder (Appendix C).

3.2.3 Fungal DNA Marker Amplification

Three DNA markers were selected for the molecular identification and phylogenetic analysis (Table 3.2). The internal transcribed spacer (ITS) region is the universal barcoding marker that is commonly used in fungal identification because it has a more defined barcode gap and relatively high resolving power for discriminating closely related species, with high polymerase chain reaction (PCR) and sequencing success rate across a broad range of fungal species (Schoch et al., 2012). The 28S ribosomal RNA gene, LSU, contains D1 and D2 hypervariable domains that can facilitate species identification, when combined with the ITS region (Raja et al., 2017), whereas the minichromosome maintenance complex component 7 (MCM7) is a parsimony-informative protein-coding gene that has been used in the phylogenetic evaluation of *Pseudogymnoascus* and allies (Minnis & Lindner, 2013). All markers were amplified with Labnet MultiGene™ gradient PCR Thermo Cycler (Labnet, USA) using 2X ExPrime Taq Polymerase (Genet Bio, KOR) (Table 3.3) following the thermocycling parameters specified in Table 3.4. The partial sequence of the 28S ribosomal RNA gene

region was amplified and sequenced using the primers LROR and LR6. The full length of the internal transcribed region including ITS1, *2.8S* and ITS2 region was amplified and sequenced using the primers ITS5 and ITS4. The protein coding gene *MCM7* was amplified and sequenced partially using the primers Mcm7-709for and Mcm7-1348. Amplified products were then stored at -20°C until further analysis.

Table 3.2: Selected DNA markerss with primer sequences for fungal identification and phylogenetic analysis.

DNA Marker	Primer	Primer Sequence	References
ITS	ITS5	$^{5'}$GGAAGTAAAAGTCGTAACAAGG$^{3'}$	(Gardes & Bruns, 1993)
	ITS4	$^{5'}$TCCTCCGCTTATTGATATGC$^{3'}$	(White et al., 1990)
LSU	LROR	$^{5'}$ACCCGCTGAACTTAAGC$^{3'}$	(Moncalvo et al., 2000)
	LR6	$^{5'}$CGCCAGTTCTGCTTACC$^{3'}$	(Vilgalys & Hester, 1990)
MCM7	Mcm7-709for	$^{5'}$ACIMGIGTITCVGAYGTHAARCC$^{3'}$	(Schmitt et al., 2009)
	Mcm7-1348	$^{5'}$GAYTTDGCIACICCIGGRTCWCCCAT$^{3'}$	

Table 3.3: Components of PCR master mix.

Reagents	Volume per reaction (µL)	5 reactions Master Mix (µL)
PCR water	17.2	86.0
10× PCR Buffer	2.5	12.5
10mM dNTPs	0.5	2.5
Forward Primer (10 µM)	1.0	5
Reverse Primer (10 µM)	1.0	5
ExPrime Taq Polymerase (5 U μL^{-1})	0.2	1.0
DNA template	2.6	-
Total Volume	25.0	89.2

Table 3.4: Cycling parameters for ITS, LSU and *MCM7*.

PCR stage	ITS		LSU		*MCM7*	
	Temp (°C)	Time	Temp (°C)	Time	Temp (°C)	Time
Initial Denaturing	95	2 min	94	10 min	94	2 min
Denaturing	95	40 s	94	30 s	94	1 min
Annealing	50	40 s	50	30 s	55	1 min
Extension	72	90 s	72	30 s	72	100 s
Final Extension	72	5 min	72	7 min	72	10 min
PCR Cycles	30		35		47	

AGE was then conducted to assess the quality of PCR products and to confirm single sequence amplification by loading 5 µL PCR products. The fragment size and intensity of PCR products were compared to 1kb Plus DNA ladder and the expected size of fragments is approximately 600 bp (ITS), 1200 bp (LSU) and 700 bp (*MCM7*) (Appendix C).

3.2.4 DNA Sequencing and BLAST

The purification and sequencing of PCR products from 3.2.3 were outsourced and completed by Apical Scientific (MYS) using BigDye® Terminator v3.1 cycle sequencing kit (Applied Biosystem, USA). Each isolate was sequenced in both forward and reverse direction to maximize sequencing coverage and the interpretation of sequence reads. Sequencing results were viewed and edited using 4Peaks (Version 1.8; by A. Griekspoor and Tom Groothuis, Nuclobytes BV, nucleobytes.com). Sequence trace with low-quality areas (< 20 Q value) was trimmed and the reverse sequence was then converted to its reverse complement sequence and merged with the forward sequence of each isolate using the Emboss merger program (http://www.bioinformatics.nl/cgi-bin/emboss/merger), to produce a consensus sequence of the fungal isolate. The consensus sequence (i.e. sequence of the isolate) was then searched against the GenBank database at National Centre for Biotechnology Information (NCBI) (http://www.ncbi.nlm.nih.gov) using BLASTN with the default pairwise alignment parameters. Sequence hits with IdentScore higher than 97% homology and 97% query coverage were accepted for identification.

3.2.5 Sequence Alignment and Concatenation

Multiple sequence alignment was performed using the generated DNA sequences and known reference sequences to recognize sequence domains that may provide information on functional, structural and evolutionary relationships among the sequences. A total of 63 reference sequences (Appendix D) was retrieved from NCBI GenBank database. For each gene, sequences were aligned using multiple sequence comparison by log-expectation (MUSCLE) algorithm and adjusted manually using Molecular Evolutionary Genetic Analysis (MEGA) version 7.0 (Kumar et al., 2016). Eight taxa of *Leuconeurospora* were assigned as the outgroup to root the ITS phylogenetic tree construction and only four were included during the construction of the multigene-tree (based on the concatenated ITS, LSU and *MCM7* sequences). Concatenation of the three partitions (ITS, LSU and *MCM7*) was performed using Mesquite version 3.2 (Maddison & Maddison, 2017). Any taxa without having all of the three sequence partitions were excluded during the multi-gene sequence alignment and tree construction. For the protein coding gene *MCM7*, the reading frame was designated and set, and partial nucleotide sequences were aligned and trimmed according to the codon sequence. All new sequences generated from the present study were deposited into NCBI database (Appendix E).

3.2.6 Basic Sequence Analysis

Analysis of DNA sequence variation, nucleotide composition and genetic distance was also performed using MEGA version 7.0 (Kumar et al., 2016). Basic sequence statistics, including conserved, variable, parsimony-informative sites and singletons were also completed for ITS, LSU and *MCM7* sequences separately as well as the concatenated sequences.

3.3 Phylogenetic Analyses

3.3.1 Best-Substitution Model Test

The best substitution model for phylogenetic analyses was tested using jModel Test 2.2.2 (Darriba et al., 2012). Akaike information criterion (AIC) (Posada & Buckley, 2004) was implemented in jModelTest 2.1.1 (Darriba et al., 2012) to select the best evolutionary model for the ITS and concatenated sequence datasets.

3.3.2 Neighbour-Joining Analysis

Neighbour-joining (NJ) trees were constructed using PAUP* 4.0a (Swofford, 2002). For the analysis of both datasets, 1000 bootstrap replicates were performed. Full heuristic search was performed with 10 random sequence additions and tree bisection-reconnection (TBR) branch swapping. Corresponding evolutionary models suggested by jModeltest 2.2.1 (Section 3.3.1) were appended to the Nexus files for the NJ tree construction with *Leuconeurospora* species defined as the outgroup. Majority rule consensus tree for each dataset was generated with a cut-off value at 70% bootstrap support.

3.3.3 Maximum Likelihood Analysis

Maximum likelihood (ML) analysis of both datasets was performed with Randomized Axelerated Maximum Likelihood (RAxML) (Stamatakis, 2014) using raxmlGUI v1.5 (Silvestro & Michalak, 2012). All parameters were set on default settings except for the best scoring ML tree and bootstrap (BS) analysis (Felsenstein, 1985) which were made in a single run with 1000 BS iterations. The GTRGAMMAI model was used for the bootstrapping phase and final tree construction. All trees were rooted with *Leuconeurospora* species.

3.3.4 Maximum Parsimony Analysis

Maximum parsimony (MP) phylogenetic trees were constructed using PAUP* 4.0a (Swofford, 2002). For both analyses, 1000 replicates were bootstrapped. Full heuristic search was performed with 10 random sequence additions and tree bisection-reconnection (TBR) branch swapping. *Leuconeurospora* sequences were defined as the outgroup and majority rule consensus tree was generated with a cut-off value of 70% bootstrap support.

3.3.5 Bayesian Inference Analysis

For Bayesian (BI) analyses, the posterior probability (PP) distribution was estimated using The Markov chain Monte Carlo (MCMC) as implemented in MrBayes v3.2.6 (Huelsenbeck & Ronquist, 2001). The parameters for both datasets were fixed based on the best model and the effective sample size (ESS) values were checked in Bayesian Evolutionary Analysis Sampling Trees (BEAST) v2.4.7 (Drummond et al., 2012) and Tracer v1.6 (Rambaut et al., 2007). The ITS and concatenated datasets (both using *Leuconeurospora* sequences as the outgroup) were ran for 3×10^6 and 1×10^7 generations, respectively, trees were then sampled at every 100^{th} and 1000^{th} generations, respectively, and both PP were estimated with 25% burn-in. For each dataset, the remaining trees were pooled and used to construct a 50% major rule consensus tree.

3.3.6 Pairwise Genetic Distance Analysis

The genetic distances between and within different clades of *Pseudogymnoascus* were calculated using the Tamura-Nei Model with gamma distribution rate of .537 implemented in MEGA version 7.0 (Kumar et al., 2016). Pairs of sequences were classified as “within clade” or “between clade” according to the classification of clades in *Pseudogymnoascus* as defined by Minnis and Lindner (2013).

3.4 Physiological Responses of Experimental Cultures to UVB Radiation

3.4.1 Exposure of Experimental Cultures to UVB Radiation

UVB was illuminated in a temperature-controlled UV chamber (Vortex Technology Industries, MYS). Photosynthetically active radiation (PAR) was provided by two daylight fluorescent lamps (TL-K 40W/10R, Philips, NZL) resulting in an intensity of 33 µmol photons m^{-2} s^{-1}, applied in a 12/12 h day/night cycle. UVB was irradiated using one UVB lamp tube (TL 20W/01, Philips, NZL) at an intensity of 0.8 W m^{-2}, giving an approximately dosage of 6.1 kJ m^{-2} d^{-1} in 130-min exposure in the middle of the photoperiod. The exposure was carried out in a temperature chamber of 15°C. To ensure uniformity of UVB and PAR intensity over the experiments, lamp tubes were pre-aged before use and UVB was eliminated from control plates using overhead projector (OHP) film.

3.4.2 Fungal Growth Profiling under UVB

CDA was prepared as described in section 3.1.1 with each plate contained 8 ml media to ensure uniformity of the media volume throughout the experiments and to allow the isolates to grow in a horizontal direction. Fungal isolates were acclimatized for 15 d at 15°C under PAR in a 12/12 h day/night cycle before inoculation for UVB treatment (section 3.4.1). Colony diameters of the culture were measured at its perpendicular angle, following lines drawn after isolate inoculation, every 24 h for a period of 10 d under a stereomicroscope (Nikon, JAP) using Fisherbrand™ Traceable™ digital carbon fiber calipers (± 0.2 mm) (Thermo Fisher Scientific Inc, USA). This ensures the conformity of measurements while avoiding any technical error. Fungal colony extension rate was then determined by plotting mean colony diameter against time (day), from which the slope of linear regression represents the rate of extension.

3.4.3 Pigmentation and Conidia Observation

Changes in pigmentation were investigated using observational assessment continuously throughout the experimental period of 10 d. Photographs of the fungal cultures are taken using a Canon EOS 1000D digital single-lens reflex camera (Canon, JAP) placed perpendicularly over the culture plate every 24 h. Conidia production under UVB radiation was first observed using a compound microscope then assessed at the end of the experiment (day 10) using scanning electron micrograph (SEM).

3.4.3.1 Sample Preparation for Scanning Electron Micrograph

Conidia samples were prepared for SEM after exposing fungal isolates to UVR for 10 days as described in section 3.4.1. In preparation for SEM, a 5-mm plug of the culture biomass was first removed from the culture plate and treated in 8% glutaraldehyde mixed with Fostat Sørencen Buffer in 1:1 volume ratio for 1 h at room temperature then rinsed with FSB mixed with distilled water in 1:1 volume ratio. The samples were then fixed overnight at 4ºC in 4% OsO_4 mixed with distilled water in a volume ratio of 1:3. After dehydration in increasing concentrations of ethanol (10, 20, 30, 40, 50, 60, 70, 80, 90, 95, and 100%, 15 min in each concentration with one repetition for 100% ethanol dehydration), the samples were further dehydrated in mixing 3:1, 1:1, and 1:3 ratio of 100% ethanol and acetone with subsequent dehydration in absolute acetone twice for 20 min in each dehydration step. Following dehydration, samples were processed *via* critical point drying using Leica EM CPD030 (Leica Microsystems, USA) with carbon dioxide as the transitional medium. Processed samples were then mounted onto an aluminium pin using double-sided foam mounting tape and sputter-coated with a thin layer of the fine-grained gold film using Leica EM SCD005 (Leica Microsystems, USA) with argon purge for clean vacuum condition. Sputter coating aids the charge dissipation while imaging under SEM. Ultra-structure of the specimens was then viewed with Quanta™ 650 FEG (FEI, USA).

3.5 Fungal UVB-induced DNA Damage and Recovery Assessment

Fungal isolates were cultured on 0.45µm nylon membranes (Merck, DEU) placed on top of CDA at 15ºC for 10 d in dark condition to reach the mid-log phase. This is to inhibit any upregulation of light-dependent genes which could then affect the measurement of UVB induced damage and repair. To asses DNA damage and recovery, the isolates were incubated under each of two incubation conditions, dark and light conditions, after exposure to UVB radiation for 130 min inducing UV dosage of 6.1 kj m^{-2} d^{-1}, intended to promote either NER or Phr, as demonstrated by Chelico et al. (2006). In the first condition, petri dishes with UV-irradiated fungal strains were wrapped with aluminium foil in order to exclude light. In the second condition, fungal cultures were incubated under fluorescent lamps giving PAR of 33 µmol photons m^{-2} s^{-1}. The fungi were maintained at 15°C during the repair incubation in both conditions.

3.5.1 Quantification of UV Induced DNA Lesions

Irradiated and control cultures were sampled at 0, 2, 6 and 10-h time points during DNA repair incubations, with fungal biomass being harvested by scraping the surface of the nylon membrane with a clean sterile spatula, transferred into a 1.5 ml microcentrifuge tube and then flashed-frozen immediately using liquid nitrogen. The frozen biomass was then stored in a -80ºC freezer until homogenization for DNA extraction.

3.5.1.1 DNA Extraction and preparation for ELISA

To quantify the DNA lesions induced by UVB radiation, gDNA of experimental cultures was extracted using DNeasy® Plant Mini Kit (BioTeke, KOR) following the manufacturer's instructions and re-suspended in 200 µL of elution buffer. The quality of extracted gDNA was assessed by AGE (Appendix J) and gDNA concentration was determined using the Nanodrop (Thermo Scientific™, USA). gDNA samples were then

diluted to 4 ng μL^{-1} with cold 0.1 mM EDTA TE buffer (Alfa Aesar, USA) and stored at -80ºC freezer until ELISA analysis.

3.5.1.2 ELISA for DNA Lesions Quantification

CPD and 6-4PP quantification was performed using OxiSelect™ UV-Induced DNA Damage ELISA kit (Cell Biolabs Inc, USA) according to the manufacturer's protocol. Briefly, 50 µl of diluted DNA samples and DNA binding solution was added to each well of the 64-well plate and incubated overnight at 16ºC on a modified WiseShake® SHO-2D digital orbital shaker (DAIHAN scientific, KOR). DNA solution was removed and the wells washed twice with phosphate-buffered saline (PBS) solution (iNtRON Biotechnology, KOR). Excess fluid was removed by blotting plate on paper towels, followed by plate blocking by adding 200 µl of assay diluent into each well and incubating for 1 h at room temperature. Assay diluent was removed and 100 µl of the diluted anti-CPD or anti-6-4PP antibody was added to each well and incubated for 1 h at room temperature on the modified flask shaker. After incubation, the wells were washed five times with 250 µl of 1× wash buffer followed by incubation with 100 µl of the diluted secondary antibody-HRP conjugate for 1 h at room temperature on the shaker. The wells were then washed again with 250 µl of 1× wash buffer and the enzyme reaction was stopped by adding 100 µl of stop solution and absorbance at 450 nm was read immediately with Epoch™ microplate reader (BioTek, USA) and Gen5™ software (BioTek, USA). A dilution series was prepared according to the manufacturer's protocol and was included in each plate to be normalized. PBS was diluted using ultra-pure water obtained from arium® pro VF ultrapure water system (Sartorius Stedim Biotech, DEU). Each DNA sample including unknown and standard was assessed in two technical replicates and three biological replicates.

3.5.2 Determine the Expression Level of DNA Repair Genes

Irradiated and control cultures were sampled following section 3.5.1 at 0 and 2-h time points during DNA repair incubations and stored at -80ºC freezer until homogenized for total RNA extraction.

3.5.2.1 RNA Extraction and DNAse Treatment

Total RNA was extracted using TRIzol Reagent (Invitrogen, USA) according to the manufacturer's protocol, after which it was re-suspended in diethylpyrocarbonate (DEPC)-treated water (Invitrogen, USA). Extracted RNA samples were then quantified using NanoDrop and the quality was assessed through AGE (Appendix K). To eliminate possible gDNA contamination, the extracted RNA samples were treated with DNase I (Thermo Fisher Scientific Inc, USA) to ensure amplification in RT-PCR is solely generated from mRNA. RNA samples were heated at 65°C for 5 min using WiseTherm® HB-48P digital heating block (DAIHAN Scientific, KOR) , placed on ice and briefly centrifuged. 1 µg of total RNA diluted in DEPC-treated water to 7.5 µL and mixed with 1 µL of 10× DNAsel buffer, 0.5 µL RiboLock (Thermo Fisher Scientific Inc, USA), and 1 µL of DNAseI. Samples were then incubated at 37°C for 30 min. After 30 min of incubation, 1 µL of 50 mM EDTA was added to each tube and incubated at 65°C for 10 min.

3.5.2.2 RNA Quality Assessment

2% agarose gel was prepared by dissolving 0.60 g of molecular grade agarose powder (NextGene, MYS) in 30 mL 1× TAE buffer (1st Base, SGP) stained with 1: 10,000 (v/v) SYBR® Safe (Thermo Fisher Scientific Inc, USA). AGE was carried out by loading 500 ng of total RNA sample in a total volume of 10 µL DEPC-treated water mixed with 2 µL of 6× DNA loading dye (Thermo Fisher Scientific Inc, USA), and loading 5 µL of 100bp DNA ladder (Thermo Fisher Scientific Inc, USA) as the marker, into the 2%

agarose gel submerged in 1× TAE buffer. The fragment size and intensity of RNA products were compared to the 100 bp DNA ladder and the expected size of fragments are around 1,500 bp (28 rRNA) and 1,000 bp (18 rRNA) (Appendix L).

3.5.2.3 Reverse Transcription of mRNA

cDNA was synthesized form DNAse-treated RNA samples using RevertAid First Strand cDNA synthesis kit (Thermo Fisher Scientific Inc, USA). 1 µL RNAse-free water and oligo-dT (500 µg mL^{-1}) was added to the DNAse-treated samples and incubated at 65°C for 5 min, then placed on ice and centrifuged briefly. Then, 4 µL 5× RT buffer, 2 µL 10 Mm dNTPs and 1 µL RevertAid H Minus RevertTranscriptase (200 U μL^{-1}) were added to the samples. All the tubes were incubated at 42°C for 60 min followed by 70°C for 5 min. cDNA samples were then stored at -80°C until further analysis.

3.5.2.4 Confirmation of cDNA Synthesis

To confirm that cDNA was successfully synthesized, PCR was conducted using 2× ExPrime Taq Polymerase. A master mix was prepared following Table 3.5 and aliquoted to each 0.2 mL PCR tube. 2 µL of cDNA product was then added to each of the PCR tubes containing 23 µL of master mix. PCR was performed using the following cycling conditions: denaturing at 95ºC for 30 s, annealing at 60ºC for 30 s, and extension at 75ºC for 30 s for 35 cycles with a final extension of 7 min. AGE was then conducted to ensure the cDNA was synthesized with successful amplification products (Appendix L).

Table 3.5: Components of master mixes PCR reaction for cDNA synthesis confirmation.

Reagents	**Volume per reaction (µL)**
PCR water	17.8
10× PCR Buffer	2.5
10mM dNTPs	0.5
Forward Primer (10 µM)	1.0
Reverse Primer (10 µM)	1.0
ExPrime Taq Polymerase (5 U μL^{-1})	0.2
cDNA template	2.0
Total Volume	25.0

3.5.2.5 Gene Selection and Primer Design

To select genes for studying gene expression levels post UV-exposure, the Class 1 NER genes *RAD1, RAD2, RAD3, RAD4, RAD10, RAD14,* and *RAD25* were first examined, as mutations in these genes confer to a high degree of sensitivity to UV irradiances and to other DNA damaging agents (Prakash & Prakash, 2000). Of the genes, those that are involved in fewer other DNA regulating mechanisms based on the *Kyoto Encyclopedia of Genes and Genomic* (KEGG) *Pathway* database were selected and finally *RAD14*, *RAD2*, and *RAD1* were targeted for this study. Only one primer set for the target gene, *RAD2* was successfully designed and qualified to be used in our study. Meanwhile, only one gene, namely *PHR1*, has been extensively described to function in Phr and was selected to be used to investigate response under light repair. Table 3.6 shows the function of the target genes and the accession number for the sequences retrieved from GenBank database for primer design.

Table 3.6: Functional annotation of selected target genes, gene names and human orthologue.

Gene	**Gene name**	**Human ortholog**	**Biochemical activities**
RAD2	Single-stranded DNA endonuclease	*XPG*	Nuclease that cuts damaged DNA on the 3'-side of the lesion
PHR1	Deoxyribodipyrimidine photolyase	-	DNA photolyase involved in photoreactivation

For real-time PCR, gene-specific primers were designed according to sequences retrieved from the whole genome shotgun sequence of *Pseudogymnoascus destructans* isolate 20631-21 as the reference species (Drees et al., 2016). Primer3Plus (Untergasser et al., 2007) was used to design primers using default parameter settings with the adjustment of product size ranging from 90 to 130 bp. Suggested primer pairs for qPCR amplification were screened for hairpins, self- and cross-dimers using NetPrimer (http://www.premierbiosoft.com/netprimer/). Then, candidate primer sets were screened using NCBI Primer-BLAST to ensure binding specificity. The primer sequences used to amplify all target and reference genes are listed in Table 3.7, as are the corresponding primer sizes, annealing temperature, amplicon size, and amplification efficiency.

Table 3.7: List of primers used for expression analysis with the accession number of sequences used for primer design, primer sequence, primer size, melting temperature and amplicon size.

Reference Gene	Accession Number	Primer Name	Sequence	Primer Size, bp	Tm, ºC	Amplicon size, bp
GAPDH	JPKE01001866.1	GAPDH_3F	5'CCTCCTCCATCTTCGATGCC3'	20	60.0	91
		GAPDH_3R	5'GAGTAGCCCCACTCGTTGTC3'	20	60.0	
ACT1	JPKE01001290.1	ACT1_2F	5'TACCGAGGCACCAATCAACC3'	20	60.0	120
		ACT1_2R	5'GAAGCGTAGAGGGACAGGAC3'	20	60.0	
β-TUB	JPKE01003075.1	β-TUB_2F	5'ACTTGACCTGCTCTGCCATC3'	20	60.0	124
		β-TUB_2R	5'GTCTGGACGTTGTTGGGGAT3'	21	60.0	
DLD	JPKE01001174.1	DLD_1F	5'CTGGAATCTCGGCATACGCT3'	20	60.0	145
		DLD_1R	5'AACGCTGCCTTGACCTCTAC 3'	20	60.0	
SAR1	JPKE01004290.1	SAR1_2F	5'CGACCCTGTTGCACATGTTG 3'	20	60.0	148
		SAR1_2R	5'TCTTTCCATAGACGGCGAGC3'	20	60.0	
PGK1	JPKD01002266.1	PGK1_1F	5'GACAAGTTTTCCCCTGATGC3'	21	60.0	121
		PGK1_1R	5'CGTTGATGGTCTGGTTGATG3'	20	60.0	
5.8S	KC461555.1	5.8S_2F	5'AACGGATCTCTTGGTTCTGG3'	20	60.0	104
		5.8S_2R	5'GCAATGTGCGTTCAAAGATT3'	20	60.0	
Target Gene						
RAD2	XM_012888916.1	RAD2_2F	5'AGGATGGGGTTGAGCAAAGA3'	20	60.0	107
		RAD2_2R	5'CGCTGCGTTAATTCGTTTCG3'	20	60.0	
PHR1	JPJY01000583.1	PHR1_1F	5'CGGCATCTTTCCTTGCGAAG3'	20	60.0	115
		PHR1_1F	5'CTAAATCCCCAGCCACCGTT3'	20	60.0	

3.5.2.6 Preliminary Primer Testing

For preliminary primer testing, primer pairs were tested against a selected strain's cDNA and gDNA as templates using standard PCR with the following thermocycling conditions: denaturing at 95ºC for 30 s, annealing at 60ºC for 30 s, and extension at 75ºC for 30 s for 35 cycles with a final extension of 7 min. Specificity, product length

and primer dimer of PCR products were assessed with AGE as described in section 3.5.2.2. Only primers with no primer dimer formation and single product generated were further validated, and primers that were not qualified were re-designed and re-tested.

3.5.2.7 Validation of Primers

Standard curve and melt curve analysis was performed on the primer sets to determine their R^2 values, efficiency and suitability for use in reverse transcriptase quantitative PCR. The standard curve for each primer pair was generated with a 1:5 dilution series of cDNA template and amplified using Thunderbird® SYBR® Green qPCR mix (Toyobo, JAP) following thermocycling parameters in section 3.5.2.9 on the Applied Biosystem® 7500 Real-Time PCR systems (Applied Biosystems, USA). 18 cDNA products from section 3.5.2.3 were pooled prior for the generation of the standard curve to ensure the uniformity of mRNA from different treatments. The standard curve is required to calculate the efficiency of the qPCR reaction; ideally a perfectly efficient reaction should be 100% amplification efficiency, corresponding to doubling the sequence during each replication cycle. Primer pairs with amplification efficiency between 90-110% were generally accepted in this study to ensure the efficiencies of all the primers used in the qPCR reaction are approximately equal for accurate comparison. Correlation coefficients (R^2 values) represent how well qPCR generated data fit the regression line and it should be > 0.99. Melt-curve analysis was also performed at the end of the qPCR cycles to confirm the specificity of the primer and ensure the absence of primer-dimer formation.

3.5.2.8 Selection of Reference Genes

Three independent applications, namely BestKeeper (Pfaffl et al., 2004), geNorm (Vandesompele et al., 2002), and NormFinder (Andersen et al., 2004) were used to evaluate the expression stability of the 7 candidate reference genes (previous Table 3.7) under the experimental conditions. geNorm is a Microsoft Excel application that derives internal control gene-stability measure (*M*) as the average pairwise variation of a particular gene with all other control genes in the same analysis (Vandesompele et al., 2002). Genes that were not co-regulated were considered least stable (highest *M* value) and were stepwise excluded resulting in a stability ranking. Genes with $M \leq 1.5$ were considered high expression stability and genes with $M > 1.5$ were not used for internal control genes, whereas genes with the lowest *M* value were considered to be the most stable and were considered to be used in our analysis. BestKeeper generates the BestKeeper index (r) of internal control genes based on pairwise comparisons of raw cycle threshold (C_t) values of each gene (Pfaffl et al., 2004). Stable internal control genes with strong correlation with BestKeeper index (r) were considered as our reference genes. NormFinder estimates intra- and inter-group variation in gene expression levels to measure gene stability value (Andersen et al., 2004). Normfinder also determines the two-gene normalization factor and its corresponding stability value using the best combination of two genes. Raw C_t values of reference genes obtained from qPCR as described in section 3.5.2.9 were used directly for stability calculations in BestKeeper analysis. For the other algorithms, the reference gene with the highest relative quantity was set to 1 and other raw C_t values were converted into relative quantities and imported into Normfinder and GeNorm to be analyzed. All reference genes were then ranked according to their stability in the tested sample sets and the top three ranked reference genes were selected to be normalized in section 3.5.2.9.

3.5.2.9 Gene Expression Analysis

mRNA expression of target genes was quantified in 96-well plates on the Applied Biosystem® 7500 Fast Real-Time PCR systems using Thunderbird® SYBR® Green qPCR mix (Toyobo, JP). 20µl of reaction mixtures were prepared following Table 3.8. The reaction conditions were following thermocycling parameters: pre-denaturation at 95°C for 20 s, followed by 40 cycles of 95°C for 3 s and 60°C for 30 s, then followed by a melt curve stage of 95°C for 15 s, 60°C for 1 min, 95°C for 15 s and 60°C for 15 s. Relative gene expression was obtained by normalizing with the expression of 3 most stable internal control genes (selected from section 3.5.2.8) using the $2^{-\Delta\Delta Ct}$ method (Livak & Schmittgen, 2001; Schmittgen & Livak, 2008). Relative expression in terms of fold change is derived from the differences in C_t values in the UV-treated samples in relative to its control (non-UV-treated) at a particular time-point and repair condition. Each RT-qPCR reaction was performed in three technical replicates. A non-template control was also included for each gene.

Table 3.8: Components of master mixes for qPCR.

Reagents	**Volume per reaction (µL)**	**Volume for 19 reactions (µL)**
PCR water	6.96	132.24
2× SYBR® qPCR mix	10.00	0.76
50× ROX reference dye	0.04	190.00
Forward Primer (10 µM)	0.50	9.50
Reverse Primer (10 µM)	0.50	9.50
cDNA template	2.00	-
Total Volume	20.00	342.00

3.6 Statistical Analyses

Means, standard deviations and standard errors of the mean of the data sets of fungal growth, DNA lesion and fold change (for the relative gene expression) were calculated and analysed using the SPSS Mac Statistical package ver. 23.0 (IBM, USA). Different statistical analyses were performed to assess the effects of the treatments investigated, with significance level set at $\alpha = 0.05$. The effect of UVB radiation on fungal growth rate on each isolate was assessed using linear regression analysis to compare the slope of the means colony diameter over a 10-d period. The interactive effect of UVB treatments and the duration of incubation on fungal growth was also assessed separately using two-way multivariate analysis of variance (MAVONA). MANOVA was used to investigate the interactive effects of incubation condition and the duration of repair on the concentration of DNA lesions, including CPD and 6-4PP, separately for each of the isolates and type of lesions. Univariate analysis was also conducted to investigate the sole effect of the independent variables. Similarly, the expression of DNA repair genes was also analysed using MANOVA to investigate three different conditions: 1) the effect of UVB radiation, 2) the effects of repair conditions and 3) the sole effect of light. Pairwise comparisons with Bonferroni adjustment were also performed with the significance level set at $\alpha = 0.05$.

CHAPTER 4: RESULTS

4.1 Verification of *Pseudogymnoascus* Isolates

All ITS, LSU and *MCM7* sequences of four isolates, AK07KGI1202 R1-1 sp.3 (AKSP3), AK07KGI1202 R1-1 sp.4 (AKSP4), HND16 R4-1 sp.1 (HNDR4) and HND16 R2-1 sp.2 (HNDR2) were successfully sequenced for preliminary species identification using BLAST (Table 4.1). BLAST analysis revealed the sequences were best matched with the ITS, LSU and *MCM7* sequences on GenBank that belonged to either genus *Pseudogymnoascus* or *Geomyces*. Although some sequences were best matched with *Geomyces* from the database, they are in fact recognized as *Pseudogymnoascus* after the reclassification of *Pseudogymnoascus* by Minnis and Lindner (2013). Thus, the isolates used in this study were identified as *Pseudogymnoascus* spp. with high identity sequence scores from the BLAST analysis.

Table 4.1: BLAST result of ITS, LSU and *MCM7* sequences between isolates used in this study and GenBank sequences.

Strain code	Accession number	Sequence Length	Best match in BLAST		Identity Scores (%)	Query coverage (%)
			Accession number	Identity		
ITS						
AKSP3	MK448238	564	KP411572.1	*Pseudogymnoascus pannorum*	100	100
AKSP4	MK448239	571	KM816682.1	*Geomyces* sp.	99	100
HNDR4	MK448240	581	KM816682.1	*Geomyces* sp.	99	99
HNDR2	MK448241	549	DQ317337.1	*Geomyces* sp.	100	99
LSU						
AKSP3	MK443474	989	JQ768405.1	*Geomyces pannorum*	99	100
AKSP4	MK443475	973	LN714595.1	*Pseudogymnoascus pannorum*	100	100
HNDR4	MK443476	962	LN714595.1	*Pseudogymnoascus pannorum*	100	100
HNDR2	MK443477	973	LN714595.1	*Pseudogymnoascus pannorum*	100	100
MCM7						
AKSP3	MK448242	615	KF017664.1	*Pseudogymnoascus* sp.	98	99
AKSP4	MK448243	614	KF017664.1	*Pseudogymnoascus* sp.	98	100
HNDR4	MK448244	639	KF017664.1	*Pseudogymnoascus* sp.	98	96
HNDR2	MK448245	636	KF017664.1	*Pseudogymnoascus* sp.	98	97

4.2 Sequence Alignment and Variation of ITS, LSU, *MCM7* and Concatenated Sequences of *Pseudogymnoascus*

The basic sequence statistics were calculated and the results are shown in Table 4.2. A total number of 67 ITS sequences belonging to *Pseudogymnoascus, Geomyces* and *Leuconeurospora* spp. formed final sequence alignment length of 493 nucleotide sites, of which 84 were variables, 75 were parsimony informative (PI) and 9 were singletons. Sequence alignment of LSU contained 1345 total nucleotides, of which 41 were variables, 31 were PI and 10 were singletons, whereas, the sequence alignment of *MCM7* contained 616 nucleotides, of which 256 were variables, 221 were PI and 37 singletons. The percentage of PI was the highest in the sequences of *MCM7* (35.88%) following ITS (15.21%) and LSU (2.3%).

The aligned concatenated sequences of 31 taxa contained 2442 nucleotides, of which 351 were variables and 52 were singletons. Although only 12.24% was PI, 299 PI sites could provide sufficient information to delineate species within the genus *Pseudogymnoascus.*

Table 4.2: Results of basic sequence statistics including number of sequences, total base pair (BP), conserved sites (CS), variable sites (VS), singletons (SS), parsimony-informative sites (PIS) and its percentage for ITS, LSU, *MCM7* and concatenated sequences of *Pseudogymnoascus, Geomyces* and *Leuconeurospora* spp.

Domain	No. Taxa	No. BP	No. CS	No. VS	No. SS	No. PIS	PIS (%)
ITS	63	493	405	84	9	75	15.21
LSU	31	1345	1304	41	10	31	2.3
MCM7	31	616	358	256	37	221	35.88
Concatenated	31	2442	2088	351	52	299	12.24

4.3 Evolutionary Models for Phylogenetic Analyses

The best-fitted evolutionary model calculated for ITS and the concatenated dataset were GTR + I + G; I = 0.544; G = 0.422 and TIM2 + G + I; I = 0.71; G = 0.537, respectively. However, the more conservative HKY + G + I model was chosen instead for analysing the ITS dataset in the Bayesian analysis. This model fits with the requirement of having an effective sample size of 200 in all statistical parameters, hence allowing posterior distributions of trees to be accurately inferred in the Bayesian analysis (Drummond et al., 2006)

Base frequencies for ITS sequences were 0.193 (A), 0.2776 (C), 0.2633 (G) and 0.2662 (T). The incorporated rates of matrix for ITS sequences were 1.7816 (AC), 6.9141 (AG), 3.3649 (AT), 0.1567 (CG), 11.1426 (CT) and 1.0000 (GT). Whereas the base frequencies for concatenated sequences were 0.2463 (A), 0.2412 (C), 0.2742 (G) and 0.2383 (T), with incorporated rates matrix for substitution model in phylogenetic analyses were 1.6621 (AC), 8.9166 (AG), 1.6621 (AT), 1.0000 (CG), 14.1561 (CT) and 1.0000 (GT).

4.4 Phylogenetic Analyses for ITS and Concatenated Aligned Sequences

An alignment data set comprising of 67 ITS sequences – 63 reference sequence from Genbank and 4 *Pseudogymnoascus* sequences from the present study – were analysed for the NJ, ML, MP and BI phylogenetic analysis of *Pseudogymnoascus*. The 50% majority rule consensus tree of the Bayesian analysis is presented in Figure 4.1 with BS values from NJ, MP, ML test and PPs of BI analysis. The phylogram constructed using only ITS sequence alignment alone provided sufficient resolution to separate *Pseudogymnoascus* from its sister clade, *Geomyces* in all phylogenetic tree analyses with strong BS and PP supporting values (96/85/91/1). In contrast, the phylogram failed to group the taxa according Minnis and Lindner (2013) and same species were separated or different species were grouped into a single clade such as *P. verrucosus* and *P. destructans* in Clade B (Figure 4.1). The phylogram was also able to separate *Pseudogymnoascus* spp. into six different clades but with poor supportive values. Clade A contains *P. roseus* and its complex species. Clade B consists of two different species: *P. destructans* and *P. verrucosus*. Clade C and E were unresolved and contain mostly undescribed *Pseudogymnoascus* sp. Only two clades were resolved with well-supported BS and PP values including an undescribed group of *Pseudogymnoascus* sp. (Clade D) and *P. appendiculatus* (Clade F).

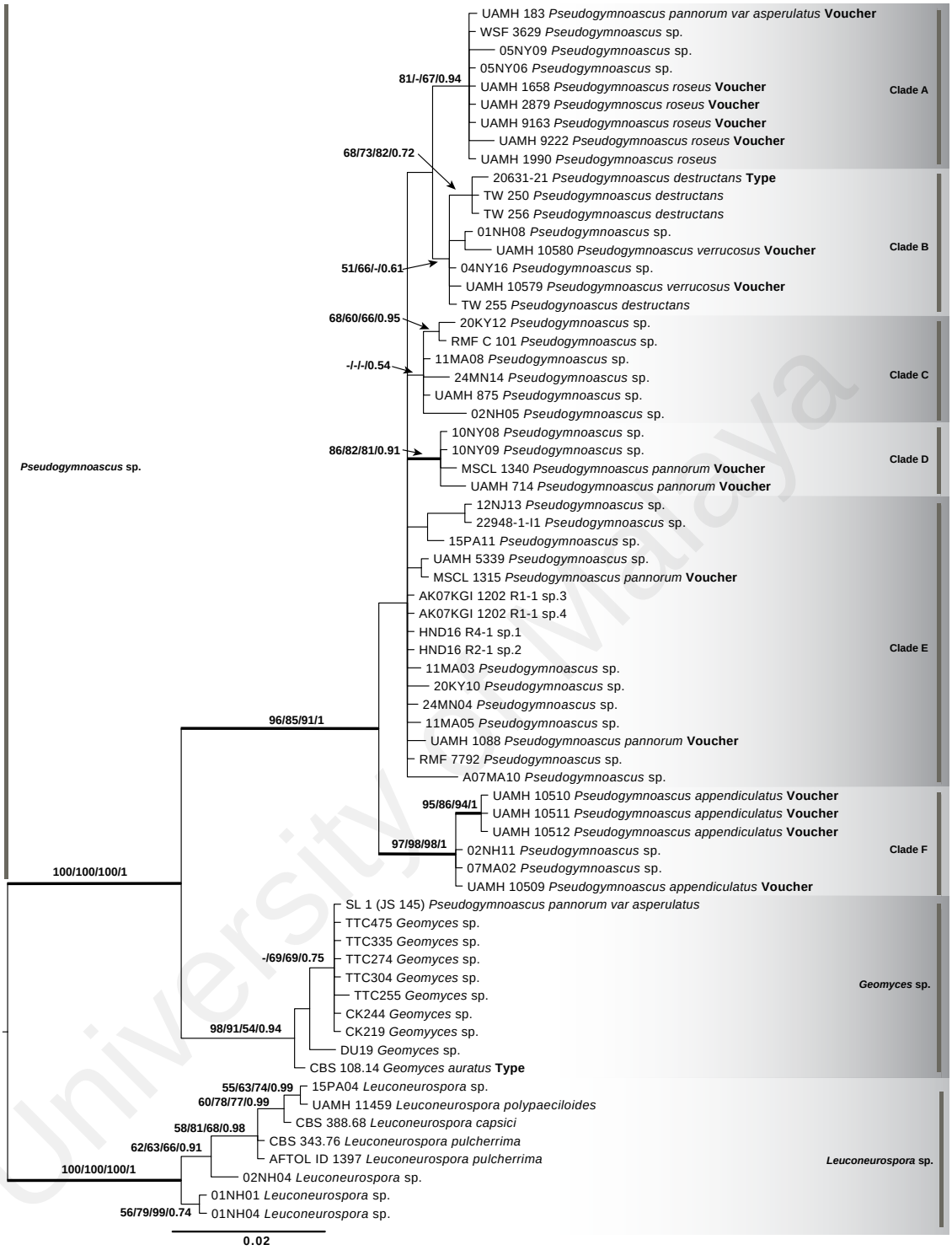

Figure 4.1: Bayesian phylogram (50% majority rule consensus) of the final aligned ITS sequences of *Pseudogymnoascus*, *Geomyces* and *Leuconeurospora* sp.. Value for the branch is presented as BS and PP value of NJ/MP/ML/PP and thick lines indicate values more than 70/70/70/0.90, respectively.

The 50% majority rule consensus tree of the combined results of two independent Bayesian runs using concatenated aligned sequences is presented in Figure 4.2 with percentages of BS replicates from NJ, MP, ML analyses, and PP values generated from BI analysis. Similar tree topologies were recovered from the other three analyses (NJ, MP and ML). Clades presented in the study of Minnis and Lindner (2013) were incorporated into Figure 4.2 to identify the four *Pseudogymnoascus* isolates used in our study. The phylogram of *Pseudogymnoascus* fungi generated from three DNA markers was able to separate into seven genetic clades (A-C, B, E, G, H, J, and L) that were supported by high BS and PP values. Clade A and C were not resolved as two different clades based on our concatenated sequence data. *Pseudogymnoascus* isolates used in this study clustered with *Pseudogymnoascus* sequences (*Pseudogymnoascus* sp.) that were classified as clade B in the phylogram with well-supported BS and PP values; however, they are still undescribed.

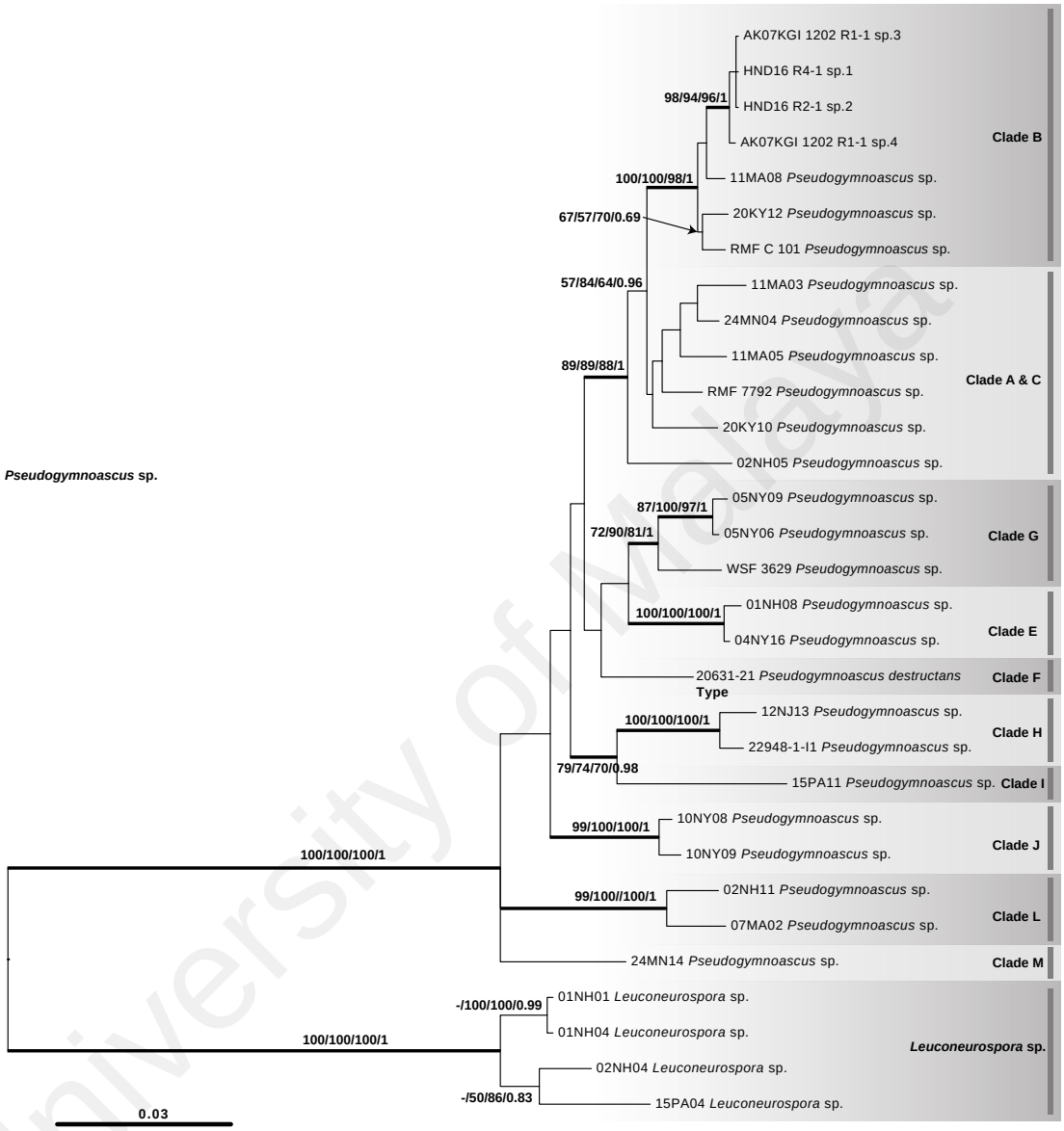

Figure 4.2: Bayesian phylogram (50% majority rule consensus) of the final concatenated alignment of ITS, LSU and *MCM7* of *Pseudogymnoascus* and *Leuconeurospora* sp.. Value for branches is presented as BS and PP value of NJ/MP/ML/BI and bold lines indicate values more than 70/70/70/0.90, respectively. Clade A-M represents different monophyletic groups derived from Minnis and Lindner (2013).

4.5 Genetic Distance, Intra- and Inter-Specific Variation

Our results demonstrated no overlapping values between the intra-specific variation in the combined sequences, except the variation within clade A&C (1.69%) and the variation between clade A&C and B (1.69%) (Table 4.3). Thus, the barcode gap only exists for other clades, except clade A, B and C to delineate species within the genus *Pseudogymnoscuas*. The multi-gene tree from section 4.4 also showed a very strong supportive BS and PP values that these two clades (B and A&C) are grouped together. Thus, the maximum intraspecific variation less than 1.69% shall be used in current study to accurately delineate into specific clades within the genus of *Pseudogymnoascus*.

Table 4.3: Genetic pairwise distance between 11 clades of *Pseudogymnoascus*. Bolded values indicate the value of intra-specific variation.

Clade	A&C	B	E	F	G	H	I	J	L	M
A&C	**1.69**									
B	1.69	**0.48**								
E	2.86	2.58	**0.11**							
F	2.97	3.16	2.90	–						
G	3.18	2.86	2.63	2.59	**1.19**					
H	3.80	3.69	4.10	3.54	4.13	**0.70**				
I	3.92	4.07	4.12	3.80	3.93	3.52	–			
J	3.56	3.81	3.25	2.92	3.19	3.82	4.05	**0.41**		
L	3.98	4.13	4.11	4.91	4.22	5.70	5.12	5.04	**1.36**	
M	4.08	4.19	4.48	4.04	3.77	4.64	4.94	3.64	4.24	–
Leuconeurospora	12.00	12.27	12.46	11.75	11.58	11.79	12.55	11.46	12.14	11.87

4.6 Effects of UVB Radiation on Growth Rates Derived from Colony Diameters

The physiological effect of UVB radiation on the growth of polar soil fungi in terms of colony diameter was demonstrated in the four isolates of *Pseudogymnoascus* spp. isolated from the Arctic and Antarctic region used in our study. We first aimed to compare the growth rates of *Pseudogymnoascus* spp. under UVB treatment (UVB+PAR) and control (PAR only) conditions. Growth profiles of the four *Pseudogymnoascus* isolates were plotted using mean colony diameters measured continuously on the same fungal colonies over a 10 d duration in laboratory simulated conditions. Figure 4.3 shows the growth profile of four *Pseudogymnoascus* isolates in terms of mean colony diameters during the 10 d period. The linear growth curves of UVB-treated samples were less steep compared to the controls. The slopes of the growth curves represented the growth rates of the fungal colonies; therefore, linear regression lines were plotted to determine the growth rate of each isolate in both conditions. Table 4.4 shows the slope value, R^2 and standard error of the regression lines plotted. UVB-treatment caused the greatest reduction in growth rate in HNDR2 (35.32%), followed by AKSP3 (34.47%) AKSP4 (33.03%), whereas HNDR4 was the least inhibited by UVB irradiation with 21.74% reduction.

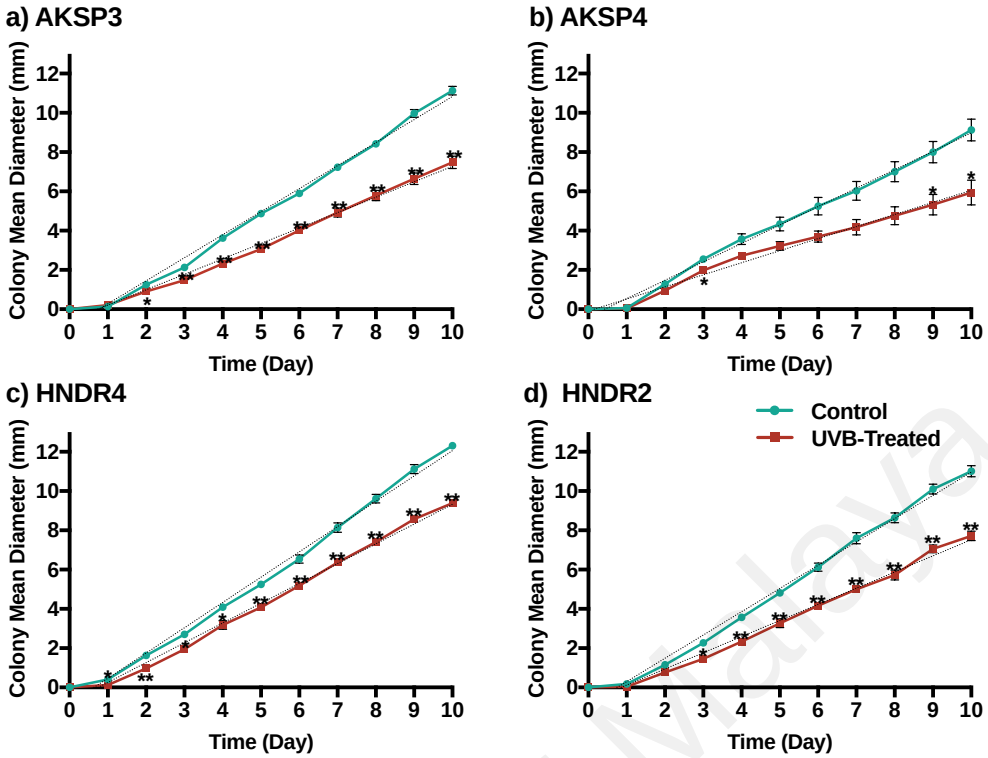

Figure 4.3: Mean colony diameter of *Pseudogymnoascus* strains recorded under UVB and control conditions across an experimental course of 10 d. Error bars are SEM of six biological replicates in a single experiment and dotted line represents the best fit linear regression of the mean value. *, $p < 0.05$; **, $p < 0.01$ indicate the significant difference between the two conditions determined by t-test within the same time point.

Table 4.4: Colony extension rates observed in each strain (five replicates per treatment). Slopes denoted with asterisk are significantly different compared to its respective control ($p < 0.05$).

Strain code	Treatment	Slope	R2	Standard deviation of residual, Sy.x
AKSP3	Control	1.1730	0.985	0.4589
	UVB-treated	0.7856*	0.962	0.5006
AKSP4	Control	0.9383	0.922	0.8738
	UVB-treated	0.6149*	0.862	0.7895
HNDR4	Control	1.2880	0.984	0.5229
	UVB-treated	1.0080*	0.980	0.4591
HNDR2	Control	1.1850	0.979	0.5643
	UVB-treated	0.8228*	0.968	0.4836

In this study, we hypothesized that colony diameter extension rates of the isolates will be reduced under UVB radiation. Linear regression analysis was performed to compare the slopes between two treatments and to test the significance of the treatment effects on colony diameter extension rates against our null hypothesis. The colony extension rates in UVB treated samples were significantly lower ($p < 0.05$) than the controls for all *Pseudogymnoascus* isolates. Hence, it was concluded that UVB radiation significantly inhibited the growth rates derived from colony growth diameters of *Pseudogymnoascus* spp.

Further analysis with two-way MANOVA was conducted to determine the interactive effects of the different treatments and duration of culture on the mean colony diameters across all the isolates. Box's equality (covariance matrixes) was tested prior to the analysis of MANOVA. Results showed that the homogeneity of variance of the data was violated. Therefore, Pilai's trace test was selected for the multivariate analysis. Findings showed that the interactive effects were significant ($p < 0.05$). This indicates that the effects of UVB radiation was significant influenced the mean colony diameters of the cultures. Pairwise comparisons with Bonferroni adjustment between different treatments showed that mean colony diameter was significantly reduced ($p < 0.05$) after 1 d of UVB exposure in HNDR4 and after 2 d in AKSP3 and HNDR2, whereas the significant difference between the treatments were only observed after 3 d in AKSP4.

4.7 Pigmentation of Cultures Exposed to UVB Radiation

No visible changes in mycelium pigmentation were observed during the exposure to UVB in the course of 10 d incubation period (Figure 4.4). Red pigments observed in two colonies (Figure. 4.4b) under UVB treatments were diffusible pigments that were presented and transferred from the previous culture into new plates for the treatments. The Arctic isolate, HNDR2, is one of the isolates that produced yellow-pigmented mycelium, however there was no increase in colour intensity under UVB-treated condition compared to the controls (Figure 4.4d).

4.8 Conidia Production Under UVB Radiation

The inhibition of conidia production in *Pseudogymnoascus* isolates was first observed under the compound microscope after 10 d of UVB exposure. To validate, SEM observation was conducted on the fungal colonies at the end of 10 d incubation under two treatments. Micrographs (Figure 4.5) show that more conidia were visible in colonies that were cultured under the control condition (PAR only) in isolates AKSP3, AKSP4, and HNDR2, whereas under UVB exposure, conidia production was inhibited except for the Arctic isolate HNDR4. Conidia production in HNDR4 was also relatively low compared to other isolates in the control condition.

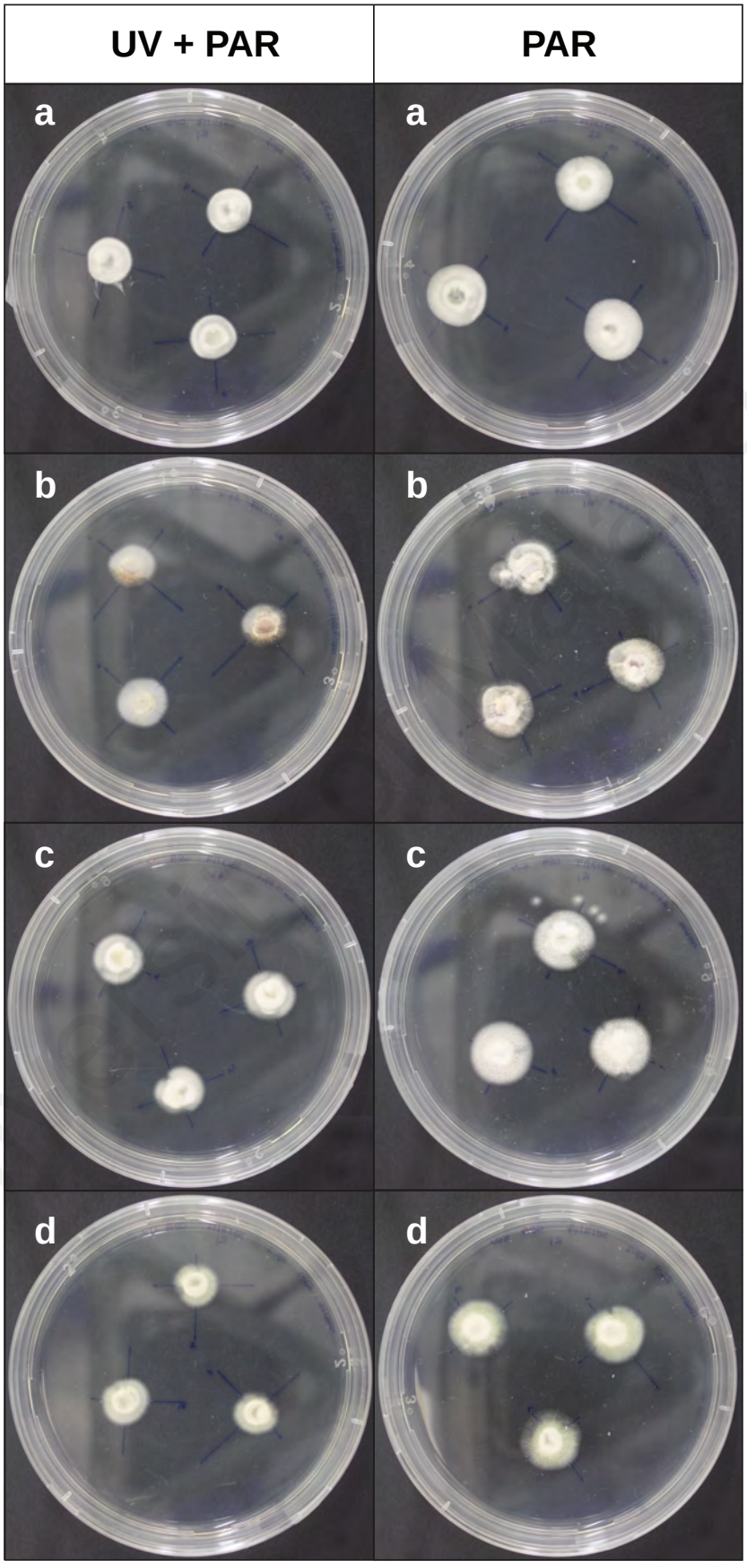

Figure 4.4: Fungal colony colours of four *Pseudogymnoascus* strains a) AKSP3, b) AKSP4, c) HNDR4 and d) HNDR2 after incubating 10 d in two different conditions: UV with PAR and PAR only.

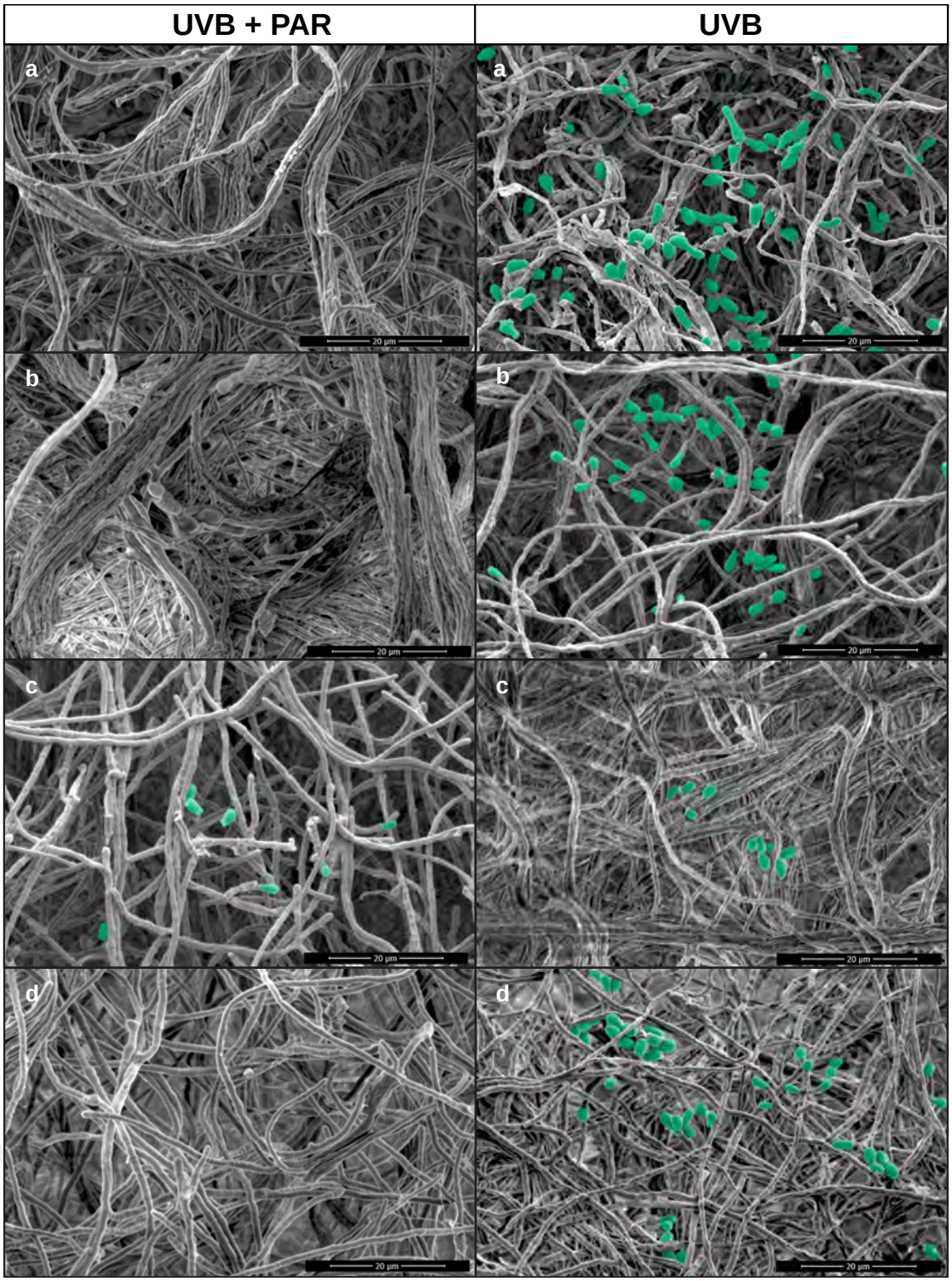

Figure 4.5: Panel of SEM micrographs illustrating the conidia (highlighted in green) and mycelium of *Pseudogymnoascus* spp., a) AKSP3, b) AKSP4, c) HNDR4 and c) HNDR2, after exposing to UVB+PAR or PAR for 10 d. Scale bar = 20 µm; magnification = 5000×.

4.9 Repair of CPD Under Light and Dark Conditions

The concentrations of CPD in *Pseudogymnoascus* isolates during the different repair conditions were quantified using ELISA after UVB exposure (Figure 4.6). CPD concentrations in the Antarctic isolates, AKSP3 ($\mu = 0.03$, SD = 9.2×10^3) and AKSP4 ($\mu = 0.029$, SD = 8×10^2), were two and three-fold greater than the concentrations recorded in the Arctic isolates, HNDR4 ($\mu = 0.018$, SD = 5.4×10^3) and HNDR ($\mu = 0.011$, SD = 1.2×10^2), respectively after UVB exposure. Antarctic isolates were more susceptible to UVB-induced CPD damage as they generated higher concentration of CPD compared to the Antarctic isolates.

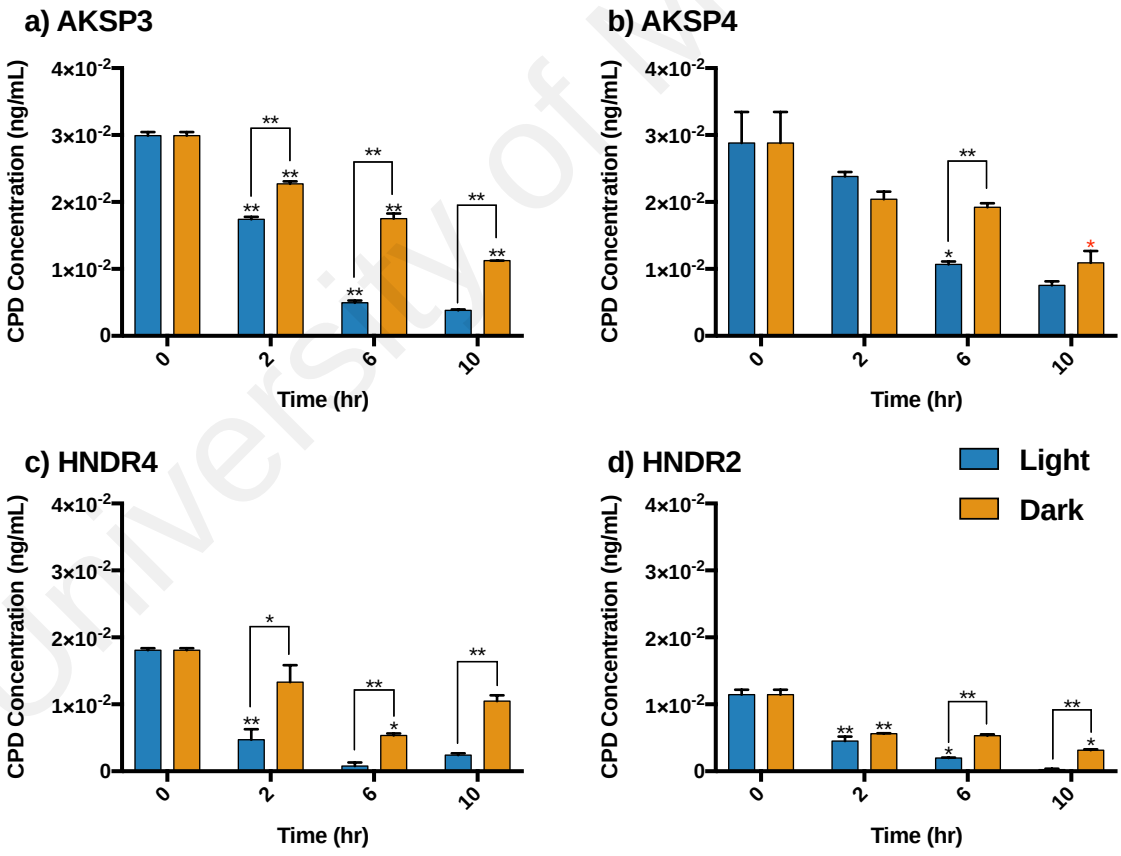

Figure 4.6: Amount of cyclobutane pyrimidine dimer (CPD) quantified using ELISA under light and dark repair conditions after UVB exposure. Error bars are SEM of three biological replicates. *, $p < 0.05$; **, $p < 0.01$ indicate significant difference compared to previous time point or as indicated; *, $p < 0.05$ is compared to the initial concentration under its respective condition.

A two-way MANOVA was conducted with the concentrations of CPD in four *Pseudogymnoascus* isolates as the dependent variable and with the duration of repair and incubation conditions as independent variables. The independent variables included four different repairing duration, 0, 2, 6 and10 h of incubations and two repairing conditions, light or dark conditions. Levene's test of equality of error variances across the groups was tested prior to two-way MANOVA. Dependent variables of three isolates had violated the assumption of homogeneity of variance-covariance, AKSP4 (p = 0.02), HNDR4 (p = 0.01) and HNDR2 (p = 0.03). Therefore, Pillai's Trace test in multivariate analysis is appropriate and was used in our statistical analysis.

The interactive effect of repair duration and incubation conditions was significant (p < 0.05) in the concentration of CPD across the four *Pseudogymnoascus* isolates, indicating both duration and incubation conditions contributed to the reduction of CPD concentration. On the other hand, all isolates demonstrated the concentrations of CPD were significantly reduced (p < 0.05) under light condition except AKSP4 (p = 0.13). Thus, there was no significant difference in the concentration of CPD in AKSP4 between the light (μ = 0.018, SD = 0.001) and the dark repair conditions (μ = 0.20, SD = 0.001).

Pairwise comparisons with Bonferroni adjustment were conducted and shown in Figure 4.6. Pairwise-comparisons between dark and light conditions within each time point in isolates AKSP3 and HNDR4 showed significant reduction of CPD concentrations in the presence of light, except for those recorded after 2 and 10 h repair incubation in AKSP4 (p = 0.06 and p = 0.14, respectively) and after 2 h repairing in HNDR2 (p = 0.19). This indicates the effects of light availability on the CPD concentration were not significant during the first two hours of repair after UVB exposure in these two isolates.

Pairwise comparisons in the light conditions showed there were significant reductions in the mean CPD concentrations in all isolates within the first 2 h of incubation, except in AKSP4 (p = 1.0), in which significant reduction was only observed after 6 h of repairing (p = 0.004). On the other hand, in the dark condition, AKSP3 and HNDR2 showed a significant reduction in mean CPD concentrations after 2 h of incubation but not AKSP4 (p = 0.30) and HNDR4 (p = 0.14), in which the CPD concentrations were significantly reduced only after 10 (p = 0.005) and 6 h (p = 0.001), respectively. These findings suggest that UVB-induced CPDs were repaired faster in the presence of light in *Pseudogymnoascus* spp.

Repair of 6-4PPs were measured in the four *Pseudogymnoascus* isolates after exposure to UVB radiation and repair under similar conditions (Figure 4.7). 6-4PP concentrations generated after exposure to UVB radiation were generally higher in AKSP3 ($\mu = 1.41 \times 10^{-3}$, SD = 1.45×10^{-4}) and HNDR4 ($\mu = 1.4 \times 10^{-3}$, SD = 1.21×10^{-4}), whereas only 5.56×10^{-4} and 7.71×10^{-4} ng ml^{-1} were recorded in AKSP4 and HNDR2, respectively. The concentrations of 6-4PP were reduced further when the repair incubation was done in the dark condition compared to the light condition.

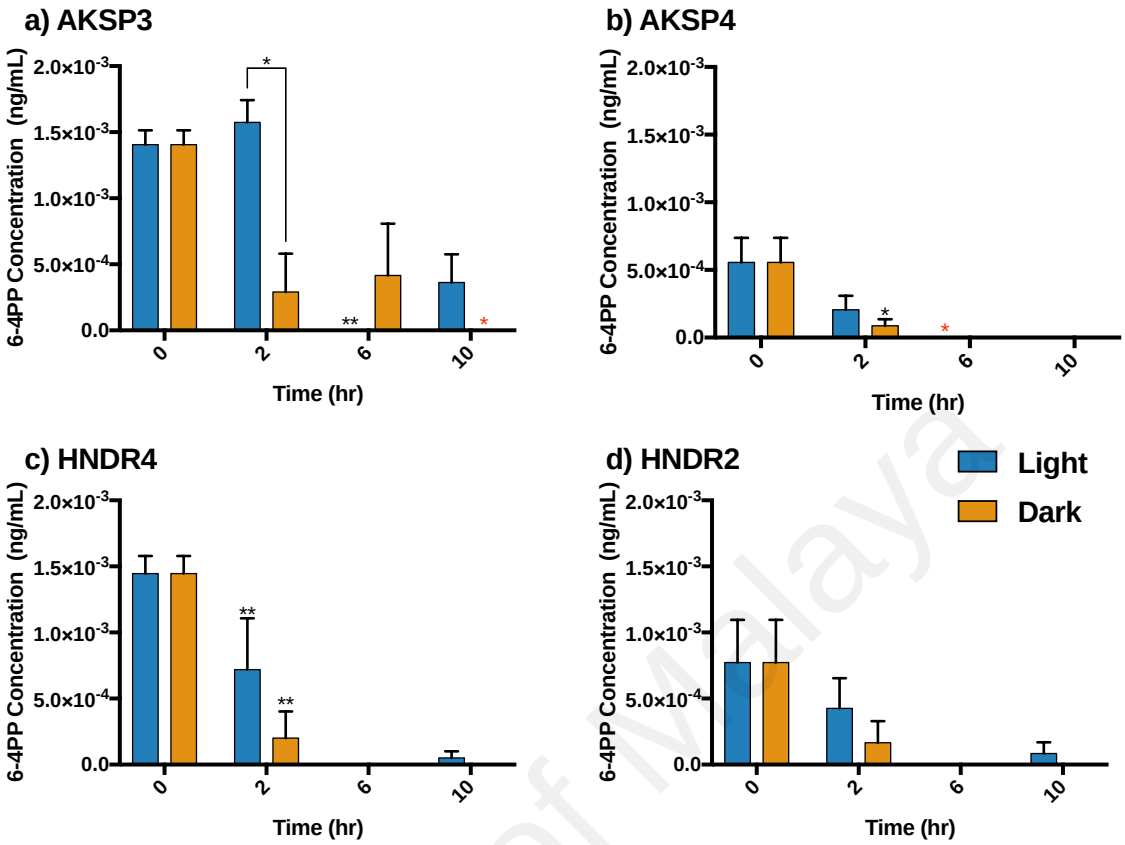

Figure 4.7: Concentration of pyrimidine 6-4 pyrimidone photoproducts (6-4PPs) quantified using ELISA under light and dark repair conditions after UVB exposure. Error bars are SEM of three biological replicates. *, $p < 0.05$; **, $p < .01$ indicate significant difference compared to control or as indicated; *, $p < 0.05$ is compared to the initial concentration under its respective condition.

Two-way MANOVA was conducted to determine the interactive effects of repair duration and incubation on the 6-4PP concentrations. Levene's test of equality of error variance was violated from the data recorded across all the isolates ($p < 0.05$). Therefore, Pillai's Trace test was used in our statistical analysis. The findings showed that the interactive effects of repair duration and incubation conditions were not significant ($p = 0.40$) in the concentrations of 6-4PP recorded across the isolates, except in isolate AKSP3 ($p = 0.01$).

The effect of light and dark incubation conditions on the concentrations of 6-4PP also showed no significant difference, with an *F*-test value of 1.320 (p = 0.31) and a medium to small effect size η^2_p of 0.29 across all the *Pseudogymnoascus* isolates. Comparisons of the sole effect of incubation condition within each isolate also demonstrated a similar result (p > 0.05). This suggest that the repair of 6-4PP in *Pseudogymnoascus* was not influenced by the incubation condition.

Pairwise comparisons with Bonferroni adjustment were tested (Figure 4.7). There were no significant differences in 6-4PP concentrations (p > 0.05) between the different incubation conditions at each time-point, except in AKSP3 after 2 h of repair (p = 0.02), in which 6-4PP concentration in the light conditions was 4.4-fold higher. In the comparisons across different time points, the 6-4PP concentrations were significantly reduced (p < 0.05*)* in HNDR4 after 2 h of incubation in both incubation conditions and after 2 h in AKSP4 (p = 0.0047) in only the dark condition. Meanwhile, significant difference was only observed after 6 (p = 0.001) and 8 h (p = 0.017) of incubation in light and dark, respectively, in AKSP3, whereas there was no significant reduction in 6-4PP concentrations throughout the entire repairing duration in HNDR2 (p > 0.05).

4.10 Validation of Primers for Relative Gene Expression

Primer amplification efficiencies of all the genes used in this study were determined by using the slope of the graph plotting threshold cycle (C_T) against the quantity of the samples (ng) ($E = 10^{(1/slope)}$). Figure 4.8 shows the results of the standard curves of all primer pairs used in this study. All primers tested showed efficiencies between 95-115% with R^2 values more than 0.99 (Table 4.5).

Table 4.5: Amplification efficiencies, and R^2 values of qPCR primer pairs.

Gene	R^2	Efficiency (%)	Gene	R^2	Efficiency (%)
GAPDH	0.999	98.94	*5.8S*	0.999	101.98
ACT1	0.999	100.61	*PGK1*	0.995	100.87
β-TUB	0.998	106.13	*RAD2*	0.995	100.99
SAR1	0.998	106.97	*PHR1*	0.997	99.79
DLD	0.994	103.58			

Amplified qPCR products were verified by sequencing and BLAST through NCBI database. As shown by the best matched from BLAST listed in Table 4.6, all of our qPCR primers amplified the intended target genes in *Pseudogymnoascus*, except *DLD* primer sets and PHR1_1F primer, which were found to have best-match with sequence encoding for unknown hypothetical protein, whereas sequence amplified by PHR1_1R was unable to match with any sequence. Further BLASTP verification was done using protein sequence from the best-match sequence and the results were listed in Table 4.6. Successfully sequenced qPCR products lack of overlapping region to merge the sequences (forward and reverse) as one, so the BLAST was done in separate to ensure the products amplified by the primer pairs were the intended target genes.

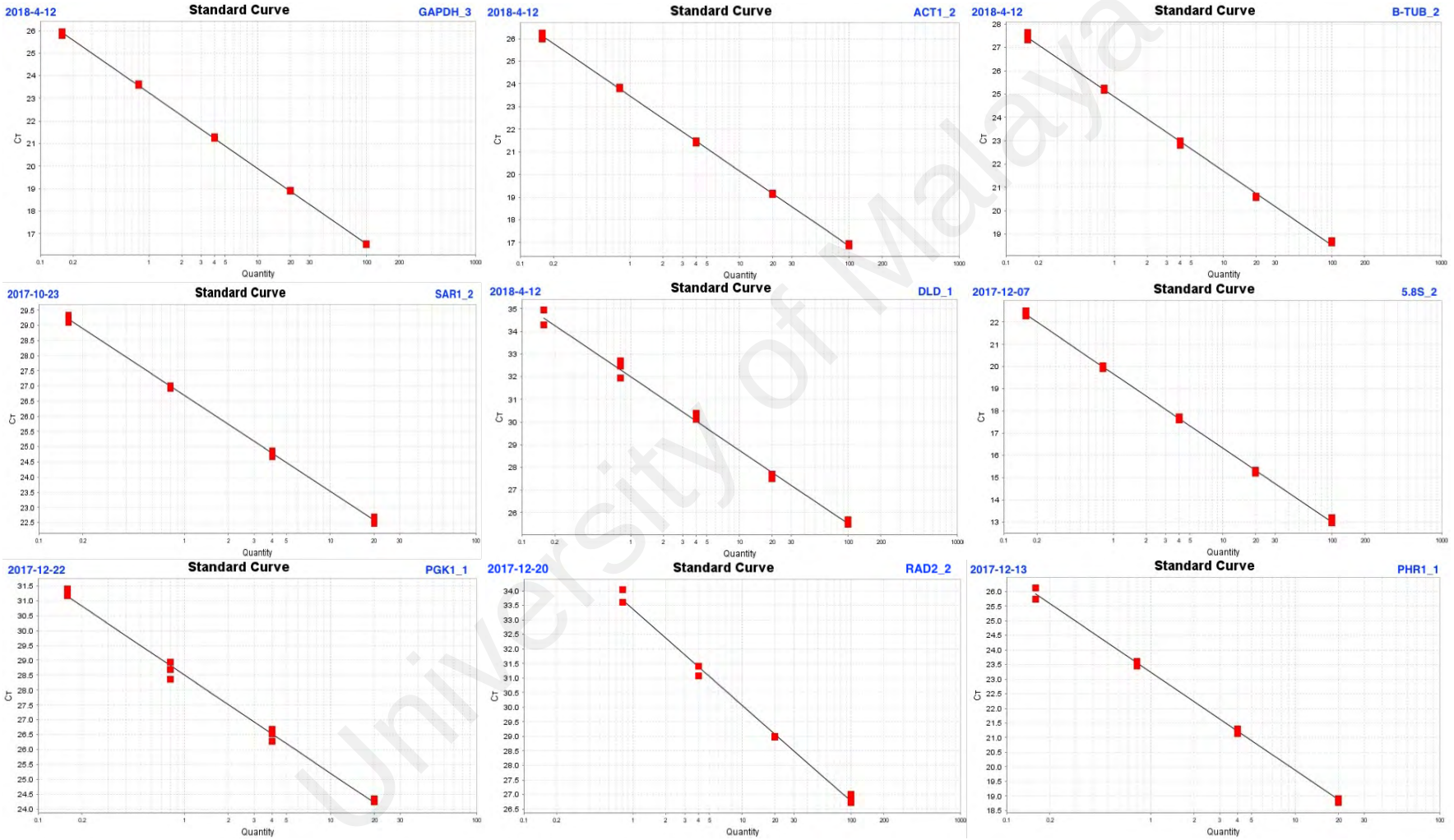

Figure 4.8: Standard curves of each primer pairs for target and reference genes; *GAPDH*, *ACT1*, *β-TUB*, *SAR1*, *DLD*, *5.8S*, *PGK1*, *RAD2*, and *PHR1*; plotted using five-fold dilutions of cDNA pooled from HNDR4.

Table 4.6: BLAST results of sequenced qPCR products using newly designed primers with gene names, product size, primer name, GenBank accession number, percentage of query coverage and identity matches.

Gene	Sequenced product size (nt)	Primer	BLAST result	Accession number	Query coverage (%)	Identity (%)
GAPDH	37	GAPDH_3F	*Pseudogymnoascus verrucosus* glyceraldehyde 3-phosphate-dehydrogenase mRNA	XM_018272569.1	100	100
	42	GAPDH_3R	*Pseudogymnoascus destructans* glycerol-3-phosphate dehydrogenase (GPD1_1),mRNA	XM_024464445.1	100	100
β-TUB	47	β-TUB_2F	*Pseudogymnoascus verrucosus* tubulin beta chain mRNA	XM_018269756.1	100	100
	75	β-TUB_2R	*Pseudogymnoascus destructans* Tubulin beta chain (Beta tubulin) (TUB2), mRNA	XM_024464846.1	100	99
DLD	64	DLD_1F	*Pseudogymnoascus verrucosus* hypothetical protein mRNA;	XM_018272077.1	98	97
	62	DLD_1R	*Pseudogymnoascus verrucosus* hypothetical protein mRNA;	XM_018272077.1	100	94
		BLASTP:	*Pseudogymnoascus destructans* hypothetical protein VC83_02315; **region name:** FAD-oxidase_c	XP_024326496.1	100	96
ACT1	67	ACT1_2F	*Pseudogymnoascus destructans* actin (ACT1), mRNA	XM_024471408.1	100	99
	61	ACT1_2R	*Pseudogymnoascus verrucoses* actin mRNA	XM_018271846.1	100	97
PGK1	61	PGK1_1F	*Pseudogymnoascus destructans* phosphoglycerate kinase (PGK1), mRNA	XM_024464817.1	93	92
	47	PGK1_1R	*Pseudogymnoascus verrucosus* phosphoglycerate kinase mRNA	XM_018269790.1	83	96
SAR1	93	SAR1_2F	*Pseudogymnoascus destructans* COPII coat GTPase (SAR1), mRNA	XM_024471700.1	97	99
	88	SAR1_2R	*Pseudogymnoascus destructans* COPII coat GTPase (SAR1), mRNA	XM_024471700.1	100	97
5.8S	45	5.8S_2F	*Pseudogymnoascus* sp. isolate FI23 small subunit ribosomal RNA gene, partial sequence; internal transcribed spacer 1 and 5.8S ribosomal RNA gene, complete sequence; and internal transcribed spacer 2, partial sequence	MH128305.1	100	100
	52	5.8S_2R	*Pseudogymnoascus* sp. isolate FI23 small subunit ribosomal RNA gene, partial sequence; internal transcribed spacer 1 and 5.8S ribosomal RNA gene, complete sequence; and internal transcribed spacer 2, partial sequence	MH128305.1	100	100
PHR1	67	PHR1_1F	*Pseudogymnoascus verrucosus* hypothetical protein mRNA	XM_018278541.1	100	96
		BLASTP:	*Pseudogymnoascus verrucosus* hypothetical protein VE01_09125; **region name:** Deoxyribodipyrimidine photolyase, *PHRB*	OBT92751.2	100	100
	54	PHR1_1R	N/A	N/A	N/A	N/A
RAD2	57	RAD2_2F	*Pseudogymnoascus destructans* DNA repair protein (RAD2), partial mRNA	XM_024467097.1	100	98
	52	RAD2_2R	*Pseudogymnoascus destructans* DNA repair protein (RAD2), partial mRNA	XM_024467097.1	100	96

4.11 Melt Curve Analysis

Melt curve analysis was performed for every real-time qPCR run at the end of the reaction. It is an important step to demonstrate the specificity of the primers and to ensure the accuracy of the expression level measured. All of our primer sets yielded single peaks, demonstrating no non-specific amplicons or primer dimers occurred in the qPCR reactions with *Pseudogymnoascus* cDNA as templates. Figure 4.9a shows a single peak melt curve graph in a real-time qPCR reaction, whereas Figure 4.9b demonstrates a melt curve graph containing non-specific amplicon and primer dimer during primer validation for efficiency test. For gene expression analysis, only primers yielding single melt-curve peaks were used. The melt curve graph for each primer pairs is attached in Appendix I.

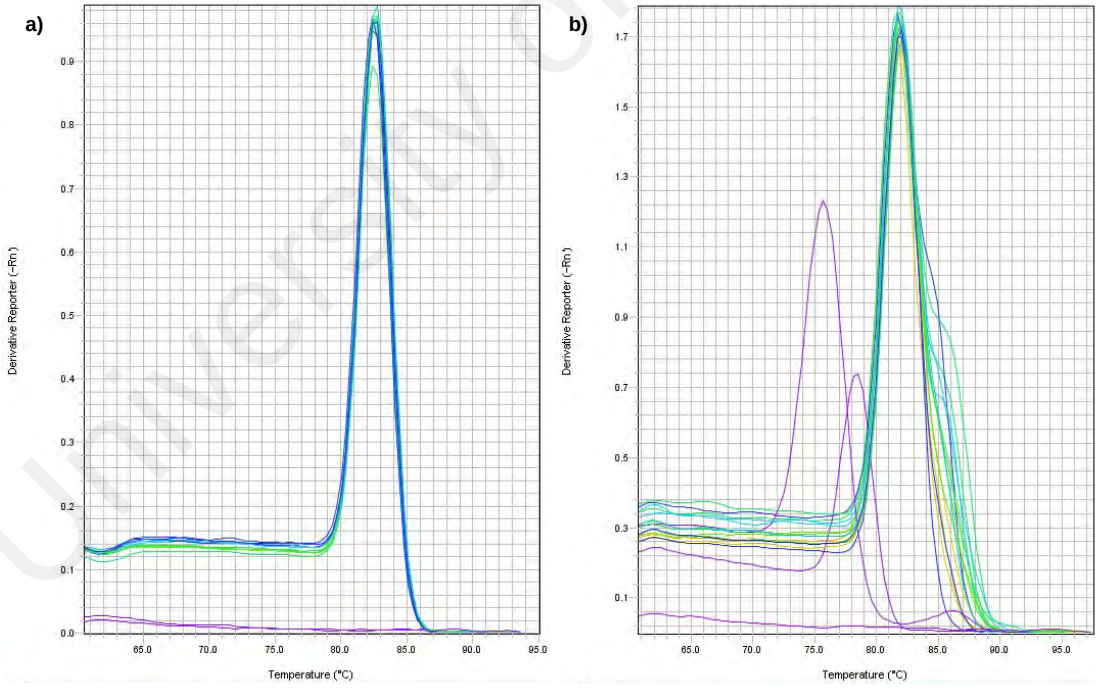

Figure 4.9: Melt curve graphs of real-time qPCR runs that generate a) single peak for each sample at the temperature and b) nonspecific PCR products in *Pseudogymnoascus* cDNA samples.

4.12 Selection of Reference Genes

The expression stability of each gene was validated using three different programs, geNorm (Vandesompele et al., 2002), Bestkeeper (Pfaffl et al., 2004) and NormFinder (Andersen et al., 2004), to identify the most stable genes for normalization. Table 4.7 shows the ranking of candidate reference genes according to the expression stability calculated by these programs. Consistently, all three programs demonstrated that *ACT1* and *GAPDH* were the most stable genes, ranked in the top three despite the different algorithms applied. Although the combination of *β-TUB* and *PGK1* demonstrated the best stability value of 0.54 on GeNorm, *ACT1* was selected as the most stable gene with a stability value of 0.714. Thus, these two genes were first selected as our reference genes for normalization. NormFinder found *GAPDH* and *SAR1* to be the best combination for reference genes with a stability value of 0.174. Although Bestkeeper showed that *SAR1* was not the most stable to serve as an internal control gene, it was consistently ranked within the top three in geNorm and NormFinder, thus *SAR1* was selected as the third gene to be included for normalization in our gene expression analysis.

Table 4.7: Rank of candidate reference genes according to the expression stability calculated by geNorm, Bestkeeper and NormFinder. The candidate reference genes are listed with corresponding stability values and ordered by decreasing expression stability.

Ranking order	geNorm		Bestkeeper		NormFinder	
	Gene name	Stability value (M)	Gene name	Stability value (r)	Gene name	Stability value
1	*ACT1*	0.714	*ACT1*	0.853	*ACT1*	0.249
2	*GAPDH*	0.729	*PGK1*	0.790	*GAPDH*	0.252
3	*SAR1*	0.736	*GAPDH*	0.746	*SAR1*	0.293
4	*β-TUB*	0.835	*β-TUB*	0.724	*DLD*	0.359
5	*PGK1*	0.842	5.8S	0.699	*PGK1*	0.368
6	5.8S	0.843	*SAR1*	0.694	*β-TUB*	0.387
7	*DLD*	0.913	*DLD*	0.534	5.8S	0.403

4.13 Relative Expression of *PHR1* and *RAD2* After UVB Exposure

The expression profiles of DNA repair genes were evaluated in four isolates of *Pseudogymnoascus* under light and dark repair conditions following UVB treatment. qPCR was performed to profile the expression of *RAD2* and *PHR1* to determine the principle DNA repair machinery employed by *Pseudogymnoascus* spp. to repair UVB-induced DNA damage. Relative mRNA expression of targeted genes was then derived by normalizing with three most stable genes, *GAPDH*, *SAR1* and *β-TUB* and using the $2^{-\Delta\Delta Ct}$ method.

The expression of *RAD2* was found to increase at least three-fold in all *Pseudogymnoascus* isolates after 130 min of UVB exposure, whereas *PHR1* was found to be repressed by up to four-fold after exposure to UVB radiation (Figure 4.10). To determine the effects of the UVB radiation on the relative expression of the target genes, a separate MANOVA was performed with the UV treatments as the independent variable, and the relative fold change in the target genes in four separate isolates as the dependent variable.

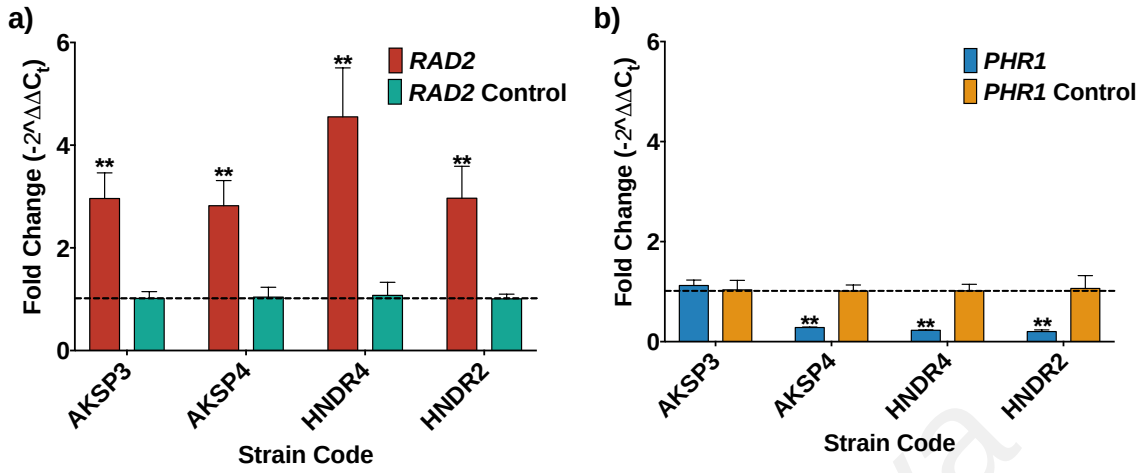

Figure 4.10: Expression of DNA repair genes a) *RAD2* and b) *PHR1* in four *Pseudogymnoascus* spp after UVB exposure. Expression levels are presented as fold change (± SEM) relative to control. Fold change ~ 1, indicated by dotted line. The significant difference between the treatments are indicated by *, $p < 0.05$ and **, $p < 0.01$.

Findings revealed no significant multivariate effects of different UV treatments in relation to the relative expression of target genes, *RAD2* ($p = 0.74$) and *PHR1* ($p = 0.122$) across four different isolates. This indicates that all *Pseudogymnoascus* isolates responded similarly in the expression of the target genes after exposure to UVB radiation. As shown in Figure 4.10, univariate testing in the relative expression of *RAD2* gene indicated the effects of different treatments are significance ($p < 0.05$) across four *Pseudogymnoascus* isolates. In contrast, the effects of different treatments in the expression of *PHR1* gene are significant ($p < 0.05$) in all three isolates except in AKSP3 ($p = 0.71$).

4.14 Relative Expression of *PHR1* and *RAD2* During Repairing Period

After UVB exposure, the isolates were incubated in two conditions, light and dark, to induce Phr and NER, respectively. The expression of the target genes was then profiled across the *Pseudogymnoascus* isolates to investigate the effect of light on the induction of Phr and NER. Figure 4.11 shows the expression profile of *RAD2* in both repair conditions across four *Pseudogymnoascus* isolates after 2 h of incubation. The expression of *RAD2* was induced by approximately 3-fold in Antarctic strains in both light and dark conditions, but in Arctic strains, only HNDR4 expression was induced by 2.42 ± 1-fold, whereas the rest remained similar to the control.

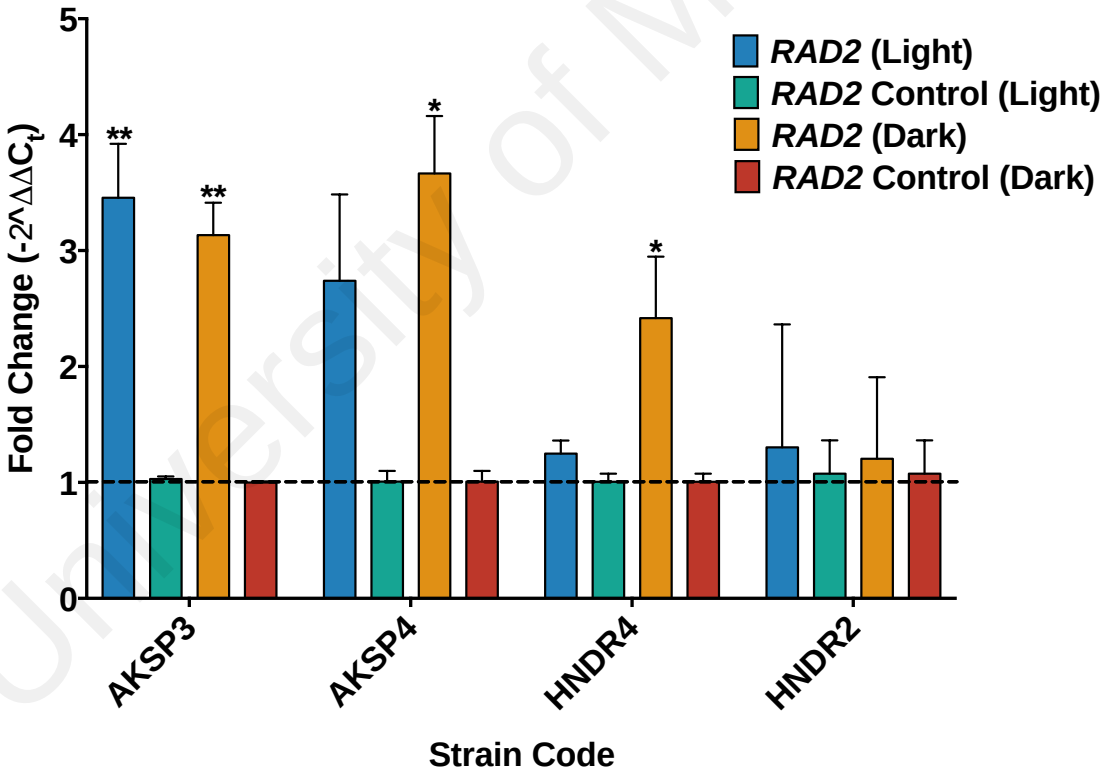

Figure 4.11: Relative expression of *RAD2* in Arctic and Antarctic *Pseudogymnoascus* spp. after UVB exposure. Expression levels are presented as fold change (± SEM) relative to control. Fold change ~ 1, indicated by dotted line. Significant difference between the UV-treated and controls are indicated by *, $p < 0.05$ and **, $p < 0.01$.

The interaction of *RAD2* expression with four repair incubation conditions across the isolates was examined by MANOVA. The four independent variables included: UV-treated and then incubated in light and dark conditions [*RAD2* (Light) and *RAD2* (Dark)] and non-UV-treated [*RAD2* Control (Light) and *RAD2* Control (Dark)]. As expected, the findings of the multivariate test showed statistical significance ($p = 0.015$) with a strong observed power of 0.92 and a moderate to high effect size, η^2_p of 0.63. This indicates that the *Pseudogymnoascus* isolates did not respond similarly in terms of the *RAD2* expression in the different repairing conditions.

Univariate analysis was performed to determine the effect of different repair conditions in each isolate. Results showed significant difference in all tested isolates except HNDR2 ($p = 0.99$), which showed a small effect size, η^2_p of 0.01, indicates the treatments accounted only 1% of the overall variance in *RAD2* expression in HNDR2. Multiple comparisons with Bonferroni adjustment was performed (Figure 4.11). The findings demonstrated no significant difference between the light and dark repair conditions in both UV-treated and controls, but significant *RAD2* upregulation in both light and dark repair conditions, 3.46 ± 0.80-fold and 3.13 ± 0.49-fold, respectively in UV-treated AKSP3 ($p = 0.001$ and $p = 0.003$, respectively) and between the UV treated and controls in dark repair condition of UVB-treated AKSP4 (3.66 ± 0.86-fold, $p = 0.019$), and HNDR4 (2.42 ± 0.92-fold, $p = 0.04$).

In the expression profile of *PHR1*, downregulation of the target gene was observed across the four isolates after exposure to UVB radiation and incubated in either light or dark conditions, except in AKSP4, in which 2.92 ± 0.05-fold upregulation was recorded (Figure 4.12). The down-regulation of *PHR1* ranged from the least in AKSP3 incubated in light condition after UVB exposure (2.63 ± 0.10-fold) to the most in AKSP4 incubated in light condition after UVB exposure (5.56 ± 0.02-fold). Similarly, the interaction of the relative expression of *PHR1* in four conditions [*PHR1* (Light), *PHR1* (Dark), *PHR1* Control (Light) and *PHR1* Control (Dark)] across the isolates was examined by MANOVA. Findings showed that there is a significant difference in the interactive effects of different conditions across the four isolates of *Pseudogymnoascus* (p = 0.01). This indicates that the expression of *PHR1* was significantly downregulated after exposure to UVB radiation regardless of the incubation conditions, either light or dark, except in AKSP4.

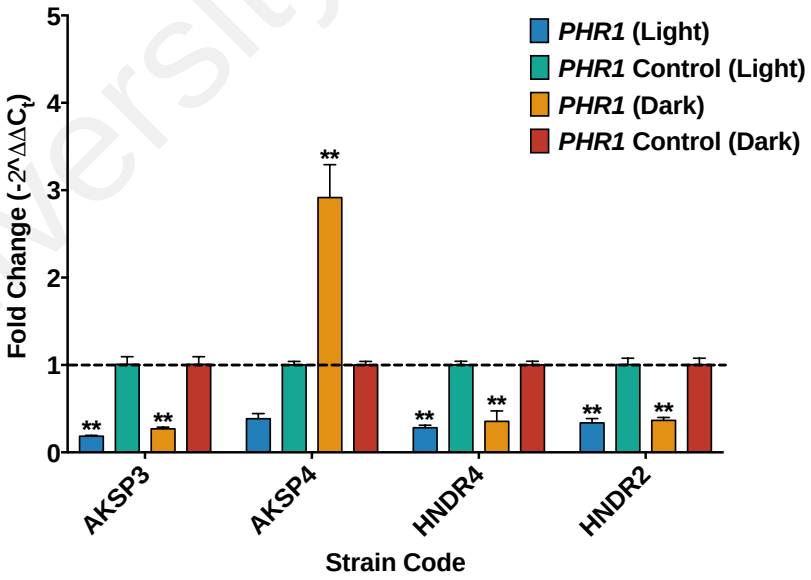

Figure 4.12: Relative expression of *PHR1* in Arctic and Antarctic *Pseudogymnoascus* spp. after UVB exposure. Expression levels are presented as fold change (± SEM) relative to control. Fold change ~ 1, indicated by dotted line. Significant difference between the UV-treated and controls are indicated by *, p < 0.05 and **, p < 0.01.

Univariate analysis was then conducted to determine the effect of different repair conditions in each isolate. Similar results were obtained, in which all isolates showed a significant difference ($p < 0.05$) with high effect size, η^2_p of 0.93 to 0.95. Multiple comparisons with Bonferroni adjustment was tested (Figure 4.12). Briefly, there is no significant difference between different repair conditions within UV-treated samples and controls, but significant difference was observed between UV-treated samples and controls across all tested isolates ($p < 0.01$) except light repair condition in AKSP4 ($p = 0.32$). The rest of the comparisons demonstrated downregulation of *PHR1* with *p* values less than 0.01, except the expression was significantly upregulated at 2.92 ± 0.19-fold in AKSP4 ($p = 0.001$) when incubated in dark condition.

4.15 Relative Expression of *PHR1* and *RAD2* Without UVB Exposure

In order to demonstrate that the expression of *PHR1* was responsive to the exposure of white light, the expression of the *RAD2* and *PHR1* was compared between the controls incubated in light and dark conditions for 2 h without UVB exposure (Figure 4.13). Three isolates of *Pseudogymnoascus* showed induction of *PHR1* in response to white light with 2.30 ± 0.80, 2.86 ± 0.33 and 1.8 ± 0.02-fold *PHR1* upregulation in AKSP3, AKSP4 and HNDR2, respectively (Figure 4.13b). The expression of *RAD2* was also upregulated under white light exposure but in a relatively less degree compared to the expression of *PHR1*, ranging from 1.12 to 1.98-fold elevation

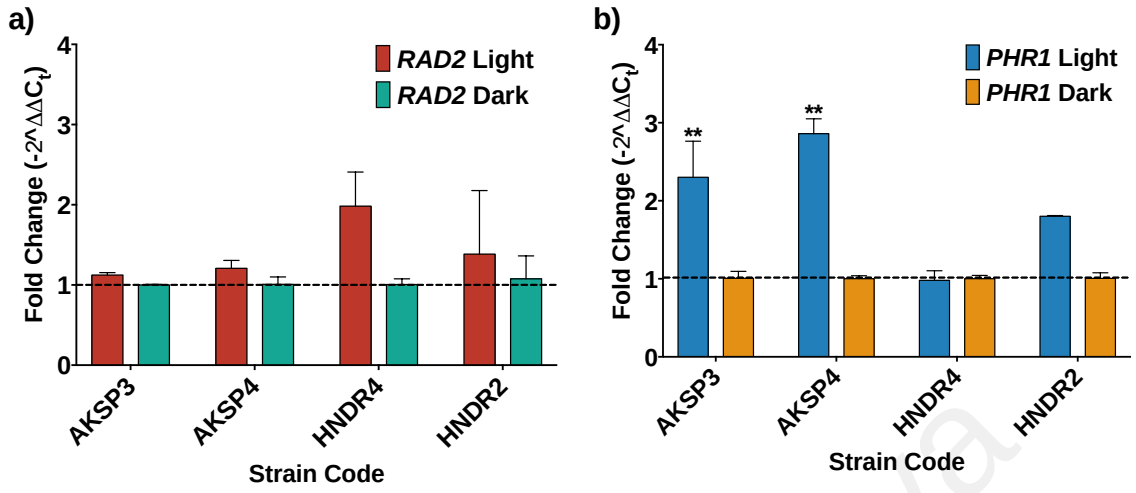

Figure 4.13: Expression of DNA repair genes a) *RAD2* and b) *PHR1* in four *Pseudogymnoascus* spp. after incubation in light and dark condition for 2 h without UVB exposure. Expression levels are presented as fold change (± SEM) relative to control. Fold change ~ 1, indicated by dotted line. The significant difference between the treatments are indicated by *, $p < 0.05$ and **, $p < 0.01$.

MANOVA analysis was performed to determine the effect of light's availability on the expression of *RAD2* and *PHR1*. The test showed that there was no significant difference in the expression of *RAD2* and *PHR1* across the isolates in response to white light exposure ($p = 0.17$ and $p = 0.14$, respectively). This indicates all isolates responded similarly toward the exposure of white light. Multiple comparisons revealed that despite the upregulation of *RAD2* was observed toward white light exposure, the differences were insignificant ($p > 0.05$) except in AKSP3 ($p = 0.017$), in which *RAD2* was upregulated by 0.12 ± 0.03-fold with a great effective size, η^2_p of 0.80. Meanwhile, the expression of *PHR1* was significantly upregulated toward white light exposure in AKSP4 (1.86 ± 0.19-fold, $p < 0.01$) and HNDR2 (0.8 ± 0.07-fold, $p < 0.01$), except in AKSP3 (1.29 ± 0.47-fold, $p = 0.05$) and HNDR4 (0.02 ± 0.13-fold, $p = 0.88$).

CHAPTER 5: DISCUSSION

5.1 Sequence Variation and Phylogenetic Analysis of *Pseudogymnoascus*

The identification of *Pseudogymnoascus, Geomyces* and their allies has been a challenging due to shared similar morphological structures and the lack of DNA marker sequences in the GenBank database in the last few decades. This issue begun to be resolved after the emergence of white-nose syndrome (WNS) in bats, which caused by *P. destructans,* that leading to a great depletion on bat's population (Gargas et al., 2009) and the reclassification of *Geomyces* and its allies by Minnis and Lindner (2013). Through the phylogenetic tree we constructed, it is evident that ITS alone provided poor resolution for use as a bar coding gene for *Pseudogymnoascus* and has limited value for species identification in this genus. Although *P. appendiculatus* is able to be resolved by ITS, but the majority of the members in *Pseudogymnoascus* is scattered among distantly related species (Figure 4.1, page 58). This observation is in congruence with the findings of Lindner et al. (2011), Lorch et al. (2013) and Minnis and Lindner (2013) that ITS sequence is apparently lacks sufficient genetic variation and additional markers are required to resolve this issue; however, the ITS sequence provides sufficient inter-genus variation to differentiate *Pseudogymnoascus* from *Geomyces* that is still frequently being misidentified.

The phylogeny based on the work of Minnis and Lindner (2013) has successfully delineated the clades A, B and C that were not able to be inferred through the tree constructed in our study. These groups of *Pseudogymnoascus* share similar geographical distribution behavior (Minnis & Lindner, 2013). Although the tree successfully grouped clade B (where our isolates are grouped) apart from clade A&C with high supporting values, the barcoding gap is absent due to overlapping of the inter-species variation of 1.69% between clade A&C and clade B, and the intra-species

variation of 1.69% within clade A&C. This observation might be due to the differences of DNA markers used in phylogenetic analysis compared to Minnis and Lindner (2013). The exclusion of two DNA markers, *RPB2* and *TEF1*, from the analysis in this study has lowered the percentage of parsimony-informative base pairs by 6% (and 1207 characters shorter), and this shortage might have contributed to the failure in separating clades A, B and C. Thus, we suggest to identify these three clades as a single clade due to the lack of barcoding gap until further taxonomic work, especially morphological characterization, is conducted.

5.2 The Effects of UVR Exposure on the Growth of Fungi

The survival of an organism in natural environments depends on its ability to respond appropriately to the changes in their external environment. Fungi are the most cosmopolitan organisms that have evolved to employ complex and conserved molecular mechanisms and regulatory signaling pathways to adapt and respond to a variety of stress induced by the environment. When fungi and other microbial organisms have to deviate themselves from optimal growth in order to adapt and survive in the environmental niche, they are considered as being in a stress condition.

The stress induced by UVB radiation was investigated using *Pseudogymnoascus* isolates in our study and the results showed significant reduction in colony growth rates between 22 to 35% relative to cultures that exposed to only PAR in a duration of 10 d. The reduction of growth rates observed was smaller compared to what was reported by Hughes et al. (2003), who investigated the growth of five Antarctic fungal species under UVB radiation. Hughes et al. (2003) reported a reduction of 33 to 100% in surface hyphal extension rates under UVB DNA-weighted flux of 6.23×10^{-4} kJ m^{-2} s^{-1}. In the same study, *P. pannorum* showed a greater reduction in surface and submerged hyphal extension rates (94 and 42%, respectively) compared to the values recorded in our

study. The differences observed might be due to different UVB dosage introduced in current study. In addition, the duration of UVB exposure might be one of the factor contributing to the differences observed. A short duration of UVB radiation was introduced in our treatments, whereas, Hughes et al. (2003) exposed their cultures to continuous UVB irradiation for 24 h. Although, we provided a large dosage in a short time exposure, but the resting period without UVB exposure in our study allowed the culture to recover from the damage. Furthermore, the irradiances were weighted according to the DNA action spectrum of Setlow (1974) in the study conducted by Hughes et al. (2003), whereas we provided daily unweighted UVB radiation dosage due to lack of facilities for the measurement of DNA action spectrum. DNA action spectrum is a plot of the rates of chemical reactions on DNA to calculate carcinogenic effectiveness as a function of the wavelength of light reaction (Sancar, 2004; Setlow, 1974). The carcinogenic effectiveness might have been much more lower in our study compared to Hughes et al. (2003), leading to lower reduction rates observed.

In another study on fungal growth response to UV, litter and phylloplane fungi from temperate regions showed growth inhibition under the UVB_{DNA} exposure of 1.7 kJ m^{-2} d^{-1} (Moody et al., 1999). The mean hyphal extension rate reduction of litter fungi was 23.3%, in the phylloplane fungi it was 0.71%. In comparisons to our findings, our data suggests that some resistance to UVB has ostensibly developed in the polar *Pseudogymnoascus* fungi, with an average of 31% growth rate reduction under a three times stronger UVB dosage than was used by Moody et al. (1999).

Growth inhibition under UVB radiation can be explained by several reasons. Under suboptimal conditions, environmental stress response (ESR) is activated to increase the chances for stress survival. The transient changes in the expression of ESR genes always come at the cost of optimal cellular growth to allow the cell to rapidly adjust its

internal milieu in order to adapt to new conditions (Gasch, 2003; Medina et al., 2015). For instance, genes involved in growth-related processes, RNA metabolism, nucleotide biosynthesis, secretion and other metabolic processes in fungi were reported to be repressed upon the activation of ESR (Causton et al., 2001; Gasch et al., 2000). Similarly, many genes involved in RNA metabolism, cell cycle and organelle organization and biogenesis were repressed under the irradiation of UV in *Saccharomyces cerevisiae* (Wade et al., 2009), suggesting a similar ESR could be activated under UVB exposure in *Pseudogymnoascus* leading to the growth retardation observed. However, more investigation on the stress signaling pathway in *Pseudogymnoascus* is required to elucidate the possible enrollment of a similar pathway.

In addition, the expression of *RAD2* might provide another reason for the growth retardation under UVB exposure. Our results demonstrated an upregulation of *RAD2*, a gene associated with UV-induced DNA damage, CPDs and 6-4PPs, upon UVB radiation. The upregulation of *RAD2* suggests the possible activation of a checkpoint pathway leading to growth inhibition in *Pseudogymnoascus.* In proliferating cells, the integrity of DNA is tightly controlled by comprehensive mechanisms to avoid the passing of damaged DNA to the next generations, which could lead to mutation or apoptosis. This control has been reported to be achieved via cell-cycle arrest involving the expression of *RAD9*, which is essential for the activation of G1 (first growth phase) and G2 (growth and mitosis preparation phase) checkpoints (Al-Moghrabi et al., 2001; Siede et al., 1993). A recent study reported the tight coordination between *RAD9* and *RAD2*, in which *RAD9* deletion impaired RAD2-induced cell growth arrest in *S. cerevisiae*, whereas overexpression of RAD2 caused cell growth arrest (Kang et al.,

2010). This observation further supports the possible involvement of *RAD2* in the promotion of cell-cycle arrest in *Pseudogymnoacus* upon UVB radiation.

5.3 The Effects of UVB Radiation on Fungal Asexual Reproduction Activities

Asexual reproduction plays a crucial component in completing the life cycle of fungi that lack of heterothallic system. Fungi have evolved to form various shapes and structures to aid asexual reproduction activities and to survive in the natural environment. Despite the asexual reproduction activities in fungi have been frequently reported to be regulated by light and near UV light (Braga et al., 2015; de Menezes et al., 2015; Ruger-Herreros et al., 2011), however there is a lack of research on the negative impact of UV radiation on conidiogenesis.

Our results from scanning electron microscopy demonstrated that the conidia production in *Pseudogymnoascus* was inhibited under UVB exposure. In contrast, other species have been reported to promote conidia production under UV radiation. For instance, UVA radiation has been shown to enhance the spore production in *Alternaria solani*, whereas UVB and enhanced levels of UVA radiation had a suppresive effect on spore production (Fourtouni et al., 1998). On the other hand, the Antarctic fungus, *Phoma herbarum* also has been reported to produce conidia within 24 h of UVB exposure accompanied by pigmentation (Hughes et al., 2003). Spore production in fungi appears to depend on the balance between different UV wavelengths and the intensity of light being provided. As reported in other *Alternaria* spp., spore production was enhanced by near ultraviolet radiation and inhibited by blue light spectrum (Kumagai & Oda, 1969, 1973; Vakalounakis & Christias, 1981). Thus, this indicates that the induction or repression of conidiogenesis in response to different light wavelengths is often species-dependent.

In concordance to the inhibition of asexual reproduction activities, the expression of *PHR1* was significantly repressed after UVB exposure, suggesting that the *PHR1* gene, encoding CPD photolyase I, might play a role in regulating asexual reproduction activities in *Pseudogymnoascus* rather than in the repair of UV-induced DNA repair. This is supported by Bluhm and Dunkle (2008), who reported the conidiogenesis and cercosporin biosynthesis in *Cercospora zea-maydis* were influenced by the expression of *PHL1* (cryotochrome/6-4 photolyase-like gene). The disruption of *PHL1* completely affected the production of conidia, although in the wild type strain conidiation was also dramatically reduced under constant light exposure but was enhanced during growth in constant darkness (Bluhm & Dunkle, 2008). In a similar study, the disruption of a DNA photolyase gene, *PHR1* in *Beauveria bassiana* conferred a defect in conidiogenesis, further supporting the roles of photolyase genes in regulating asexual reproduction activities in certain fungi (Chelico & Khachatourians, 2008; Lee et al., 2018). Although a separate photosensory pathway has been proposed for Phr and sporulation in *Trichoderma* (Berrocal-Tito et al., 1999; Sametz-Baron et al., 1997), it remains possible that similar photoreceptor might be involved in both responses but distinct transduction steps are employed.

Recent studies have shed some light on understanding the regulation of conidia production by multiple cryptochrome/photolyase family proteins in fungi. The expression of *CRY1* (encoding CPD photolyase I) has been reported to not be responsible in regulating asexual reproduction activities in *Botrytis cinerea*, but the conidia production was influenced by the CRY-DASH protein, CRY2 which acts as the negative regulator of photoinduced conidiation (Cohrs & Schumacher, 2017). The deletion of *CRY2* induced conidiation in white and black light, whereas overexpression of *CRY2* resulted in fewer conidia in *B. cinerea*. Similarly, the CRY-DASH protein,

CRYD in *Fusarium fujikuroi* and CRYA in *Aspergillus nidulans* also demonstrated similar negative regulatory responses (Bayram et al., 2008; Castrillo et al., 2013), further supporting the possible regulation of sexual and asexual activities by cryptochrome/photolyase family genes in fungi. If this is true, decrease in snow coverage and the melting of ice following climate change could expose to UVB radiation and affect its survival and reproduction of *Pseudogymnoascus* in the polar regions.

5.4 Chemical Protective Strategy in Fungi Against UVB-induced Damages

Pigments form the first defense protective layer in certain species of fungi to absorb and limit the penetration of UV wavelengths that induce various cellular damages. Besides absorbing UV wavelength, certain fungi has developed abilities to utilize these secondary metabolites for other functions such as cell wall strengthening or as a quencher of photosensitization products and ROS induced by UV radiation (Irazusta et al., 2013; Pihet et al., 2009).

Our results demonstrated no visible increase in pigment production in *Pseudogymnoascus* isolates under UVB radiation for a duration of 10 d. Similarly, carotenoid production in *Cystofilobasidium capitatum* was reported not significantly induced under UVB radiation, which also did not result in a change in UVB survival rate (Moliné et al., 2009). In contrast, Libkind et al. (2004) demonstrated water yeasts with high constitutive levels of carotenoids were less stimulated by UV radiation than those with low basal carotenoids content. Presumably, the differences reported were due to different wavelengths of UV radiation and the intensity of UV light provided in both studies.

In the Antarctic fungus, *P. herbarum,* brown pigments were produced within 24 h of UVB exposure, which was accompanied by the production of conidiomate and conidia (Hughes et al., 2003). *P. herbarum* was also reported to be the most UVB resistant among the strains tested, thus indicating that the UV stress induced might not have reached the threshold for the activation of ESR. Although we observed no pigmentation change in *Pseudogymnoascus* isolated but inhibition in conidia production was observed. These observations suggest that pigment and conidia production in fungi might share a similar signaling pathway under UV radiation. This is also supported by the observation that the disruption of genes involved in melanin synthesis, including *BMR2* and *CMK1* encoding 1,3,8-trihydroxynaphthalene and mitogen-activated protein (MAP) kinase, in *Alternaria alternata* and *Collctotrichum lagenarium*, respectively can affect pigment synthesis and conidia production (Kawamura et al., 1999; Takano et al., 2000).

According to a study of *Arabidopsis thaliana*, a R2R3 MYB-related transcription factor, *AtMYB4* that functions as a transcriptional repressor, has been reported to control the production of pigments under UVB radiation. (Jin et al., 2000). Prolonged exposure of UVB radiation downregulated the expression of *AtMYB4*, in association with decreased sinapate esters (source of protectant sunscreen in *Arabidopsis*) levels and increased UV sensitivity in *Arabidopsis*. Similar MYB-like protein, *BAS1* has been identified in certain fungal species including *S. cerevisiae*, *A. niger,* and *Fusarium graminearum* (Arratia-Quijada et al., 2012; Kim et al., 2014b). The deletion of *BAS1* has been reported to enhance the pigment production (riboflavin) in *Ashbya gossyppii*, whereas overexpression of *BAS1* promotes fungal growth and sporulation in *Magnaporthe oryzae* (Mateos et al., 2006; Yang et al., 2017). Thus, it is possible that the pigment production and conidiogenesis might share a similar signaling pathway in

response to UVB radiation, with the involvement of MYB-related transcription factors, leading to the observation made in our study.

5.5 DNA Repair in Fungi Under Light and Dark Conditions

Various DNA repair mechanisms are available in both eukaryotes and prokaryotes to repair damage caused by various types of stresses. NER and Phr are two particular mechanisms that are involved in repairing UV-induced DNA lesions, CPDs and 6-4PPs, which were quantified and analysed in our study. Our observations opened up more questions on which is the key mechanisms that function in the regulation of DNA repair processes in *Pseudogymnoascus*. Different approaches have been used to investigate the principal machinery to repair these two types of DNA damage. For instance, Chelico et al. (2006) investigated the key mechanisms of DNA damage repair pathway following UV radiation in entomopathogenic fungi using a physiological approach by determining spore viability under two incubation conditions, light and dark, which were assumed to induce Phr and NER, respectively. Multiple studies have shown that the survival rate of spores was improved in light condition (Braga et al., 2002; Chelico et al., 2006; Chelico & Khachatourians, 2008), but there is a lack of direct evidence to support that the improvement was due to Phr in repairing the damage caused by UV radiation. It is important to determine if Phr is transcriptionally induced by different treatments *in vivo* to explain its functional role in DNA repair. In this study, we investigated the expression of two DNA repair genes in *Pseudogymnoascus* spp., *RAD2* and *PHR1*, which were selected from genes known to be involved in NER and Phr (Costa et al., 2003; Rastogi et al., 2010; Sinha & Häder, 2002; Wang et al., 2015).

Our results showed that the expression of *RAD2* was upregulated significantly by 3-fold, whereas, the expression of *PHR1* was downregulated significantly by 4-fold after UVB radiation. This indicates that NER was likely responsible for the repairing of

UVB-induced DNA damage in *Pseudogymnoascus* prior to the repairing conditions applied. Our observations are in agreement with the roles of NER in executing their functions in a non-light dependent manner, commonly regarded as a dark repair (Dijk et al., 2014). The mechanism of NER is dependent on damage recognition, which initiates the repairing process and recruitment of other components in response to genetic insult (Costa et al., 2003).

On the other hand, Phr repairs lesions in a light-driven process, in which the photon energy is captured and utilized to break the covalent bond between two pyrimidines (Sancar, 1994). The induction of cryotochrome/photolyase family genes including *PHR1* and *CRY1* is regulated by light *via* the blue light receptor protein, *BLR-1* and *BLR-2*, and white-collar proteins, WC-1 and WC-2, in *Trichoderma atroviride* and *Neurospora crassa*, respectively (Cheng et al., 2002; García-Esquivel et al., 2016). Thus, the UV-irradiated *Pseudogymnoascus* cultures were incubated in the presence of light to induce photoreactivation. Surprisingly, the expression of *PHR1* remained suppressed upon incubating for 120 minutes.

A similar response has been reported by Radziejwoski et al. (2011) in *A. thaliana*. The transcription level of *PHR1* was found to be regulated by the expression of the atypical E2F transcription factor DP-E2F-like 1 (E2Fe/DEL1), which has been found to be important regulator of endocycling (Radziejwoski et al., 2011). The E2Fe/DEL1 acts as a transcriptional repressor of the *PHR1* gene in *A. thaliana* upon UVB radiation, leading to the down regulation of *PHR1* and reduced DNA repair ability (Radziejwoski et al., 2011). A different protein called SBF-transcription factor (a SWI4-SWI6 complex) in fungi also performs a similar role as E2F/DEF1 in plant and animals (Medina et al., 2016). Although E2F/DEL1 and SBF are two different proteins that do not share a common ancestor, but they contain similar binding sites (Medina et al., 2016),

indicating a similar regulatory pathway may be employed in fungi. Although the functions of SBF-transcription factor in regulating the expression of *PHR1* in fungi remains unknown, we infer that *Pseudogymnoascus* might share a similar regulatory pathway leading to the suppression of *PHR1* transcription upon UVB radiation.

In contrast to our results, the expression of *CPD1* (gene encoding CPD photolyase) in *C. zeae-maydis* was reported upregulated by 1.5-fold after UV irradiation (Bluhm & Dunkle, 2008). In general, three proteins have been identified to regulate the expression of *PHR1* in *S. cerevisiae* including UME6 (transcriptional regulator involved in chromatin remodelling) (Sweet et al., 1997), RPH1 and GIS1 (histone demethylase and DNA damage-responsive repressors of *PHR1*) (Jang et al., 1999; Liang et al., 2011). UME6 binds specifically to the upstream activation sequence of *PHR1* acting as a positive regulator (Sweet et al., 1997), whereas both RPH1 and GIS repress the expression of *PHR1* through modulation of histone proteins in the absence of UV irradiation (Liang et al., 2011). Upon UV radiation, RAD53 modulates the phosphorylation and dissociation of RPH1 leading to the de-repression of *PHR1*. Thus, a different regulatory pathway in *C. zeae-maydis* may lead to the differences in our findings.

In order to determine the sole effect of light on the regulation of DNA repair genes, the transcription level of *RAD2* and *PHR1* was quantified in relative to dark without exposure to UVB radiation. Our results showed that the expression of *PHR1* was upregulated by 2.3-fold under the illumination of white light. This indicates the ability of *Pseudogymnoascus* to regulate the expression of *PHR1* in a light-dependent manner. This observation has also been frequently reported in many fungal species including, *Trichoderma harzianum* (Berrocal-Tito et al., 1999; 2000), *T. atroviride* (García-Esquivel et al., 2016), *Aspergillus fumigatus* (Fuller et al., 2013), *A. nidulans* (Ruger-

Herreros et al., 2011), *N. crassa* (Chen et al., 2009), and *Ustilago maydis* (Brych et al., 2016). However, transcriptional levels of *RAD2* remained consistent between dark and light conditions, indicating that the expression of *RAD2* was not influenced by the expression of *PHR1*, which many have reported to be regulated by *PHR1* gene in the case of other fungal species (Bluhm & Dunkle, 2008; Guzmán-Moreno et al., 2014). Nevertheless, it remains possible that they may share a similar signal transduction in DNA repair.

5.6 Alternative Repair Pathway in Fungi

The oxygen radicals generated by visible light may act as a triggering factor for the induction of DNA repair pathway in fungi, and much research has focused on the role of light as a signal for inducing DNA repair under light condition in fungi. Our results demonstrated significantly higher CPD repair activity in the presence of light, despite the downregulation of *PHR1* in both conditions. This observation indicates that the improved CPD repair efficiency in light condition was not attributed to the CPD photolyase I. Furthermore, there was no significant difference in the expression of *RAD2* between light and dark conditions suggesting that the improved repairing efficiency was unlikely due to NER.

The effects of light on DNA repair have also been demonstrated by Chelico et al. (2006) and Chelico and Khachatourians (2008) in their investigations on NER and Phr in *B. bassiana*. Both studies reported significantly higher germination of *B. bassiana* conidia in the presence of light, and it was proposed that the increased survival rate was due to photoreactivation. Similar observations were also reported in *T. atroviride* and *Trichoderma reesei* (García-Esquivel et al., 2016; Guzmán-Moreno et al., 2014). In contrast, the conidia in *T. reesei* with knocked out *BLR1* and *CRY1* demonstrated

greater survival rate after UV radiation in the presence of light, even though the disruption of these genes should have impaired Phr ability in *T. reesei*. Hence, this suggests the presence of an alternative repair pathway to repair UV-induced DNA damage in fungi.

Verma and Idnurm (2013) have recently reported the regulation of UVDE-dependent excision repair (UVER) pathway (an alternative excision pathway) by white collar complex (BWC1-BWC2) in response to light in the pathogenic fungus *Cryptococcus neoformans*. The disruption of *BWC1* impaired *in vivo* transcription of *UVE1* (gene involve in UVER) and increased UV sensitivity in *C. neoformans*. Similar regulatory responses were demonstrated in *N. crassa* and *Phycomyces blakesleeanus*, suggesting that the signaling pathway of UVER is conserved in fungi (Verma & Idnurm, 2013). In addition, the loss of the key enzyme, UV endonuclease (UVE1) in *P. destructans* greatly impaired its ability in repairing UV-induced DNA damage and increased sensitivity toward UV radiation and the DNA alkylating agent methyl methane sulfonate (MMS) compared to other *Pseudogymnoascus* spp. (Palmer et al., 2018). With the evidence provided, we propose that improved CPD repair efficiency in the presence of light in *Pseudogymnoascus* was highly likely contributed by alternative excision repair pathway following insignificant differences observed in the expression of *RAD2* and *PHR1* in our study, however further investigations are required to provide direct evidence to further support this inference.

5.7 Future Studies

Our findings serve as a foundation for future studies to further investigate into UV-induced DNA repair in *Pseudogymnoascus* and other fungal species. Following the outcomes of this study, we propose the following aspects to be investigated to further expand our understanding in fungal DNA repair mechanisms.

a) Identify the pigment compounds and quantify the change of the pigmentation under UVB radiation in *Pseudogymnoascus*.
b) Determine the effects of UVB radiation on the genes involved in ESR and regulation of the cell cycle.
c) Characterize the roles and functions of phytolyase/cryptochrome family proteins in *Pseudogymnoascus*.
d) Elucidate the roles of SBF-transcription factor and MYB-like protein in fungi in response to UVR.
e) Investigate AER in the UV-induced damage repair under light conditions.

CHAPTER 6: CONCLUSION

In conclusion, we have successfully verified taxonomic identity of the isolates used in our study, as shown by the phylogenetic trees of three DNA markers (ITS, LSU, *MCM7*) we suggested that they clustered into a single clade that is undistinguished between clade A, B and C in the genus of *Pseudogymnoascus*. Our findings show that the growth, fungal pigmentation and conidia production in *Pseudogymnoascus* were inhibited under artificial UVB dosage of 6.1 kJ m^{-2} d^{-1} at 15°C. Colony extension rates were reduced by 35.32% (HND16 R2-1 sp.2), 34.47% (AK07KGI1202 R1-1 sp.3), 33.03% (AK07KGI1202 R1-1 sp.4) and 21.74% (HND16 R4-1 sp.1) compared with controls cultured in PAR only. Fungal pigmentation was not induced by UVB radiation in an incubation duration of 10 d. Inhibition of conidia production was found in all tested isolates, except HND16 R4-1 sp.1 as shown by the number of conidia visualized in SEM. These observations suggest that these three physiological responses might share a similar signalling pathway in response to UVB-induced stress and damage. Moreover, a higher amount of CPDs was generated by UVB radiation in the Arctic strains compared to the Antarctic strains, indicating the Antarctic strains have developed higher resistance toward UVB. The presence of light promoted the repair of CPDs in *Pseudogymnoascus*, whereas 6-4PPs were found to be repaired faster in dark conditions, though not statistically significant. Meanwhile, the transcriptional repression of *PHR1* upon UVB radiation suggests that the increase in CPD repair efficiency in the presence of light was possibly associated with an alternative repair mechanism. The lack of significance difference in *RAD2* expression between the two repair conditions further supports this inference.

REFERENCES

Al-Moghrabi, N. M., Al-Sharif, I. S., & Aboussekhra, A. (2001). The Saccharomyces cerevisiae *RAD9* cell cycle checkpoint gene is required for optimal repair of UV-induced pyrimidine dimers in both G1 and G2/M phases of the cell cycle. *Nucleic Acids Research, 29*(10), 2020-2025.

Alejandre-Durán, E., Roldán-Arjona, T., Ariza, R. R., & Ruiz-Rubio, M. (2003). The photolyase gene from the plant pathogen *Fusarium oxysporum f. sp. lycopersici* is induced by visible light and α-tomatine from tomato plant. *Fungal Genetics and Biology, 40*(2), 159-165.

Ali, S. H. (2016). *Diversity and keratinase enzyme production of psychrophilic and psychrotolerant soil microfungi from Hornsund, Spitsbergen, High Arctic* (*University of Malaya*), Pages (Master of Science Conventional Format), Malaysia.

Almeida-Paes, R., Frases, S., de Sousa Araújo, G., de Oliveira, M. M. E., Gerfen, G. J., Nosanchuk, J. D., & Zancopé-Oliveira, R. M. (2012a). Biosynthesis and functions of a melanoid pigment produced by species of the *Sporothrix* complex in the presence of L-tyrosine. *Applied and Environmental Microbiology, 78*(24), 8623-8630.

Almeida-Paes, R., Nosanchuk, J. D., & Zancope-Oliveira, R. M. (2012b). Fungal melanins: biosynthesis and biological functions. *Melanin: biosynthesis, functions, and health effects. New York: Nova Science Publishers*, 77-107.

Alves, S., Risco, S., & Almeida, L. (1984). Influence of photoperiod and temperature on the development and sporulation of *Metarhizium anisopliae* (Metsch.) Sorok. *Journal of Applied Entomology, 97*(1‐5), 127-129.

Amalfi, M., Yombiyeni, P., & Decock, C. (2010). Fomitiporia in sub-Saharan Africa: morphology and multigene phylogenetic analysis support three new species from the Guineo-Congolian rainforest. *Mycologia, 102*(6), 1303-1317.

Andersen, C. L., Jensen, J. L., & Ørntoft, T. F. (2004). Normalization of real-time quantitative reverse transcription-PCR data: a model-based variance estimation approach to identify genes suited for normalization, applied to bladder and colon cancer data sets. *Cancer Research, 64*(15), 5245-5250.

Arcangeli, C., & Cannistraro, S. (2000). In situ Raman microspectroscopic identification and localization of carotenoids: Approach to monitoring of UV‐B irradiation stress on antarctic fungus. *Biopolymers, 57*(3), 179-186.

Arratia-Quijada, J., Sánchez, O., Scazzocchio, C., & Aguirre, J. (2012). FlbD, a Myb transcription factor of *Aspergillus nidulans* is uniquely involved in both asexual and sexual differentiation. *Eukaryotic Cell*, EC. 00101-00112.

Avalos, J., & Estrada, A. F. (2010). Regulation by light in *Fusarium*. *Fungal Genetics and Biology, 47*(11), 930-938.

Avalos, J., & Limón, M. C. (2015). Biological roles of fungal carotenoids. *Current Genetics, 61*(3), 309-324.

Aziz, N. M. A., Esa, Y., & Arshad, A. (2016). DNA barcoding and phylogenetic analysis of Malaysian groupers (Subfamily: *Epinephelinae*) using mitochondrial Cytochrome c oxidase I (COI) gene. *Journal of Environmental Biology, 37*(4 Spec No), 725-733.

Bago, B., Pfeffer, P. E., Abubaker, J., Jun, J., Allen, J. W., Brouillette, J., . . . Shachar-Hill, Y. (2003). Carbon export from arbuscular mycorrhizal roots involves the translocation of carbohydrate as well as lipid. *Plant Physiology, 131*(3), 1496-1507.

Bais, A., McKenzie, R., Bernhard, G., Aucamp, P., Ilyas, M., Madronich, S., & Tourpali, K. (2015). Ozone depletion and climate change: Impacts on UV radiation. *Photochemical & Photobiological Sciences, 14*(1), 19-52.

Bais, A. F., Tourpali, K., Kazantzidis, A., Akiyoshi, H., Bekki, S., Braesicke, P., . . . Garny, H. (2011). Projections of UV radiation changes in the 21st century: impact of ozone recovery and cloud effects. *Atmospheric Chemistry and Physics, 11*(15), 7533-7545.

Baldrian, P., & Valášková, V. (2008). Degradation of cellulose by basidiomycetous fungi. *FEMS Microbiology Reviews, 32*(3), 501-521.

Baldrian, P., Voříšková, J., Dobiášová, P., Merhautová, V., Lisá, L., & Valášková, V. (2011). Production of extracellular enzymes and degradation of biopolymers by saprotrophic microfungi from the upper layers of forest soil. *Plant and Soil, 338*(1-2), 111-125.

Bayram, Ö., Biesemann, C., Krappmann, S., Galland, P., & Braus, G. H. (2008). More than a repair enzyme: *Aspergillus nidulans* photolyase-like CryA is a regulator of sexual development. *Molecular Biology of the Cell, 19*(8), 3254-3262.

Becker, M. M., & Wang, Z. (1989). Origin of ultraviolet damage in DNA. *Journal of Molecular Biology, 210*(3), 429-438.

Beckmann, M., Václavík, T., Manceur, A. M., Šprtová, L., Wehrden, H., Welk, E., & Cord, A. F. (2014). glUV: a global UV ‐ B radiation data set for macroecological studies. *Methods in Ecology and Evolution, 5*(4), 372-383.

Begerow, D., Nilsson, H., Unterseher, M., & Maier, W. (2010). Current state and perspectives of fungal DNA barcoding and rapid identification procedures. *Applied Microbiology and Biotechnology, 87*(1), 99-108.

Belozerskaya, T. A., Gessler, N. N., & Aver‘yanov, A. A. (2017). Melanin pigments of fungi *Fungal Metabolites* (pp. 263-291): Springer.

Bernillon, J., Bouillant, M.-L., Pittet, J.-L., Favre-Bonvin, J., & Arpin, N. (1984). Mycosporine glutamine and related mycosporines in the fungus *Pyronema omphalodes*. *Phytochemistry, 23*(5), 1083-1087.

Berrocal-Tito, G., Sametz-Baron, L., Eichenberg, K., Horwitz, B. A., & Herrera-Estrella, A. (1999). Rapid blue light regulation of a *Trichoderma harzianum* photolyase gene. *Journal of Biological Chemistry, 274*(20), 14288-14294.

Berrocal-Tito, G. M., Esquivel-Naranjo, E. U., Horwitz, B. A., & Herrera-Estrella, A. (2007). *Trichoderma atroviride* PHR1, a fungal photolyase responsible for DNA repair, autoregulates its own photoinduction. *Eukaryotic Cell, 6*(9), 1682-1692.

Berrocal-Tito, G. M., Rosales‐Saavedra, T., Herrera‐Estrella, A., & Horwitz, B. A. (2000). Characterization of Blue‐light and Developmental Regulation of the Photolyase gene *phr1* in *Trichoderma harzianum*. *Photochemistry and Photobiology, 71*(5), 662-668.

Bischoff, J. F., Rehner, S. A., & Humber, R. A. (2009). A multilocus phylogeny of the *Metarhizium anisopliae* lineage. *Mycologia, 101*(4), 512-530.

Blackwell, M. (2011). The Fungi: 1, 2, 3… 5.1 million species? *American Journal of Botany, 98*(3), 426-438.

Blanc, P., Tuveson, R., & Sargent, M. (1976). Inactivation of carotenoid-producing and albino strains of *Neurospora crassa* by visible light, blacklight, and ultraviolet radiation. *Journal of Bacteriology, 125*(2), 616-625.

Bluhm, B., & Dunkle, L. (2008). PHL1 of *Cercospora zeae-maydis* encodes a member of the photolyase/cryptochrome family involved in UV protection and fungal development. *Fungal Genetics and Biology, 45*(10), 1364-1372.

Borkovich, K. A., Alex, L. A., Yarden, O., Freitag, M., Turner, G. E., Read, N. D., . . . Plesofsky, N. (2004). Lessons from the genome sequence of *Neurospora crassa*: tracing the path from genomic blueprint to multicellular organism. *Microbiology and Molecular Biology Reviews, 68*(1), 1-108.

Bouillant, M.-L., Pittet, J.-L., Bernillon, J., Favre-Bonvin, J., & Arpin, N. (1981). Mycosporins from *Ascochyta pisi, Cladosporium herbarum* and *Septoria nodorum*. *Phytochemistry, 20*(12), 2705-2707.

Bowman, K. K., Sidik, K., Smith, C. A., Taylor, J.-S., Doetsch, P. W., & Freyer, G. A. (1994). A new ATP-independent DNA endonuclease from *Schizosaccharomyces pombe* that recognizes cyclobutane pyrimidine dimers and 6–4 photoproducts. *Nucleic Acids Research, 22*(15), 3026-3032.

Braga, G. U., Rangel, D. E., Fernandes, É. K., Flint, S. D., & Roberts, D. W. (2015). Molecular and physiological effects of environmental UV radiation on fungal conidia. *Current Genetics, 61*(3), 405-425.

Braga, G. U., Rangel, D. E., Flint, S. D., Miller, C. D., Anderson, A. J., & Roberts, D. W. (2002). Damage and recovery from UV-B exposure in conidia of the entomopathogens *Verticillium lecanii* and *Aphanocladium album*. *Mycologia, 94*(6), 912-920.

Braghini, R., Pozzi, C., Aquino, S., Rocha, L., & Corrêa, B. (2009). Effects of γ-radiation on the fungus *Alternaria alternata* in artificially inoculated cereal samples. *Applied Radiation and Isotopes, 67*(9), 1622-1628.

Brancini, G. T., Bachmann, L., Ferreira, M. E. d. S., Rangel, D. E., & Braga, G. Ú. (2018). Exposing *Metarhizium acridum* mycelium to visible light up-regulates a photolyase gene and increases photoreactivating ability. *Journal of Invertebrate Pathology, 152*, 35-37.

Brancini, G. T., Rangel, D. E., & Braga, G. Ú. (2016). Exposure of *Metarhizium acridum* mycelium to light induces tolerance to UV-B radiation. *FEMS Microbiology Letters, 363*(6).

Bridge, P. D., & Newsham, K. K. (2009). Soil fungal community composition at Mars Oasis, a southern maritime Antarctic site, assessed by PCR amplification and cloning. *Fungal Ecology, 2*(2), 66-74.

Britt, A. B. (2004). Repair of DNA damage induced by solar UV. *Photosynthesis Research, 81*(2), 105-112.

Bryan, R., Jiang, Z., Friedman, M., & Dadachova, E. (2011). The effects of gamma radiation, UV and visible light on ATP levels in yeast cells depend on cellular melanization. *Fungal Biology, 115*(10), 945-949.

Brych, A., Mascarenhas, J., Jaeger, E., Charkiewicz, E., Pokorny, R., Bölker, M., . . . Batschauer, A. (2016). White collar 1 ‐ induced photolyase expression contributes to UV ‐ tolerance of *Ustilago maydis*. *MicrobiologyOpen, 5*(2), 224-243.

Cadet, J., Grand, A., & Douki, T. (2014). Solar UV radiation-induced DNA bipyrimidine photoproducts: formation and mechanistic insights *Photoinduced phenomena in nucleic acids II* (pp. 249-275): Springer.

Cadet, J., Mouret, S., Ravanat, J. L., & Douki, T. (2012). Photoinduced damage to cellular DNA: direct and photosensitized reactions. *Photochemistry and Photobiology, 88*(5), 1048-1065.

Cai, L., Giraud, T., Zhang, N., Begerow, D., Cai, G., & Shivas, R. G. (2011). The evolution of species concepts and species recognition criteria in plant pathogenic fungi. *Fungal Diversity, 50*(1), 121.

Caldwell, M. M., & Flint, S. D. (1997). Uses of biological spectral weighting functions and the need of scaling for the ozone reduction problem. *Plant Ecology, 128*(1-2), 67-76.

Čandek, K., & Kuntner, M. (2015). DNA barcoding gap: reliable species identification over morphological and geographical scales. *Molecular Ecology Resources, 15*(2), 268-277.

Canessa, P., Schumacher, J., Hevia, M. A., Tudzynski, P., & Larrondo, L. F. (2013). Assessing the effects of light on differentiation and virulence of the plant pathogen *Botrytis cinerea*: characterization of the White Collar Complex. *PloS One, 8*(12), e84223.

Castrillo, M., García-Martínez, J., & Avalos, J. (2013). Light-dependent functions of the *Fusarium fujikuroi* CryD DASH cryptochrome in development and secondary metabolism. *Applied and Environmental Microbiology, 79*(8), 2777-2788.

Causton, H. C., Ren, B., Koh, S. S., Harbison, C. T., Kanin, E., Jennings, E. G., . . . Young, R. A. (2001). Remodeling of yeast genome expression in response to environmental changes. *Molecular Biology of the Cell, 12*(2), 323-337.

Chelico, L., Haughian, J. L., & Khachatourians, G. G. (2006). Nucleotide excision repair and photoreactivation in the entomopathogenic fungi *Beauveria bassiana*, *Beauveria brongniartii*, *Beauveria nivea*, *Metarhizium anisopliae*, *Paecilomyces farinosus* and *Verticillium lecanii*. *Journal of Applied Microbiology, 100*(5), 964-972.

Chelico, L., Haughian, J. L., Woytowich, A. E., & Khachatourians, G. G. (2005). Quantification of ultraviolet-C irradiation induced cyclobutane pyrimidine dimers and their removal in *Beauveria bassiana* conidiospore DNA. *Mycologia, 97*(3), 621-627.

Chelico, L., & Khachatourians, G. G. (2008). Isolation and characterization of nucleotide excision repair deficient mutants of the entomopathogenic fungus, *Beauveria bassiana*. *Journal of Invertebrate Pathology, 98*(1), 93-100.

Chen, C. H., Ringelberg, C. S., Gross, R. H., Dunlap, J. C., & Loros, J. J. (2009). Genome ‐ wide analysis of light ‐ inducible responses reveals hierarchical light signalling in *Neurospora*. *The EMBO journal, 28*(8), 1029-1042.

Cheng, P., Ma, Z., Wang, X., Wang, C., Li, Y., Wang, S., & Wang, H. (2014). Impact of UV-B radiation on aspects of germination and epidemiological components of three major physiological races of *Puccinia striiformis* f. sp. *tritici*. *Crop Protection, 65*, 6-14.

Cheng, P., Yang, Y., Gardner, K. H., & Liu, Y. (2002). PAS domain-mediated WC-1/WC-2 interaction is essential for maintaining the steady-state level of WC-1 and the function of both proteins in circadian clock and light responses of *Neurospora*. *Molecular and Cellular Biology, 22*(2), 517-524.

Choudhury, R. A., & McRoberts, N. (2017). Temperature and light effects on in vitro germination of *Peronospora effusa* sporangia. *Tropical Plant Pathology*, 1-5.

Christiaens, F., Moyal, D., Seité, S., & Frederick, J. (2011). Comments to the article by Kollias, Ruvolo and Sayre entitled “the value of the ratio of UVA to UVB in sunlight”. *Photochemistry and Photobiology, 87*(6), 1476-1477.

Coblentz, W. (1932). The Copenhagen meeting of the second international congress on light. *Science, 76*(1975), 412-415.

Cohen, Y. (1976). Interacting effects of light and temperature on sporulation of *Peronospora tabacina* on tobacco leaves. *Australian Journal of Biological Sciences, 29*(3), 281-290.

Cohen, Y., Eyal, H., & Sadon, T. (1975). Light-induced inhibition of sporangial formation of *Phytophthora infestans* on potato leaves. *Canadian Journal of Botany, 53*(22), 2680-2686.

Cohen, Y., Vaknin, M., Ben-Naim, Y., & Rubin, A. E. (2013). Light suppresses sporulation and epidemics of *Peronospora belbahrii*. *PloS One, 8*(11), e81282.

Cohrs, K. C., & Schumacher, J. (2017). The two cryptochrome/photolyase family proteins fulfill distinct roles in DNA photorepair and regulation of conidiation in the gray mold fungus *Botrytis cinerea*. *Applied and Environmental Microbiology, 89*(17), 812-817.

Comiso, J. C., Parkinson, C. L., Gersten, R., & Stock, L. (2008). Accelerated decline in the Arctic sea ice cover. *Geophysical Research Letters, 35*(1).

Conde, F. R., Churio, M. S., & Previtali, C. M. (2004). The deactivation pathways of the excited-states of the mycosporine-like amino acids shinorine and porphyra-334 in aqueous solution. *Photochemical & Photobiological Sciences, 3*(10), 960-967.

Connell, L., Barrett, A., Templeton, A., & Staudigel, H. (2009). Fungal diversity associated with an active deep sea volcano: Vailulu'u Seamount, Samoa. *Geomicrobiology Journal, 26*(8), 597-605.

Costa, R. M., Chigançcas, V., da Silva Galhardo, R., Carvalho, H., & Menck, C. F. (2003). The eukaryotic nucleotide excision repair pathway. *Biochimie, 85*(11), 1083-1099.

Courdavault, S., Baudouin, C., Charveron, M., Canguilhem, B., Favier, A., Cadet, J., & Douki, T. (2005). Repair of the three main types of bipyrimidine DNA photoproducts in human keratinocytes exposed to UVB and UVA radiations. *DNA Repair, 4*(7), 836-844.

Cox, F., Newsham, K. K., Bol, R., Dungait, J. A., & Robinson, C. H. (2016). Not poles apart: Antarctic soil fungal communities show similarities to those of the distant Arctic. *Ecology Letters, 19*(5), 528-536.

Dadachova, E., Bryan, R. A., Huang, X., Moadel, T., Schweitzer, A. D., Aisen, P., . . . Casadevall, A. (2007). Ionizing radiation changes the electronic properties of melanin and enhances the growth of melanized fungi. *PloS One, 2*(5), e457.

Dadachova, E., & Casadevall, A. (2008). Ionizing radiation: how fungi cope, adapt, and exploit with the help of melanin. *Current Opinion in Microbiology, 11*(6), 525-531.

Darriba, D., Taboada, G. L., Doallo, R., & Posada, D. (2012). jModelTest 2: more models, new heuristics and parallel computing. *Nature Methods, 9*(8), 772.

Day, T., Ruhland, C., & Xiong, F. (2001). Influence of solar ultraviolet-B radiation on Antarctic terrestrial plants: results from a 4-year field study. *Journal of Photochemistry and Photobiology B: Biology, 62*(1-2), 78-87.

de Menezes, H. D., Massola, N. S., Flint, S. D., Silva, G. J., Bachmann, L., Rangel, D. E., & Braga, G. U. (2015). Growth under visible light increases conidia and mucilage production and tolerance to UV‐B radiation in the plant pathogenic fungus *Colletotrichum acutatum*. *Photochemistry and Photobiology, 91*(2), 397-402.

Dettman, J. R., Jacobson, D. J., & Taylor, J. W. (2003). A multilocus genealogical approach to phylogenetic species recognition in the model eukaryote *Neurospora*. *Evolution, 57*(12), 2703-2720.

Dighton, J., Tugay, T., & Zhdanova, N. (2008). Fungi and ionizing radiation from radionuclides. *FEMS Microbiology Letters, 281*(2), 109-120.

Dijk, M., Typas, D., Mullenders, L., & Pines, A. (2014). Insight in the multilevel regulation of NER. *Experimental Cell Research, 329*(1), 116-123.

Douki, T., & Cadet, J. (2014). DNA damage. *Encyclopedia of Astrobiology*, 1-7.

Downes, F. (1992). *Compendium of methods for the microbiological examination of foods*: American Public Health Association.

Drees, K. P., Palmer, J. M., Sebra, R., Lorch, J. M., Chen, C., Wu, C.-C., . . . Cuomo, C. A. (2016). Use of multiple sequencing technologies to produce a high-quality genome of the fungus *Pseudogymnoascus destructans*, the causative agent of bat white-nose syndrome. *Genome announcements, 4*(3), e00445-00416.

Drummond, A. J., Ho, S. Y., Phillips, M. J., & Rambaut, A. (2006). Relaxed phylogenetics and dating with confidence. *PLoS Biology, 4*(5), e88.

Drummond, A. J., Suchard, M. A., Xie, D., & Rambaut, A. (2012). Bayesian phylogenetics with BEAUti and the BEAST 1.7. *Molecular Biology and Evolution, 29*(8), 1969-1973.

Duguay, K. J., & Klironomos, J. N. (2000). Direct and indirect effects of enhanced UV-B radiation on the decomposing and competitive abilities of saprobic fungi. *Applied Soil Ecology, 14*(2), 157-164.

Durbin, R. (1959). Some effects of light on the growth Aand morphology of *Rhizoctonia-solani* (Vol. 49, pp. 59-60): Amer phytopatholoical soc

Fabre, F. (1972). Photoreactivation in the yeast *Schizosaccharomyces pombe*. *Photochemistry and Photobiology, 15*(4), 367-373.

Fang, W., & Leger, R. J. S. (2012). Enhanced UV resistance and improved killing of malaria mosquitoes by photolyase transgenic entomopathogenic fungi. *PloS One, 7*(8), e43069.

Faraji, S., & Dreuw, A. (2017). Insights into light‐driven DNA repair by photolyases: Challenges and opportunities for electronic structure theory. *Photochemistry and Photobiology, 93*(1), 37-50.

Favre-Bonvin, J., Bernillon, J., Salin, N., & Arpin, N. (1987). Biosynthesis of mycosporines: mycosporine glutaminol in *Trichothecium roseum*. *Phytochemistry, 26*(9), 2509-2514.

Felsenstein, J. (1985). Confidence limits on phylogenies: an approach using the bootstrap. *Evolution, 39*(4), 783-791.

Fenice, M., Selbmann, L., Zucconi, L., & Onofri, S. (1997). Production of extracellular enzymes by Antarctic fungal strains. *Polar Biology, 17*(3), 275-280.

Finlay, R. D. (2008). Ecological aspects of mycorrhizal symbiosis: with special emphasis on the functional diversity of interactions involving the extraradical mycelium. *Journal of Experimental Botany, 59*(5), 1115-1126.

Finotti, E., Paolino, C., Lancia, B., & Mercantini, R. (1996). Metabolic differences between two Antarctic strains of *Geomyces pannorum*. *Current Microbiology, 32*(1), 7-10.

Fitter, A. H. (2005). Darkness visible: reflections on underground ecology. *Journal of Ecology, 93*(2), 231-243.

Flieger, M., Bandouchova, H., Cerny, J., Chudíčková, M., Kolarik, M., Kovacova, V., . . . Stodůlková, E. (2016). Vitamin B 2 as a virulence factor in *Pseudogymnoascus destructans* skin infection. *Scientific Reports, 6*, 33200.

Forsythe, A., & Xu, J. (2017). The complete mitochondrial genome of the White-Nose Syndrome pathogen, *Pseudogymnoascus destructans*. *Mitochondrial DNA Part B, 2*(1), 48-49.

Fourtouni, A., Manetas, Y., & Christias, C. (1998). Effects of UV-B radiation on growth, pigmentation, and spore production in the phytopathogenic fungus *Alternaria solani*. *Canadian Journal of Botany, 76*(12), 2093-2099.

Friedberg, E. C., Walker, G. C., Siede, W., & Wood, R. D. (2005). *DNA repair and mutagenesis*: American Society for Microbiology Press.

Fuller, K. K., Loros, J. J., & Dunlap, J. C. (2015). Fungal photobiology: visible light as a signal for stress, space and time. *Current Genetics, 61*(3), 275-288.

Fuller, K. K., Ringelberg, C. S., Loros, J. J., & Dunlap, J. C. (2013). The fungal pathogen *Aspergillus fumigatus* regulates growth, metabolism, and stress resistance in response to light. *mBio, 4*(2), e00142-00113.

Gams, W. (2007). Biodiversity of soil-inhabiting fungi. *Biodiversity and Conservation, 16*(1), 69-72.

García-Esquivel, M., Esquivel-Naranjo, E. U., Hernández-Oñate, M. A., Ibarra-Laclette, E., & Herrera-Estrella, A. (2016). The *Trichoderma atroviride* cryptochrome/photolyase genes regulate the expression of blr1-independent genes both in red and blue light. *Fungal Biology, 120*(4), 500-512.

Gardes, M., & Bruns, T. D. (1993). ITS primers with enhanced specificity for basidiomycetes ‐ application to the identification of mycorrhizae and rusts. *Molecular Ecology, 2*(2), 113-118.

Gargas, A., Trest, M., Christensen, M., Volk, T. J., & Blehert, D. S. (2009). *Geomyces destructans* sp. nov. associated with bat white-nose syndrome. *Mycotaxon, 108*(1), 147-154.

Gasch, A. P. (2003). The environmental stress response: a common yeast response to diverse environmental stresses *Yeast stress responses* (pp. 11-70): Springer.

Gasch, A. P., Spellman, P. T., Kao, C. M., Carmel-Harel, O., Eisen, M. B., Storz, G., . . . Brown, P. O. (2000). Genomic expression programs in the response of yeast cells to environmental changes. *Molecular Biology of the Cell, 11*(12), 4241-4257.

Geis, P. A., & Szaniszlo, P. J. (1984). Carotenoid pigments of the dematiaceous fungus *Wangiella dermatitidis*. *Mycologia*, 268-273.

Geiser, D., Klich, M., Frisvad, J. C., Peterson, S., Varga, J., & Samson, R. A. (2007). The current status of species recognition and identification in *Aspergillus*. *Studies in Mycology, 59*, 1-10.

Gilgado, F., Cano, J., Gené, J., & Guarro, J. (2005). Molecular phylogeny of the *Pseudallescheria boydii* species complex: proposal of two new species. *Journal of Clinical Microbiology, 43*(10), 4930-4942.

Gilmore, S. R., Graefenhan, T., Louis ‐ Seize, G., & Seifert, K. A. (2009). Multiple copies of cytochrome oxidase 1 in species of the fungal genus *Fusarium*. *Molecular Ecology Resources, 9*, 90-98.

Goldman, G. H., & Kafer, E. (2004). Aspergillus nidulans as a model system to characterize the DNA damage response in eukaryotes. *Fungal Genetics and Biology, 41*(4), 428-442.

Goldman, G. H., McGuire, S. L., & Harris, S. D. (2002). The DNA damage response in filamentous fungi. *Fungal Genetics and Biology, 35*(3), 183-195.

Gorbushina, A. A., Whitehead, K., Dornieden, T., Niesse, A., Schulte, A., & Hedges, J. I. (2003). Black fungal colonies as units of survival: hyphal mycosporines synthesized by rock-dwelling microcolonial fungi. *Canadian Journal of Botany, 81*(2), 131-138.

Grinhut, T., Hadar, Y., & Chen, Y. (2007). Degradation and transformation of humic substances by saprotrophic fungi: processes and mechanisms. *Fungal Biology Reviews, 21*(4), 179-189.

Gunasekera, T., Paul, N., & Ayres, P. (1997). Responses of phylloplane yeasts to UV-B (290–320 nm) radiation: interspecific differences in sensitivity. *Mycological Research, 101*(7), 779-785.

Gutiérrez Pozo, G., Corrochano Peláez, L. M., Luque, E. M., Navarro Sampedro, L., Olmedo, M., Rodríguez Romero, J., . . . Tagua, V. G. (2012). A relationship between carotenoid accumulation and the distribution of species of the fungus *Neurospora* in spain. *PloS One, 7*, e33658.

Guzmán-Moreno, J., Flores-Martínez, A., Brieba, L. G., & Herrera-Estrella, A. (2014). The *Trichoderma reesei* Cry1 protein is a member of the cryptochrome/photolyase family with 6–4 photoproduct repair activity. *PloS One, 9*(6), e100625.

Hamid, M. I., Zeng, F., Cheng, J., Jiang, D., & Fu, Y. (2013). Disruption of heat shock factor 1 reduces the formation of conidia and thermotolerance in the mycoparasitic fungus *Coniothyrium minitans*. *Fungal Genetics and Biology, 53*, 42-49.

Hatakeyama, S., Ito, Y., Shimane, A., Ishii, C., & Inoue, H. (1998). Cloning and characterization of the yeast *RAD1* homolog gene (*mus-38*) from *Neurospora crassa*: evidence for involvement in nucleotide excision repair. *Current Genetics, 33*(4), 276-283.

Hawksworth, D. (2012). Global species numbers of fungi: are tropical studies and molecular approaches contributing to a more robust estimate? *Biodiversity and Conservation, 21*(9), 2425-2433.

Hebert, P. D., Cywinska, A., Ball, S. L., & DeWaard, J. R. (2003). Biological identifications through DNA barcodes. *Proceedings of the Royal Society of London. Series B: Biological Sciences, 270*(1512), 313-321.

Honda, Y., & Yunoki, T. (1980). Inhibition of fungal sporulation by ultraviolet-absorbing vinyl film and its application to disease control. *Japan Agriculture Research Quarterly, 14*(2), 78-83.

Hoshino, T., Kiriaki, M., Ohgiya, S., Fujiwara, M., Kondo, H., Nishimiya, Y., . . . Tsuda, S. (2003). Antifreeze proteins from snow mold fungi. *Canadian Journal of Botany, 81*(12), 1175-1181.

Huelsenbeck, J. P., & Ronquist, F. (2001). MRBAYES: Bayesian inference of phylogenetic trees. *Bioinformatics, 17*(8), 754-755.

Hughes, K. A., Lawley, B., & Newsham, K. K. (2003). Solar UV-B radiation inhibits the growth of Antarctic terrestrial fungi. *Applied and Environmental Microbiology, 69*(3), 1488-1491.

Huijser, A., Pezzella, A., & Sundström, V. (2011). Functionality of epidermal melanin pigments: current knowledge on UV-dissipative mechanisms and research perspectives. *Physical Chemistry Chemical Physics, 13*(20), 9119-9127.

Irazusta, V., Nieto-Peñalver, C. G., Cabral, M. E., Amoroso, M. J., & de Figueroa, L. I. (2013). Relationship among carotenoid production, copper bioremediation and oxidative stress in *Rhodotorula mucilaginosa* RCL-11. *Process Biochemistry, 48*(5-6), 803-809.

Ishii, C., Nakamura, K., & Inoue, H. (1998). A new UV-sensitive mutant that suggests a second excision repair pathway in *Neurospora crassa*. *Mutation Research/DNA Repair, 408*(3), 171-182.

James, T. Y., Kauff, F., Schoch, C. L., Matheny, P. B., Hofstetter, V., Cox, C. J., . . . Miadlikowska, J. (2006). Reconstructing the early evolution of Fungi using a six-gene phylogeny. *Nature, 443*(7113), 818.

Jang, Y. K., Wang, L., & Sancar, G. B. (1999). RPH1 and GIS1 are damage-responsive repressors of *PHR1*. *Molecular and Cellular Biology, 19*(11), 7630-7638.

Jin, H., Cominelli, E., Bailey, P., Parr, A., Mehrtens, F., Jones, J., . . . Martin, C. (2000). Transcriptional repression by AtMYB4 controls production of UV ‐ protecting sunscreens in *Arabidopsis*. *The EMBO journal, 19*(22), 6150-6161.

Johnson, D. (2003). Response of terrestrial microorganisms to ultraviolet-B radiation in ecosystems. *Research in Microbiology, 154*(5), 315-320.

Johnson, L. J., Miller, A. N., McCleery, R. A., McClanahan, R., Kath, J. A., Lueschow, S., & Porras-Alfaro, A. (2013). Psychrophilic and psychrotolerant fungi on bats and the presence of *Geomyces* spp. on bat wings prior to the arrival of white nose syndrome. *Applied and Environmental Microbiology, 79*(18), 5465-5471.

Kang, M. S., Yu, S. L., Lim, H. S., Choi, B., Park, C. S., Kang, J. H., & Lee, S. K. (2010). Mitotic catastrophe induced by overexpression of budding yeast Rad2p. *Yeast, 27*(7), 399-411.

Kawamura, C., Tsujimoto, T., & Tsuge, T. (1999). Targeted disruption of a melanin biosynthesis gene affects conidial development and UV tolerance in the Japanese pear pathotype of *Alternaria alternata*. *Molecular Plant-Microbe Interactions, 12*(1), 59-63.

Kihara, J., Moriwaki, A., Matsuo, N., Arase, S., & Honda, Y. (2004). Cloning, functional characterization, and near-ultraviolet radiation-enhanced expression of a photolyase gene (*PHR1*) from the phytopathogenic fungus *Bipolaris oryzae*. *Current Genetics, 46*(1), 37-46.

Kim, H., Son, H., & Lee, Y. W. (2014a). Effects of light on secondary metabolism and fungal development of *Fusarium graminearum*. *Journal of Applied Microbiology, 116*(2), 380-389.

Kim, Y., Kim, H., Son, H., Choi, G. J., Kim, J.-C., & Lee, Y.-W. (2014b). MYT3, a Myb-like transcription factor, affects fungal development and pathogenicity of *Fusarium graminearum*. *PloS One, 9*(4), e94359.

Kochkina, G., Ivanushkina, N., Akimov, V., Gilichinskii, D., & Ozerskaya, S. (2007). Halo-and psychrotolerant *Geomyces* fungi from Arctic cryopegs and marine deposits. *Microbiology, 76*(1), 31-38.

Kogej, T., Gostinčar, C., Volkmann, M., Gorbushina, A. A., & Gunde-Cimerman, N. (2006). Mycosporines in extremophilic fungi—novel complementary osmolytes? *Environmental Chemistry, 3*(2), 105-110.

Kogej, T., Stein, M., Volkmann, M., Gorbushina, A. A., Galinski, E. A., & Gunde-Cimerman, N. (2007). Osmotic adaptation of the halophilic fungus *Hortaea werneckii*: role of osmolytes and melanization. *Microbiology, 153*(12), 4261-4273.

Konova, I., Sergeeva, Y. E., Galanina, L., Kochkina, G., Ivanushkina, N., & Ozerskaya, S. (2009). Lipid synthesis by *Geomyces pannorum* under the impact of stress factors. *Microbiology, 78*(1), 42-47.

Kosakyan, A., Mulot, M., Mitchell, E. A., & Lara, E. (2015). Environmental DNA COI barcoding for quantitative analysis of protists communities: A test using the Nebela collaris complex (Amoebozoa; Arcellinida; Hyalospheniidae). *European Journal of Protistology, 51*(4), 311-320.

Kozdroj, J., & van Elsas, J. D. (2001). Structural diversity of microorganisms in chemically perturbed soil assessed by molecular and cytochemical approaches. *Journal of Microbiological Methods, 43*(3), 197-212.

Krishnan, A., Convey, P., Gonzalez-Rocha, G., & Alias, S. A. (2016). Production of extracellular hydrolase enzymes by fungi from King George Island. *Polar Biology, 39*(1), 65-76.

Kuehne, H. A., Murphy, H. A., Francis, C. A., & Sniegowski, P. D. (2007). Allopatric divergence, secondary contact, and genetic isolation in wild yeast populations. *Current Biology, 17*(5), 407-411.

Kumagai, T., & Oda, Y. (1969). Blue and near ultraviolet reversible photoreaction in conidial development of the fungus, *Alternaria tomato*. *Development, growth & differentiation, 11*(2), 130-142.

Kumagai, T., & Oda, Y. (1973). Blue and near ultraviolet reversible photoreaction with intracellular particulate fraction of the fungus, *Alternaria tomato*. *Plant and Cell Physiology, 14*(6), 1107-1112.

Kumar, S., Stecher, G., & Tamura, K. (2016). MEGA7: Molecular Evolutionary Genetics Analysis version 7.0 for bigger datasets. *Molecular Biology and Evolution, 33*(7), 1870-1874.

Kurahashi, A., Shimoda, T., Sato, M., Fujimori, F., Hirama, J., & Nishibori, K. (2015). A putative transcription factor Gf. *BMR1* in *Grifola frondosa*, the homolog of *BMR1* in *Bipolaris oryzae*, was strongly induced by near-ultraviolet light and blue light. *Mycoscience, 56*(2), 177-182.

Kuthubutheen, A., & Pugh, G. (1979). Effects of temperature and fungicides on *Chrysosporium pannorum* (Link) Hughes. *Antonie van Leeuwenhoek, 45*(1), 65-79.

Lamoth, F., Juvvadi, P. R., Fortwendel, J. R., & Steinbach, W. J. (2012). Heat-shock protein 90 (Hsp90) is required for conidiation and cell wall integrity in *Aspergillus fumigatus*. *Eukaryotic Cell*, EC. 00032-00012.

Langematz, U. (2019). Stratospheric ozone: down and up through the anthropocene. *ChemTexts, 5*(2), 8.

Latgé, J. P. (2007). The cell wall: a carbohydrate armour for the fungal cell. *Molecular Microbiology, 66*(2), 279-290.

Leach, C. M. (1971). Chapter XXIII A Practical Guide to the Effects of Visible and Ultraviolet Light on Fungitt12 *Methods in microbiology* (Vol. 4, pp. 609-664): Elsevier.

Lee, K., Singh, P., Chung, W.-C., Ash, J., Kim, T. S., Hang, L., & Park, S. (2006). Light regulation of asexual development in the rice blast fungus, *Magnaporthe oryzae*. *Fungal Genetics and Biology, 43*(10), 694-706.

Lee, S. J., Lee, M. R., Kim, S., Kim, J. C., Park, S. E., Shin, T. Y., & Kim, J. S. (2018). Conidiogenesis-related DNA photolyase gene in *Beauveria bassiana*. *Journal of Invertebrate Pathology, 153*, 85-91.

Legrand, M., Chan, C. L., Jauert, P. A., & Kirkpatrick, D. T. (2008). Analysis of base excision and nucleotide excision repair in *Candida albicans*. *Microbiology, 154*(8), 2446-2456.

Lehmann, A. R. (1996). Molecular biology of DNA repair in the fission yeast *Schizosaccharomyces pombe*. *Mutation Research/DNA Repair, 363*(3), 147-161.

Leite, B., & Nicholson, R. L. (1992). Mycosporine-alanine: A self-inhibitor of germination from the conidial mucilage of *Colletotrichum graminicola*. *Experimental Mycology, 16*(1), 76-86.

Liang, C.-Y., Hsu, P.-H., Chou, D.-F., Pan, C.-Y., Wang, L.-C., Huang, W.-C., . . . Lo, W.-S. (2011). The histone H3K36 demethylase Rph1/KDM4 regulates the expression of the photoreactivation gene *PHR1*. *Nucleic Acids Research, 39*(10), 4151-4165.

Libkind, D., Diéguez, M. C., Moliné, M., Pérez, P., Zagarese, H. E., & Broock, M. (2006). Occurrence of photoprotective compounds in yeasts from freshwater ecosystems of northwestern Patagonia (Argentina). *Photochemistry and Photobiology*, *82*(4), 972-980.

Libkind, D., Moline, M., & van Broock, M. (2011). Production of the UVB-absorbing compound mycosporine–glutaminol–glucoside by *Xanthophyllomyces dendrorhous* (*Phaffia rhodozyma*). *FEMS Yeast Research*, *11*(1), 52-59.

Libkind, D., Pérez, P., Sommaruga, R., del Carmen Diéguez, M., Ferraro, M., Brizzio, S., . . . van Broock, M. (2004). Constitutive and UV-inducible synthesis of photoprotective compounds (carotenoids and mycosporines) by freshwater yeasts. *Photochemical & Photobiological Sciences*, *3*(3), 281-286.

Libkind, D., Sommaruga, R., Zagarese, H., & van Broock, M. (2005). Mycosporines in carotenogenic yeasts. *Systematic and Applied Microbiology*, *28*(8), 749-754.

Lindner, D. L., & Banik, M. T. (2011). Intragenomic variation in the ITS rDNA region obscures phylogenetic relationships and inflates estimates of operational taxonomic units in genus Laetiporus. *Mycologia*, *103*(4), 731-740.

Lindner, D. L., Gargas, A., Lorch, J. M., Banik, M. T., Glaeser, J., Kunz, T. H., & Blehert, D. S. (2011). DNA-based detection of the fungal pathogen *Geomyces destructans* in soils from bat hibernacula. *Mycologia*, *103*(2), 241-246.

Liu, Y., & Filler, S. G. (2011). *Candida albicans* Als3, a multifunctional adhesin and invasin. *Eukaryotic Cell*, *10*(2), 168-173.

Livak, K. J., & Schmittgen, T. D. (2001). Analysis of relative gene expression data using real-time quantitative PCR and the 2− ΔΔCT method. *Methods*, *25*(4), 402-408.

Loperena, L., Soria, V., Varela, H., Lupo, S., Bergalli, A., Guigou, M., . . . Rivas, F. (2012). Extracellular enzymes produced by microorganisms isolated from maritime Antarctica. *World Journal of Microbiology and Biotechnology*, *28*(5), 2249-2256.

Lorch, J. M., Lindner, D. L., Gargas, A., Muller, L. K., Minnis, A. M., & Blehert, D. S. (2013). A culture-based survey of fungi in soil from bat hibernacula in the eastern United States and its implications for detection of *Geomyces destructans*, the causal agent of bat white-nose syndrome. *Mycologia*, *105*(2), 237-252.

Maddison, W. P., & Maddison, D. R. (2017). Mesquite: a modular system for evolutionary analysis (Version 3.31). Retrieved from http://mesquiteproject.org/

Madronich, S., McKenzie, R. L., Björn, L. O., & Caldwell, M. M. (1998). Changes in biologically active ultraviolet radiation reaching the Earth's surface. *Journal of Photochemistry and Photobiology B: Biology*, *46*(1), 5-19.

Manney, G. L., Santee, M. L., Rex, M., Livesey, N. J., Pitts, M. C., Veefkind, P., . . . Froidevaux, L. (2011). Unprecedented Arctic ozone loss in 2011. *Nature, 478*(7370), 469-475.

Mateos, L., Jiménez, A., Revuelta, J. L., & Santos, M. A. (2006). Purine biosynthesis, riboflavin production, and trophic-phase span are controlled by a Myb-related transcription factor in the fungus *Ashbya gossypii*. *Applied and Environmental Microbiology, 72*(7), 5052-5060.

McKenzie, R. L., Aucamp, P. J., Bais, A. F., Björn, L. O., & Ilyas, M. (2007). Changes in biologically-active ultraviolet radiation reaching the Earth's surface. *Photochemical & Photobiological Sciences, 6*(3), 218-231.

Medina, A., Schmidt-Heydt, M., Rodríguez, A., Parra, R., Geisen, R., & Magan, N. (2015). Impacts of environmental stress on growth, secondary metabolite biosynthetic gene clusters and metabolite production of xerotolerant/xerophilic fungi. *Current Genetics, 61*(3), 325-334.

Medina, E. M., Turner, J. J., Gordan, R., Skotheim, J. M., & Buchler, N. E. (2016). Punctuated evolution and transitional hybrid network in an ancestral cell cycle of fungi. *Elife, 5*, e09492.

Meredith, P., & Sarna, T. (2006). The physical and chemical properties of eumelanin. *Pigment Cell & Melanoma Research, 19*(6), 572-594.

Miller, G. R., & Sarachek, A. (1974). Absence of photoreactivating enzyme in *Candida albicans, Candida stellatoidea,* and *Candida tropicalis*. *Infection and Immunity, 10*(2), 398.

Minnis, A. M., & Lindner, D. L. (2013). Phylogenetic evaluation of *Geomyces* and allies reveals no close relatives of *Pseudogymnoascus destructans,* comb. nov., in bat hibernacula of eastern North America. *Fungal Biology, 117*(9), 638-649.

Mishra, R. K., Tiwari, S., & Prasad, S. M. (2017). Interaction of UV‐B with the Terrestrial Ecosystem *UV-B Radiation: From Environmental Stressor to Regulator of Plant Growth* (pp. 65).

Moliné, M., Arbeloa, E. M., Flores, M. R., Libkind, D., Farías, M. E., Bertolotti, S. G., . . . van Broock, M. R. (2010a). UVB photoprotective role of mycosporines in yeast: photostability and antioxidant activity of mycosporine-glutaminol-glucoside. *Radiation Research, 175*(1), 44-50.

Moliné, M., Flores, M. R., Libkind, D., del Carmen Diéguez, M., Farías, M. E., & van Broock, M. (2010b). Photoprotection by carotenoid pigments in the yeast *Rhodotorula mucilaginosa*: the role of torularhodin. *Photochemical & Photobiological Sciences, 9*(8), 1145-1151.

Moliné, M., Libkind, D., del Carmen Diéguez, M., & van Broock, M. (2009). Photoprotective role of carotenoids in yeasts: response to UV-B of pigmented

and naturally-occurring albino strains. *Journal of Photochemistry and Photobiology B: Biology, 95*(3), 156-161.

Moncalvo, J.-M., Lutzoni, F. M., Rehner, S. A., Johnson, J., & Vilgalys, R. (2000). Phylogenetic relationships of agaric fungi based on nuclear large subunit ribosomal DNA sequences. *Systematic Biology, 49*(2), 278-305.

Montzka, S., Reimann, S., Engel, A., Kruger, K., Sturges, W., Blake, D., . . . Jucks, K. (2011). Scientific assessment of ozone depletion: 2010. *Global Ozone Research and Monitoring Project-Report No. 51*.

Moody, S. A., Newsham, K. K., Ayres, P. G., & Paul, N. D. (1999). Variation in the responses of litter and phylloplane fungi to UV-B radiation (290–315 nm). *Mycological Research, 103*(11), 1469-1477.

Mooney, J. L., & Yager, L. N. (1990). Light is required for conidiation in *Aspergillus nidulans*. *Genes & Development, 4*(9), 1473-1482.

Muller, E., & von Arx, J. (1982). *Pseudogymnoascus alpinus, nov. spec.* Paper presented at the Sydowia: Annales mycologici.

Nascimento, E., Da Silva, S. H., dos Reis Marques, E., Roberts, D. W., & Braga, G. U. (2010). Quantification of cyclobutane pyrimidine dimers induced by UVB radiation in conidia of the fungi *Aspergillus fumigatus*, *Aspergillus nidulans*, *Metarhizium acridum* and *Metarhizium robertsii*. *Photochemistry and Photobiology, 86*(6), 1259-1266.

Nobile, C. J., Nett, J. E., Andes, D. R., & Mitchell, A. P. (2006). Function of *Candida albicans* adhesin Hwp1 in biofilm formation. *Eukaryotic Cell, 5*(10), 1604-1610.

Norvell, L. L. (2011). Fungal nomenclature. 1. Melbourne approves a new Code. *Mycotaxon, 116*(1), 481-490.

O'Donnell, K. (2000). Molecular phylogeny of the Nectria haematococca-*Fusarium solani* species complex. *Mycologia*, 919-938.

O'Donnell, K., & Cigelnik, E. (1997). Two divergent intragenomic rDNA ITS2 types within a monophyletic lineage of the fungus *Fusarium* are non orthologous. *Molecular Phylogenetics and Evolution, 7*(1), 103-116.

Olmedo, M., Ruger-Herreros, C., Luque, E. M., & Corrochano, L. M. (2013). Regulation of transcription by light in *Neurospora crassa*: A model for fungal photobiology? *Fungal Biology Reviews, 27*(1), 10-18.

Osman, M., Elsayed, M., Mohamed, Y., & Abo-Zeid, A. (1989). Effect of ultraviolet irradiation on germination and growth in *Aspergillus flavus* and *Penicillium notatum*. *Mycological Research, 92*(3), 293-296.

Osman, M., & Valadon, L. (1979). Effect of light quality on growth and sporulation in *Verticillium agaricinum*. *Transactions of the British Mycological Society, 72*(1), 145-146.

Overland, J., Turner, J., Francis, J., Gillett, N., Marshall, G., & Tjernström, M. (2008). The Arctic and Antarctic: Two faces of climate change. *Eos, 89*(19), 177-178.

Ozerskaya, S., Kochkina, G., Ivanushkina, N., & Gilichinsky, D. A. (2009). Fungi in permafrost *Permafrost Soils* (pp. 85-95): Springer.

Palmer, J. M., Drees, K. P., Foster, J. T., & Lindner, D. L. (2018). Extreme sensitivity to ultraviolet light in the fungal pathogen causing white-nose syndrome of bats. *Nature communications, 9*(1), 35.

Palmer, J. M., Kubatova, A., Novakova, A., Minnis, A. M., Kolarik, M., & Lindner, D. L. (2014). Molecular characterization of a heterothallic mating system in *Pseudogymnoascus destructans*, the fungus causing white-nose syndrome of bats. *G3: Genes, Genomes, Genetics*, g3. 114.012641.

Pannkuk, E. L., Blair, H. B., Fischer, A. E., Gerdes, C. L., Gilmore, D. F., Savary, B. J., & Risch, T. S. (2014). Triacylglyceride composition and fatty acyl saturation profile of a psychrophilic and psychrotolerant fungal species grown at different temperatures. *Fungal Biology, 118*(9-10), 792-799.

Parniske, M. (2008). Arbuscular mycorrhiza: the mother of plant root endosymbioses. *Nature Reviews Microbiology, 6*(10), 763.

Pattison, D. I., & Davies, M. J. (2006). Actions of ultraviolet light on cellular structures *Cancer: cell structures, carcinogens and genomic instability* (pp. 131-157): Springer.

Paul, E. A. (2014). *Soil microbiology, ecology and biochemistry*: Academic press.

Paul, N. D., & Gwynn-Jones, D. (2003). Ecological roles of solar UV radiation: towards an integrated approach. *Trends in Ecology & Evolution, 18*(1), 48-55.

Pereira‐Junior, R. A., Huarte‐Bonnet, C., Paixão, F. R., Roberts, D. W., Luz, C., Pedrini, N., & Fernandes, É. K. (2018). Riboflavin induces *Metarhizium* spp. to produce conidia with elevated tolerance to UV‐B, and upregulates photolyases, laccases and polyketide synthases genes. *Journal of Applied Microbiology*.

Pfaffl, M. W., Tichopad, A., Prgomet, C., & Neuvians, T. P. (2004). Determination of stable housekeeping genes, differentially regulated target genes and sample integrity: BestKeeper–Excel-based tool using pair-wise correlations. *Biotechnology Letters, 26*(6), 509-515.

Pfeifer, G. P. (1997). Formation and processing of UV photoproducts: effects of DNA sequence and chromatin environment. *Photochemistry and Photobiology, 65*(2), 270-283.

Pfeifer, G. P., You, Y.-H., & Besaratinia, A. (2005). Mutations induced by ultraviolet light. *Mutation Research/Fundamental and Molecular Mechanisms of Mutagenesis, 571*(1), 19-31.

Pihet, M., Vandeputte, P., Tronchin, G., Renier, G., Saulnier, P., Georgeault, S., . . . Bouchara, J.-P. (2009). Melanin is an essential component for the integrity of the cell wall of *Aspergillus fumigatus* conidia. *BMC Microbiology, 9*(1), 177.

Pino‐Bodas, R., Martín, M. P., Burgaz, A. R., & Lumbsch, H. T. (2013). Species delimitation in *Cladonia* (*Ascomycota*): a challenge to the DNA barcoding philosophy. *Molecular Ecology Resources, 13*(6), 1058-1068.

Pittet, J.-L., Bouillant, M.-L., Bernillon, J., Arpin, N., & Favre-Bonvin, J. (1983). Sur la presence de mycosporines-glutamine reduites, nouvelles molecules, chez plusieurs deuteromycetes. *Tetrahedron Letters, 24*(1), 65-68.

Poole, N., & Price, P. (1971). The occurrence of *Chrysosporium pannorum* in soils receiving incremental cellulose. *Soil Biology and Biochemistry, 3*(3), 161-166.

Posada, D., & Buckley, T. R. (2004). Model selection and model averaging in phylogenetics: advantages of Akaike information criterion and Bayesian approaches over likelihood ratio tests. *Systematic Biology, 53*(5), 793-808.

Prakash, S., & Prakash, L. (2000). Nucleotide excision repair in yeast. *Mutation Research/Fundamental and Molecular Mechanisms of Mutagenesis, 451*(1), 13-24.

Radziejwoski, A., Vlieghe, K., Lammens, T., Berckmans, B., Maes, S., Jansen, M. A., . . . Bahnweg, G. (2011). Atypical E2F activity coordinates *PHR1* photolyase gene transcription with endoreduplication onset. *The EMBO journal, 30*(2), 355-363.

Raillo, A. (1929). Beitrage zur kenntnis der Boden-Pilze. *Zentralblatt fur Bakteriologie und Parasitenkunde Jena Abt, 278*, 515-524.

Raja, H., Schoch, C. L., Hustad, V., Shearer, C., & Miller, A. (2011). Testing the phylogenetic utility of *MCM7* in the Ascomycota. *MycoKeys, 1*, 63-94.

Raja, H. A., Miller, A. N., Pearce, C. J., & Oberlies, N. H. (2017). Fungal identification using molecular tools: a primer for the natural products research community. *Journal of Natural Products, 80*(3), 756-770.

Rambaut, A., Drummond, A., & Suchard, M. (2007). Tracer v1. 6 http://beast/. bio. ed. ac. uk. *Tracer (visited on 2017-06-12)*.

Rangel, D. E. (2011). Stress induced cross-protection against environmental challenges on prokaryotic and eukaryotic microbes. *World Journal of Microbiology and Biotechnology, 27*(6), 1281-1296.

Rangel, D. E., Fernandes, É. K., Braga, G. U., & Roberts, D. W. (2011). Visible light during mycelial growth and conidiation of *Metarhizium robertsii* produces conidia with increased stress tolerance. *FEMS Microbiology Letters, 315*(2), 81-86.

Rastogi, R. P., Kumar, A., Tyagi, M. B., & Sinha, R. P. (2010). Molecular mechanisms of ultraviolet radiation-induced DNA damage and repair. *Journal of Nucleic Acids, 2010*.

Rehner, S. A., & Buckley, E. (2005). A *Beauveria* phylogeny inferred from nuclear *ITS* and *EF1-α* sequences: evidence for cryptic diversification and links to *Cordyceps* teleomorph. *Mycologia, 97*(1), 84-98.

Reuveni, R., Ravivm, M., & Bar, R. (1989). Sporulation of *Botrytis cinerea* as affected by photoselective polyethylene sheets and filters. *Annals of Applied Biology, 115*(3), 417-424.

Reynolds, H. T., & Barton, H. A. (2014). Comparison of the white-nose syndrome agent *Pseudogymnoascus destructans* to cave-dwelling relatives suggests reduced saprotrophic enzyme activity. *PloS One, 9*(1), e86437.

Reynolds, H. T., Barton, H. A., & Slot, J. C. (2016). Phylogenomic analysis supports a recent change in nitrate assimilation in the White-nose Syndrome pathogen, *Pseudogymnoascus destructans*. *Fungal Ecology, 23*, 20-29.

Rhodes, J., & Fisher, M. C. (2018). Breaching Pathogeographic Barriers by the Bat White-Nose Fungus. *mBio, 9*(3), e00897-00818.

Rice, A. V., & Currah, R. S. (2006). Two new species of *Pseudogymnoascus* with *Geomyces* anamorphs and their phylogenetic relationship with *Gymnostellatospora*. *Mycologia, 98*(2), 307-318.

Riesz, J., Gilmore, J., & Meredith, P. (2006). Quantitative scattering of melanin solutions. *Biophysical Journal, 90*(11), 4137-4144.

Robinson, C. H. (2001). Cold adaptation in Arctic and Antarctic fungi. *New Phytologist, 151*(2), 341-353.

Rodríguez-Romero, J., & Corrochano, L. M. (2004). The gene for the heat-shock protein HSP100 is induced by blue light and heat-shock in the fungus *Phycomyces blakesleeanus*. *Current Genetics, 46*(5), 295-303.

Rodríguez‐Romero, J., & Corrochano, L. M. (2006). Regulation by blue light and heat shock of gene transcription in the fungus *Phycomyces*: proteins required for photoinduction and mechanism for adaptation to light. *Molecular Microbiology, 61*(4), 1049-1059.

Ruger-Herreros, C., Rodríguez-Romero, J., Fernández-Barranco, R., Olmedo, M., Fischer, R., Corrochano, L. M., & Canovas, D. (2011). Regulation of conidiation by light in *Aspergillus nidulans*. *Genetics*, genetics. 111.130096.

Rumbolz, J., Wirtz, S., Kassemeyer, H. H., Guggenheim, R., Schäfer, E., & Büche, C. (2002). Sporulation of *Plasmopara viticola*: differentiation and light regulation. *Plant Biology, 4*(3), 413-422.

Sametz‐Baron, L., Amit, R., Herrera‐Estrella, A., & Horwitz, B. A. (1997). Photoreactivation of UV‐lnactivated Spores of *Trichoderma harzianum*. *Photochemistry and Photobiology*, *65*(5), 849-854.

Samson, R. A. (1972). Notes on *Pseudogymnoascus*, *Gymnoascus* and related genera. *Acta Botanica Neerlandica, 21*(5), 517-527.

Sancar, A. (1994). Structure and function of DNA photolyase. *Biochemistry, 33*(1), 2-9.

Sancar, A. (2004). Photolyase and cryptochrome blue-light photoreceptors *Advances in Protein Chemistry* (Vol. 69, pp. 73-100): Elsevier.

Sancar, G. B. (1985). Sequence of the *Saccharomyces cerevisiae PHRI* gene and homology of the *PHRI* photolyase to *E. coli* photolyase. *Nucleic Acids Research, 13*(22), 8231-8246.

Schmitt, I., Crespo, A., Divakar, P., Fankhauser, J., Herman-Sackett, E., Kalb, K., . . . Shimp, A. (2009). New primers for promising single-copy genes in fungal phylogenetics and systematics. *Persoonia-Molecular Phylogeny and Evolution of Fungi, 23*(1), 35-40.

Schmittgen, T. D., & Livak, K. J. (2008). Analyzing real-time PCR data by the comparative C T method. *Nature Protocols, 3*(6), 1101.

Schoch, C. L., Seifert, K. A., Huhndorf, S., Robert, V., Spouge, J. L., Levesque, C. A., . . . Crous, P. W. (2012). Nuclear ribosomal internal transcribed spacer (ITS) region as a universal DNA barcode marker for Fungi. *Proceedings of the National Academy of Sciences, 109*(16), 6241-6246.

Schubert, K., Groenewald, J., Braun, U., Dijksterhuis, J., Starink, M., Hill, C., . . . Crous, P. (2007). Biodiversity in the *Cladosporium herbarum* complex (*Davidiellaceae*, *Capnodiales*), with standardisation of methods for *Cladosporium* taxonomy and diagnostics. *Studies in Mycology, 58*, 105-156.

Schuch, A. P., da Silva Galhardo, R., de Lima-Bessa, K. M., Schuch, N. J., & Menck, C. F. M. (2009). Development of a DNA-dosimeter system for monitoring the effects of solar-ultraviolet radiation. *Photochemical & Photobiological Sciences, 8*(1), 111-120.

Schumacher, J. (2017). How light affects the life of *Botrytis*. *Fungal Genetics and Biology, 106*, 26-41.

Schweitzer, A. D., Howell, R. C., Jiang, Z., Bryan, R. A., Gerfen, G., Chen, C.-C., . . . Dadachova, E. (2009). Physico-chemical evaluation of rationally designed melanins as novel nature-inspired radioprotectors. *PloS One, 4*(9), e7229.

Sebastian, J., Kraus, B., & Sancar, G. B. (1990). Expression of the yeast *PHR1* gene is induced by DNA-damaging agents. *Molecular and Cellular Biology, 10*(9), 4630-4637.

Seifert, K. A., Samson, R. A., Houbraken, J., Lévesque, C. A., Moncalvo, J.-M., Louis-Seize, G., & Hebert, P. D. (2007). Prospects for fungus identification using *CO1* DNA barcodes, with *Penicillium* as a test case. *Proceedings of the National Academy of Sciences, 104*(10), 3901-3906.

Setlow, R. B. (1974). The wavelengths in sunlight effective in producing skin cancer: a theoretical analysis. *Proceedings of the National Academy of Sciences, 71*(9), 3363-3366.

Sharifmoghadam, M. R., & Valdivieso, M. H. (2008). The *Schizosaccharomyces pombe* Map4 adhesin is a glycoprotein that can be extracted from the cell wall with alkali but not with β‐glucanases and requires the C‐terminal DIPSY domain for function. *Molecular Microbiology, 69*(6), 1476-1490.

Sheppard, D. C. (2011). Molecular mechanism of *Aspergillus fumigatus* adherence to host constituents. *Current Opinion in Microbiology, 14*(4), 375-379.

Shuryak, I., Bryan, R. A., Nosanchuk, J. D., & Dadachova, E. (2014). Mathematical modeling predicts enhanced growth of X-ray irradiated pigmented fungi. *PloS One, 9*(1), e85561.

Siede, W., Friedberg, A. S., & Friedberg, E. C. (1993). RAD9-dependent G1 arrest defines a second checkpoint for damaged DNA in the cell cycle of *Saccharomyces cerevisiae*. *Proceedings of the National Academy of Sciences, 90*(17), 7985-7989.

Silvestro, D., & Michalak, I. (2012). raxmlGUI: a graphical front-end for RAxML. *Organisms Diversity & Evolution, 12*(4), 335-337.

Sinha, R. P., & Häder, D.-P. (2002). UV-induced DNA damage and repair: a review. *Photochemical & Photobiological Sciences, 1*(4), 225-236.

Skouboe, P., Frisvad, J. C., Taylor, J. W., Lauritsen, D., Boysen, M., & Rossen, L. (1999). Phylogenetic analysis of nucleotide sequences from the ITS region of terverticillate *Penicillium* species. *Mycological Research, 103*(7), 873-881.

Smith, M. E., Douhan, G. W., & Rizzo, D. M. (2007). Intra-specific and intra-sporocarp ITS variation of ectomycorrhizal fungi as assessed by rDNA sequencing of sporocarps and pooled ectomycorrhizal roots from a Quercus woodland. *Mycorrhiza, 18*(1), 15-22.

Smith, R. C., Prezelin, B., Baker, K. e. a., Bidigare, R., Boucher, N., Coley, T., . . . Menzies, D. (1992). Ozone depletion: ultraviolet radiation and phytoplankton biology in Antarctic waters. *Science, 255*(5047), 952-959.

Smith, S. E., & Read, D. J. (2010). *Mycorrhizal symbiosis*: Academic press.

Stamatakis, A. (2014). RAxML version 8: a tool for phylogenetic analysis and post-analysis of large phylogenies. *Bioinformatics, 30*(9), 1312-1313.

Stevenson, D. S. (2009). Atmospheric science: Putting the wind up ozone. *Nature Geoscience, 2*(10), 677-679.

Suh, H.-J., Lee, H.-W., & Jung, J. (2003). Mycosporine glycine protects biological systems against photodynamic damage by quenching singlet oxygen with a high efficiency. *Photochemistry and Photobiology, 78*(2), 109-113.

Sweet, D. H., Jang, Y. K., & Sancar, G. B. (1997). Role of UME6 in transcriptional regulation of a DNA repair gene in *Saccharomyces cerevisiae*. *Molecular and Cellular Biology, 17*(11), 6223-6235.

Swofford, D. L. (2002). PAUP*. Phylogenetic analysis using parsimony (* and other methods). (Version 4). Sunderland, Massachusetts: Sinauer Associates.

Tagua, V. G., Pausch, M., Eckel, M., Gutiérrez, G., Miralles-Durán, A., Sanz, C., . . . Batschauer, A. (2015). Fungal cryptochrome with DNA repair activity reveals an early stage in cryptochrome evolution. *Proceedings of the National Academy of Sciences, 112*(49), 15130-15135.

Tajuddin, N., Rizman-Idid, M., Convey, P., & Alias, S. A. (2018). Thermal adaptation in a marine-derived tropical strain of *Fusarium equiseti* and polar strains of *Pseudogymnoascus* spp. under different nutrient sources. *Botanica Marina, 61*(1), 9-20.

Takano, Y., Kikuchi, T., Kubo, Y., Hamer, J. E., Mise, K., & Furusawa, I. (2000). The *Colletotrichum lagenarium* MAP kinase gene *CMK1* regulates diverse aspects of fungal pathogenesis. *Molecular Plant-Microbe Interactions, 13*(4), 374-383.

Tan, K. (1974). Blue-light inhibition of sporulation in *Botrytis cinerea*. *Microbiology, 82*(1), 191-200.

Tan, K. (1975). Interaction of near-ultraviolet, blue, red, and far-red light in sporulation of *Botrytis cinerea*. *Transactions of the British Mycological Society, 64*(2), 215-222.

Tan, K. K., & Epton, H. (1974). Further studies on light and sporulation in *Botrytis cinerea*. *Transactions of the British Mycological Society, 62*(1), 105-112.

Taylor, J. S., Lu, H. F., & Kotyk, J. J. (1990). Quantitative conversion of the (6–4) photoproduct of TpdC to its Dewar valence isomer upon exposure to simulated sunlight. *Photochemistry and Photobiology, 51*(2), 161-167.

Taylor, J. W., Jacobson, D. J., Kroken, S., Kasuga, T., Geiser, D. M., Hibbett, D. S., & Fisher, M. C. (2000). Phylogenetic species recognition and species concepts in fungi. *Fungal Genetics and Biology, 31*(1), 21-32.

Tedersoo, L., Bahram, M., Põlme, S., Kõljalg, U., Yorou, N. S., Wijesundera, R., . . . Suija, A. (2014). Global diversity and geography of soil fungi. *Science, 346*(6213), 1256688.

Thompson, S., Croft, N. J., Sotiriou, A., Piggins, H. D., & Crosthwaite, S. K. (2008). *Neurospora crassa* heat shock factor 1 is an essential gene; a second heat shock factor-like gene, *hsf2*, is required for asexual spore formation. *Eukaryotic Cell, 7*(9), 1573-1581.

Timling, I., Walker, D., Nusbaum, C., Lennon, N., & Taylor, D. (2014). Rich and cold: diversity, distribution and drivers of fungal communities in patterned ‐ ground ecosystems of the N orth A merican A rctic. *Molecular Ecology, 23*(13), 3258-3272.

Traaen, A. (1914). Untersuchungen über bodenpilze aus Norwegen. *Nytt Magasin for Naturvidenskapene, 52*, 1-121.

Treseder, K. K., Maltz, M. R., Hawkins, B. A., Fierer, N., Stajich, J. E., & McGuire, K. L. (2014). Evolutionary histories of soil fungi are reflected in their large ‐ scale biogeography. *Ecology Letters, 17*(9), 1086-1093.

Tretter, E. D., Johnson, E., Wang, Y., Kandel, P., & White, M. M. (2013). Examining new phylogenetic markers to uncover the evolutionary history of early-diverging fungi: comparing MCM7, TSR1 and rRNA genes for single-and multi-gene analyses of the Kickxellomycotina. *Persoonia: Molecular Phylogeny and Evolution of Fungi, 30*, 106.

Tretter, E. D., Johnson, E. M., Benny, G. L., Lichtwardt, R. W., Wang, Y., Kandel, P., . . . White, M. M. (2014). An eight-gene molecular phylogeny of the Kickxellomycotina, including the first phylogenetic placement of *Asellariales*. *Mycologia, 106*(5), 912-935.

Untergasser, A., Nijveen, H., Rao, X., Bisseling, T., Geurts, R., & Leunissen, J. A. (2007). Primer3Plus, an enhanced web interface to Primer3. *Nucleic acids research, 35*(suppl_2), W71-W74.

Vakalounakis, D. J., & Christias, C. (1981). Sporulation in *Alternaria cichorii* is controlled by a blue and near ultraviolet reversible photoreaction. *Canadian Journal of Botany, 59*(5), 626-628.

Vandesompele, J., De Preter, K., Pattyn, F., Poppe, B., Van Roy, N., De Paepe, A., & Speleman, F. (2002). Accurate normalization of real-time quantitative RT-PCR data by geometric averaging of multiple internal control genes. *Genome Biology, 3*(7), research0034. 0031.

Veluchamy, S., & Rollins, J. A. (2008). A CRY-DASH-type photolyase/cryptochrome from *Sclerotinia sclerotiorum* mediates minor UV-A-specific effects on development. *Fungal Genetics and Biology, 45*(9), 1265-1276.

Verma, S., & Idnurm, A. (2013). The Uve1 endonuclease is regulated by the white collar complex to protect *Cryptococcus neoformans* from UV damage. *PLoS Genetics, 9*(9), e1003769.

Větrovský, T., Kolařík, M., Žifčáková, L., Zelenka, T., & Baldrian, P. (2016). The *rpb2* gene represents a viable alternative molecular marker for the analysis of environmental fungal communities. *Molecular Ecology Resources, 16*(2), 388-401.

Vialle, A., Feau, N., Allaire, M., Didukh, M., Martin, F., MONCALVO, J. M., & Hamelin, R. C. (2009). Evaluation of mitochondrial genes as DNA barcode for Basidiomycota. *Molecular Ecology Resources, 9*, 99-113.

Vilgalys, R., & Hester, M. (1990). Rapid genetic identification and mapping of enzymatically amplified ribosomal DNA from several *Cryptococcus species*. *Journal of Bacteriology, 172*(8), 4238-4246.

Volkmann, M., & Gorbushina, A. A. (2006). A broadly applicable method for extraction and characterization of mycosporines and mycosporine-like amino acids of terrestrial, marine and freshwater origin. *FEMS Microbiology Letters, 255*(2), 286-295.

Volkmann, M., Whitehead, K., Rütters, H., Rullkötter, J., & Gorbushina, A. A. (2003). Mycosporine ‐ glutamicol ‐ glucoside: a natural UV ‐ absorbing secondary metabolite of rock ‐ inhabiting microcolonial fungi. *Rapid Communications in Mass Spectrometry, 17*(9), 897-902.

Wade, S. L., Poorey, K., Bekiranov, S., & Auble, D. T. (2009). The Snf1 kinase and proteasome ‐ associated Rad23 regulate UV ‐ responsive gene expression. *The EMBO journal, 28*(19), 2919-2931.

Wang, F., Liu, Q., Zhang, J., Liu, K., Li, K., Liu, G., & Dong, C. (2018). Comparative transcriptome analysis between a spontaneous albino mutant and its sibling strain of *Cordyceps militaris* in response to light stress. *Frontiers in Microbiology, 9*, 1237.

Wang, F., Song, X., Dong, X., Zhang, J., & Dong, C. (2017). DASH-type cryptochromes regulate fruiting body development and secondary metabolism differently than CmWC-1 in the fungus *Cordyceps militaris*. *Applied Microbiology and Biotechnology, 101*(11), 4645-4657.

Wang, J., Du, X., Pan, W., Wang, X., & Wu, W. (2015). Photoactivation of the cryptochrome/photolyase superfamily. *Journal of Photochemistry and Photobiology C: Photochemistry Reviews, 22*, 84-102.

Weinstein, R. N., Montiel, P. O., & Johnstone, K. (2000). Influence of growth temperature on lipid and soluble carbohydrate synthesis by fungi isolated from fellfield soil in the maritime Antarctic. *Mycologia*, 222-229.

Weinstein, R. N., Palm, M. E., Johnstone, K., & Wynn-Williams, D. D. (1997). Ecological and physiological characterization of *Humicola marvinii*, a new psychrophilic fungus from fellfield soils in the maritime Antarctic. *Mycologia*, 706-711.

White, T. J., Bruns, T., Lee, S., & Taylor, J. (1990). Amplification and direct sequencing of fungal ribosomal RNA genes for phylogenetics. *PCR protocols: a guide to methods and applications, 18*(1), 315-322.

Will, O. A., & Scovel, C. A. (1989). Photoprotective functions of carotenoids *Carotenoids* (pp. 229-236): Springer.

Williamson, C. E., Zepp, R. G., Lucas, R. M., Madronich, S., Austin, A. T., Ballaré, C. L., . . . McKenzie, R. L. (2014). Solar ultraviolet radiation in a changing climate. *Nature Climate Change, 4*(6), 434-441.

Wilson, M. B., Held, B. W., Freiborg, A. H., Blanchette, R. A., & Salomon, C. E. (2017). Resource capture and competitive ability of non-pathogenic *Pseudogymnoascus* spp. and *P. destructans*, the cause of white-nose syndrome in bats. *PloS One, 12*(6), e0178968.

WMO. (2011). *Scientific Assessment of Ozone Depletion: 2010, World Meteorological Organisation, Geneva, Switzerland Global ozone Research and Monitoring Project* (52, 438). Retrieved from https://www.wmo.int/pages/prog/arep/gaw/ozone_2010/documents/Ozone-Assessment-2010-complete.pdf

Xiong, F. S., & Day, T. A. (2001). Effect of solar ultraviolet-B radiation during springtime ozone depletion on photosynthesis and biomass production of Antarctic vascular plants. *Plant Physiology, 125*(2), 738-751.

Yajima, H., Inoue, H., Oikawa, A., & Yasui, A. (1991). Cloning and functional characterization of a eucaryotic DNA photolyase gene from *Neurospora crassa*. *Nucleic Acids Research, 19*(19), 5359-5362.

Yan, G.-l., Liang, H.-y., Wang, Z.-q., Yang, X.-f., Liu, D., Liu, J.-f., & Duan, C.-q. (2011). Important role of catalase in the production of β-carotene by recombinant *Saccharomyces cerevisiae* under H2O2 stress. *Current Microbiology, 62*(3), 1056-1061.

Yang, J., Liu, L., Wang, Y., Wang, C., Yan, J., Liu, Y., . . . Li, C. (2017). Overexpression of *BAS1* in rice blast fungus can promote blast fungus growth, sporulation and virulence in planta. *Saudi Journal of Biological Sciences, 24*(8), 1884-1893.

Yang, T., & Dong, C. (2014). Photo morphogenesis and photo response of the blue-light receptor gene *Cmwc-1* in different strains of *Cordyceps militaris*. *FEMS Microbiology Letters, 352*(2), 190-197.

Yonemasu, R., McCready, S. J., Murray, J. M., Osman, F., Takao, M., Yamamoto, K., . . . Yasui, A. (1997). Characterization of the alternative excision repair pathway of UV-damaged DNA in *Schizosaccharomyces pombe*. *Nucleic Acids Research, 25*(8), 1553-1558.

Yu, S. M., Ramkumar, G., & Lee, Y. (2013). Light quality influences the virulence and physiological responses of *Colletotrichum acutatum* causing anthracnose in pepper plants. *Journal of Applied Microbiology, 115*(2), 509-516.

Zhang, Y.-J., Huo, L.-Q., Zhang, S., & Liu, X.-Z. (2016). The complete mitochondrial genome of the cold-adapted fungus P*seudogymnoascus pannorum* syn. *Geomyces pannorum*. *Mitochondrial DNA Part A*, *27*(4), 2566-2567.

Zhang, Y.-J., Li, Z.-H., Luo, Z.-B., Zhang, J.-Q., Fan, Y.-H., & Pei, Y. (2009). Light stimulates conidiation of the entomopathogenic fungus *Beauveria bassiana*. *Biocontrol Science and Technology, 19*(1), 91-101.

Zhao, P., Luo, J., Zhuang, W., Liu, X., & Wu, B. (2011). DNA barcoding of the fungal genus *Neonectria* and the discovery of two new species. *Science China Life Sciences, 54*(7), 664-674.

Zhdanova, N. N., Tugay, T., Dighton, J., Zheltonozhsky, V., & Mcdermott, P. (2004). Ionizing radiation attracts soil fungi. *Mycological Research*, *108*(9), 1089-1096.